ECOLE DE TECHNOLOGIE SUPÉRIEURE
UNIVERSITÉ DU QUÉBEC

MANUSCRIPT-BASED THESIS
PRESENTED TO
ÉCOLE DE TECHNOLOGIE SUPÉRIEURE

IN PARTIAL FULFILLMENT OF THE REQUIREMENTS FOR
THE DEGREE OF DOCTOR OF PHILOSOPHY

BY
Hashem MORTAZAVI

AN IMPEDANCE BASED METHOD FOR DISTRIBUTION SYSTEM MONITORING

MONTREAL, 1$^{\text{TH}}$ APRIL 2016

ACKNOWLEDGMENTS

UNE MÉTHODE BASÉE SUR L'IMPÉDANCE POUR LA SURVEILLANCE DES SYSTÈMES DE DISTRIBUTION

Hashem MORTAZAVI

RÉSUMÉ

Le but principal de cette thèse est de proposer une nouvelle méthode de surveillance des systèmes de distribution traditionnels en tenant compte de l'intégration des sources d'énergie renouvelables. Les réseaux de distribution traditionnels sont principalement composés de dispositifs d'alimentation radiaux et ils sont conçus pour un flux de puissance unidirectionnel. En conséquence, la réglementation opérationnelle et les systèmes de protection et de contrôle sont souvent basés sur l'hypothèse d'un système de distribution radial.

La forte pénétration des sources d'énergie renouvelables aura un impact clair sur l'opération des systèmes de distribution. L'opération des réseaux électriques fait face à de nouveaux défis créés par les sources d'énergie renouvelables qui sont différents des défis traditionnels. L'intermittence des sources d'énergie renouvelables, la protection des systèmes électriques, la stabilité, la sécurité, la répartition économique et l'optimisation du flux de puissance sont des problèmes critiques issus de la pénétration d'un système électrique par des sources d'énergie renouvelables.

En outre, la production de la source d'énergie renouvelable peut excéder la consommation durant le jour, ce qui inverse le flux d'énergie durant certaines périodes. Un fort taux de pénétration de sources renouvelables décentralisées crée une situation de flux électrique multidirectionnel dans le réseau de distribution, qui était à l'origine conçu pour un flux unidirectionnel seulement. En conséquence de cette inversion de flux électrique, le voltage des dispositifs d'alimentation radiaux augmente.

L'importance d'un système de surveillance en ligne pour les principaux dispositifs d'alimentation dans les systèmes de distribution sera démontrée dans cette thèse. Il sera aussi montré que l'impédance mesurée sur le dispositif d'alimentation recèle un grand potentiel pour la surveillance en ligne des dispositifs d'alimentation.

L'apport principal de cette thèse est d'établir de modèle mathématique à l'état stable pour définir la zone de surveillance dans le plan R-X. Il sera montré que l'impédance apparente a un bon potentiel pour surveiller le facteur de puissance du distributeur, le flux de courant inversé, le flux de courant actif et le flux de courant réactif. En outre, il sera démontré qu'une courbe de puissance complexe peut être transférée au plan R-X pour surveiller la composante de puissance réactive imposée par la réglementation des services publics liée à l'intégration des sources d'énergie renouvelables.

VIII

Mots-clés : Calcul d'impédance, flux de puissance, sources d'énergie renouvelables, système de distribution, surveillance.

AN IMPEDANCE BASED METHOD FOR DISTRIBUTION SYSTEM MONITORING

Hashem MORTAZAVI

<ABSTRACT>

The main goal of this thesis is to propose a new monitoring technique for traditional distribution system with integration of renewable energy source. The traditional distribution network is primarily composed of radial feeders, designed for unidirectional power flow. Therefore, many operation regulation, protection and control system, in distribution network, are based on the radial distribution systems assumption.

The high penetration of the renewable energy sources, will clearly impact the distribution systems operation. Unlike other ways of electricity generation renewable energies initiate some challenges for grid operation. Intermittency of renewable energies sources, power system protection, stability, security, economic dispatch, optimal power flow are critical issues initiated by renewable energies penetration to power systems.

In addition, the renewable energy source output may exceed the consumed power during the day. Therefore, the direction of the power flow can be reversed during some periods. The high penetration of decentralized renewable sources will create a multidirectional power flow condition in the distribution grid, which was originally designed for unidirectional power flow only. Following of this reverse power flow, the distribution feeder voltage rises.

In this thesis the necessity of online monitoring system for important feeders in distribution system will be shown. It will be shown that the apparent impedance measured on the feeder has great capabilities for on line monitoring of distribution feeder.

The thesis establishes the steady-state mathematical model for defining the monitoring zone in R-X plane as the main contribution. It will be shown that the apparent impedance has a good potential for monitoring of feeder power factor, reverse and forward active and reactive power flow. In addition, it will be shown that complex power curve can be transferred to R-X plane to monitor the reactive power requirement regulation issued by utilities for RES integration.

Keywords: Distribution System, Impedance Calculation, Monitoring, Power Flow, Renewable Energy Resources.

TABLE OF CONTENTS

LIST OF FIGURES

Page

LIST OF ABREVIATIONS

AESO	Alberta Electric System Operator
APC	Active Power Curtailment
CP	Custom Power Devices
DG	Distributed Generation
DSIF	Demand And Supply Interface
DSTATCOM	Distribution-STATCOM
DSO	Distribution System Operator
EIA	U.S. Energy Information Administration
GHG	Green House Gas
IEA	International Energy Agency
HPWH	Heat Pump Water Heaters
LDC	Line Drop Compensation
kWp	Killowatt peak
MV	Medium Voltage
OECD	The Organization For Economic Co-Operation And Development
PF	Power Factor
PL	Penetration Level
PCC	Point Of Common Coupling
POI	Point Of Interconnection
PV	Photo Voltaic
RES	Renewable Energy Source
SVC	Static Var Compensator
STATCOM	Static Synchronous Compensator

INTRODUCTION

Electricity is the easiest source of energy that is used in modern society. More population, fast rate of economic growth and urbanization increase the electricity consumption. High security of supplying electricity is vital for every country in the new world, then increasing and diversifying energy sources are the main goal of governments. After the oil shocks of the 1970s, most of OECD (Organization for Economic Co-operation and Development) started focusing in developing alternative sources of energy. Atomic energy, bio alcohol, biodiesel, biofuel, biogas, biomass, wind, solar, geothermal are some of those alternative sources of energy. Global world weather warming and climate change are the main reasons of popularity of low-carbon technology. Low-carbon economic or Decarbonized Economy refers to an economy that has a minimal output of Green House Gas (GHG) emissions into the environment biosphere.

As renewable energies considered as low–carbon solution for electricity generation, they become popular in last decade. Sunlight, wind, rain, tides, waves and geothermal heat, are the most important sources of renewable energy. Therefore, most countries have an outlook for integrating new source of electricity generation to their electric grid. Unlike other ways of electricity generation renewable energies initiate some challenges for grid operation. Integration of intermittent RES, like solar and wind into a radial and unidirectional power flow distribution system, implies incorporating new monitoring devices that are sensitive to rapid changes of RES generation and power flow direction.

In this thesis, an impedance based technique is proposed as a monitoring tool in distribution systems. The performance of impedance seen at number of buses as a monitoring technique is analyzed in presence of RES devices. In this chapter, the motivation for this work along with the related objectives and challenges are described. The contributions of this work in the field of Electrical Engineering are listed. Finally, the organization of thesis is presented.

Motivation and Challenges

The traditional distribution network is primarily composed of radial feeders, designed for unidirectional power flow. Therefore, many operation regulation, protection and control system, in distribution network, are based on the radial distribution systems assumption.

The high penetration of the RESs & DGs, will clearly impact the distribution systems operation. Unlike other ways of electricity generation renewable energies initiate some challenges for grid operation. Intermittency of RE sources, power system protection, stability, security, economic dispatch, optimal power flow and etc. are critical issues initiated by RE penetration to power system.

In addition, the RES output may exceed the consumed power during the day. Therefore the direction of the power flow may be reversed during some periods of time. The high penetration of decentralized renewable sources will create a multidirectional power flow condition in the distribution grid, which was originally designed for unidirectional power flow. The distribution feeder voltage rises in consequence of reserve power flow Analyzing the impact of high penetration of RES in distribution system power flow and proposing a power flow monitoring technique is the main subject of this thesis.

Thesis Objective

It has been shown that RES connection to distribution grid may change the power flow direction and increase the voltage at the connection point; therefore, the theory that voltage is always lower with increasing distance from the substation is no longer valid in distribution system with RES integration. This voltage fluctuation along the feeder brings new challenges to the operation regulations of distribution grids. The main premise of this thesis is that; direction and magnitude of power flow are the main factors in distribution system operation, protection and voltage regulation in presence of RES. Therefore, if we can find a parameter

that be sensitive to active and reactive power flow variation then we can propose a power flow monitoring technique for distribution system with high RES penetration. The general research objective of this work are as follows:

- Proposing a power flow monitoring technique for distribution system with the RES integration.

The specific research objectives of this work are as follows:

- Reviewing the forward and reverse power flow side effects in distribution system operation;
- Finding an index sensitive to power flow variation ;
- Defining the monitoring zone for power factor, active and reactive power flow monitoring.

We put a constraint in our research objective as follow:

- Applicability of the proposed method for the traditional distribution system and smart grid.

Thesis Contributions

The major contributions of this thesis are listed below:

A Monitoring Technique for Reversed Power Flow Detection with High PV Penetration Level

A monitoring application based on the calculated apparent impedance is proposed for reversed power flow detection. It is shown that the apparent impedance has considerable capability to be used as a monitoring technique for reverse power flow detection at any condition. The proposed mathematics show that any point (r, x) on the R-X coordinates plane is in one-to-one correspondence with a point (p, q) in the P-Q coordinates plane. The main contribution of the work is based on calculated impedance that has high capability for detecting different states of distribution system in presence of various RES penetration

4

levels. The results indicate that any proposed monitoring technique shall have the capability of monitoring for balanced and unbalanced system (Mortazavi et al., 2015b).

An Impedance Based Method for Distribution System Monitoring

The steady-state mathematical model for defining the monitoring zone in R-X plane is established as one of the main contributions of this thesis. It will be shown that the apparent impedance has a good potential for monitoring of feeder power factor, reverse and forward active and reactive power flow.

An Impedance Based Method for Wind Farm Reactive Power Requirement Monitoring

In order to reliable operation of power system, the generating units must comply with certain reactive power requirement depending on the network they are connected. Although many of existing interconnection regulations have been based on traditional generating units' capabilities, the increasing rate of RES integration forces the power system regulators to consider variable type of generation in their standards and practical procedures. Therefore, it will be shown that complex power curve can be transferred to R-X plane to monitor the reactive power requirement regulation issued by utilities for RES integration.

Application of Distance Relay for Distribution System Monitoring

Based on the interconnection standard, by RES integration to distribution system, utilities need to install distance relay as the main feeder protection device. It will be shown that the so called distance relay as a protection device has the capability to monitor the RES integration to the feeder. The results indicate that a one-phase distance relay not only reacts to fault in its defined zone, but also can monitor the feeder for different PV penetration level and load variation (H. Mortazavi, 2015.).

A Modified Load Encroachment Technique for Power Factor Monitoring

A new application of distance relay load encroachment technique is proposed for power factor monitoring. During the heavy load conditions, the load encroachment of impedance into the distance relay protection zones is a well-known reason for distance relay mal-operation. Therefore, all the modern digital distance relays are equipped with the load

encroachment scheme which prevents the mal-operation of relay during the heavy load conditions. This thesis proposes the idea of using the load encroachment scheme of distance relay for monitoring purpose in presence of RES integration.

Thesis Organization

In the present research, application of an impedance based monitoring technique for distribution system monitoring is studied. In Chapter 1 a literature review of the impact of RES integration on the feeder power flow and the necessity of the feeder monitoring are presented. A monitoring technique for reversed power flow detection with high PV penetration level are presented in Chapter 2. Chapter 3 discusses the idea of an impedance based method for distribution system monitoring. In Chapter 4, application of distance relay for distribution system monitoring is presented and the modified load encroachment idea is introduced. Finally, a conclusion of the thesis is provided.

CHAPITRE 1

LITERATURE REVIEW

The traditional distribution network is primarily composed of radial feeders, designed for unidirectional power flow. Therefore, many operation regulation, protection and control system, in distribution network, are based on the radial distribution systems assumption. The high integration of the RES, will clearly impact the distribution systems operation.

In this chapter, the impacts of RES integration to the distribution system operation are explained. Then, the necessity of distribution system monitoring is explained.

1.1 RES integration impacts on power flow and voltage control

This section focuses on the main impacts of RES integration on distribution system power flow and the feeder voltage control. Traditional distribution system was designed radially with unidirectional power flow. The voltage drop is one of the main concerns of traditional distribution system design.

Meanwhile as the voltage decreases from the substation to the end of the feeder, the probability of over-voltage occurrence is relatively small. Increased integration of DGs and RES in last decade has changed this phenomenon and the probability of over-voltage occurrence especially at the end of radial feeder increases. Consequently the voltage rise; due to the increased penetration of DGS and RES, became the main limiting factor for their integration (Appen et al., 2013; Aziz et al., 2013; Demirok et al., 2011; Ehara, 2009; Turitsyn et al., 2010; Verhoeven, 1998; Viawan, 2008). Figure 1.1 shows the effect of injected power by PV on voltage profile of a feeder. The green line shows feeder voltage profile without PV. By adding the PV effect on voltage profile (black line) the voltage at end of feeder may exceed the over-voltage limit.

8
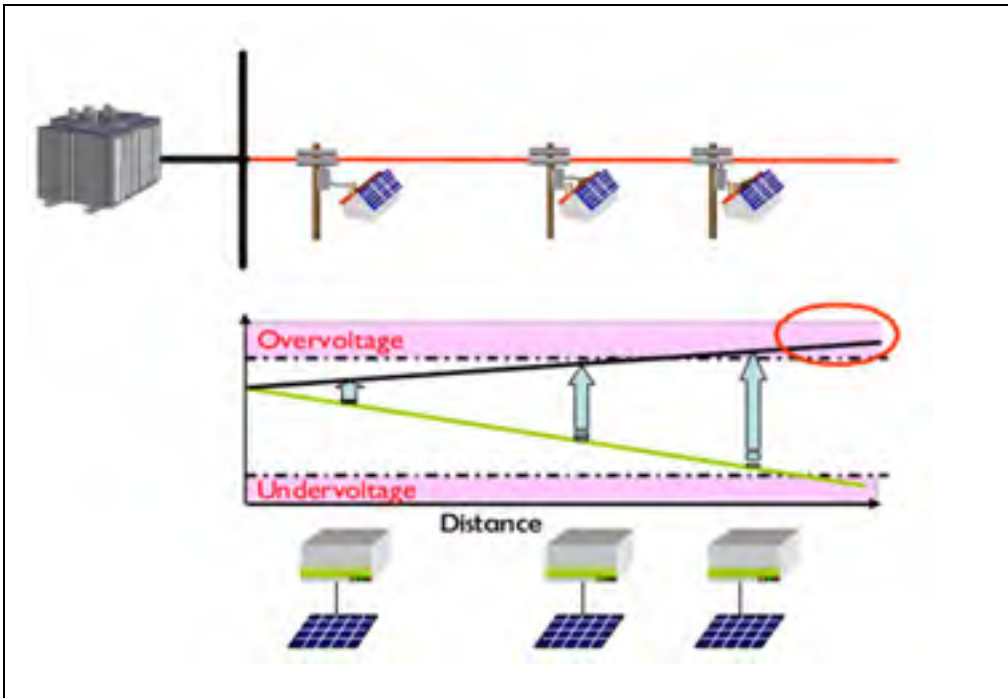
Figure 1.1 Voltage profile at presence of PV
Adapted from Ehara (2009)

The main reasons of feeder voltage profile violation are the variation of both magnitude and direction of power flow.

A basic overview on voltage drop in a simple power system is shown in a single line diagram in Figure 1.2. In radial distribution systems, the voltage-drop effect is distinguished. Here the voltage simply decreases as moving from the substation (the power source, in effect) out toward the end of a distribution feeder. This variation in voltage is known as the line drop. The line drop is described by Ohm's law, $V = IZ$, where I is the current flowing through the line, Z is the line's impedance, and V is the voltage difference between the two ends. Ohm's law also shows us that the line drop depends on the connected load, since a greater power demand implies a greater current.

While the line impedance stays the same, the voltage drop varies in proportion to the load. In practice, the voltage drops in distribution systems are quite significant, especially for long

feeders. Recognizing that it is physically impossible to maintain a perfectly flat profile, operational guidelines in the United States generally prescribe a tolerance of ±5% of the nominal voltage. This range applies throughout transmission and distribution systems, down to the customer level. For example, a customer nominally receiving 120 V should expect to measure anywhere between 114 and 126 V at their service drop.

For any feeder of figure 1.2, the current I_i as a function of the line complex apparent power $S_i = P_{Li} + jQ_{Li}$ and the load voltage V_{i+1} will be

$$I_i = \frac{P_{Li} - jQ_{Li}}{V_{i+1}^*} \tag{1.1}$$
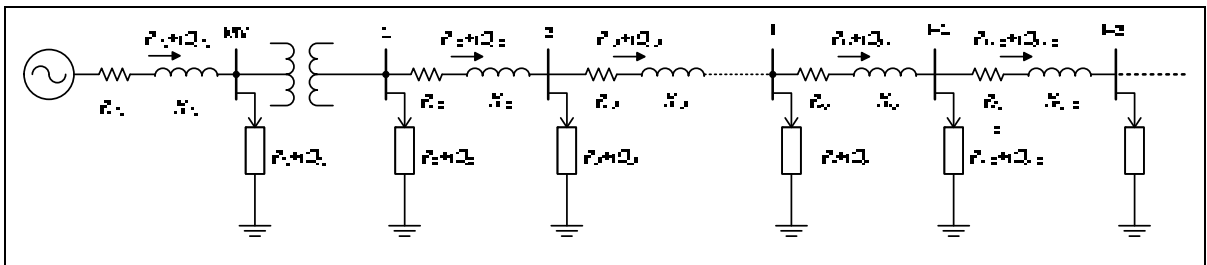
Figure 1.2 One line diagram for an illustration of the voltage drop in a distribution system

The voltage drop on the feeder i is given by

$$\Delta V_i = V_i - V_{i+1} = (R_{si} + jX_{si}) * \frac{P_{Li} - jQ_{Li}}{V_{i+1}^*} \tag{1.2}$$

$$\Delta V_i = \left[\frac{R_{si} * P_{Li} + X_{si} * Q_{Li}}{V_{i+1}^*}\right] + j * \left[\frac{X_{si} * P_{Li} - R_{si} * Q_{Li}}{V_{i+1}^*}\right] \tag{1.3}$$

For a small power flow, the voltage angle between V_{i+1} and V_i in (1.2) is small, so the imaginary part of (1.3) can be neglected, therefore; the voltage drop can be approximated by

$$\Delta V_i = \left[\frac{R_{si} * P_{Li} + X_{si} * Q_{Li}}{V_{i+1}^*}\right] \tag{1.4}$$

From Equations (1.3) - (1.4), it can be seen that the load current always causes a voltage drop and the voltage profile in conventional radial distribution systems (without integration of DG and RES) is decreasing towards the end. This voltage drop and voltage profile is the basis for voltage regulation in power systems. The transformer secondary voltage can be adjusted by changing the voltage ratio of the transformer, meanwhile the voltage drop on the feeder can be reduced by compensating the reactive power demand using shunt capacitors; which will be explained hereafter.

A simple two node radial distribution system is shown in Figure 1.3. If we conclude the RES or DG power production to formula (1. 4) and calculate the voltage drop along the feeder we will reach to formula (1.5).
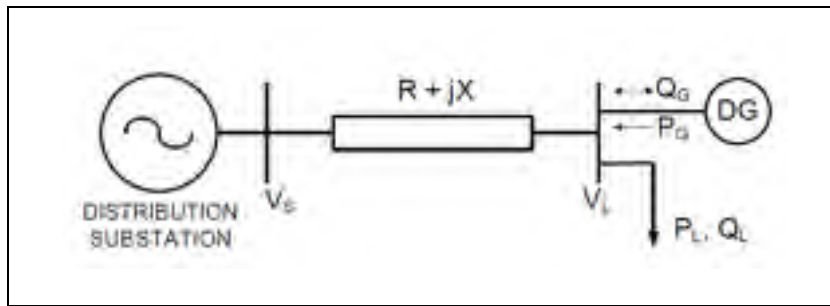
Figure 1.3 Simple two node radial distribution system

$$\Delta V = V_S - V_L = \left[\frac{R(-P_G + P_L) + X(\pm Q_G + Q_L)}{V_L}\right] \tag{1.5}$$

From this formula it is clear that different active and reactive power production of DG may produce a change in the power flow. By reversing the power flow direction there is a negative voltage drop along the feeder which is the main cause of over-voltage at the end of feeder in presence of any type of power generation.

1.2   Proposed method in the literature for detection of power flow variation and voltage control at high penetration of RES and DG

Verhoeven et al. in (Verhoeven, 1998), is one of the first authors who addressed the problems of PV penetration to power system, in 1998. In (Verhoeven, 1998), different problems initiated by PV integration are discussed such as harmonic, multiple inverters, overvoltage, protection and etc. The report emphasized on reverse power flow problem and in consequence voltage rise due to high penetration of PV. The report proposed two methods as solutions. The first recommended technique in (Verhoeven, 1998) is operation of PV system at the leading power factor. By operation at leading power factor of PV inverter, the feeder voltage raise will be regulated without decreasing the active power output of PV. The report (Verhoeven, 1998), mentioned that the effectiveness of leading factor operation of inverter is restricted by X/R ratio of feeder. If the reactance of feeder is very low in comparison of feeder resistance, feeder voltage regulation needs a huge amount of reactive power. When the feeder voltage rise cannot be compensated by leading power factor, the second recommended method is decreasing the active power output of system.

Based on the newest report published by Task 10 of "Photovoltaic Power Systems Program" of International Energy Agency (IEA) (Ehara, 2009), the over-voltage and under-voltage are the biggest barriers to high PV penetration in the distribution system. Figure 1.1 shows the problem of parallel line voltage regulation by MV transformer tap changer. In (Ehara, 2009) it was proposed that, it is possible to regulate the feeder voltage, and keep it in boundaries by decreasing the sending-end voltage controlled by MV transformer tap changer. The main problem of this method is when there are parallel lines with different PV penetration level.

As it can be seen from Figure 1.4 by decreasing the tap step of tap-changer, the feeder with no PV or any other source of DG will suffer the under-voltage at the end of the feeder. Based on the (Ogimoto et al., 2013) in Japan, they designed a power conditioner system for PV that will decrease the active power output of PV to control the voltage. The main disadvantage of

this system is lower PV system efficiency. Furthermore in a distribution line, among all users, the PV systems which located at the end of the line tend to be more restricted with higher priority.
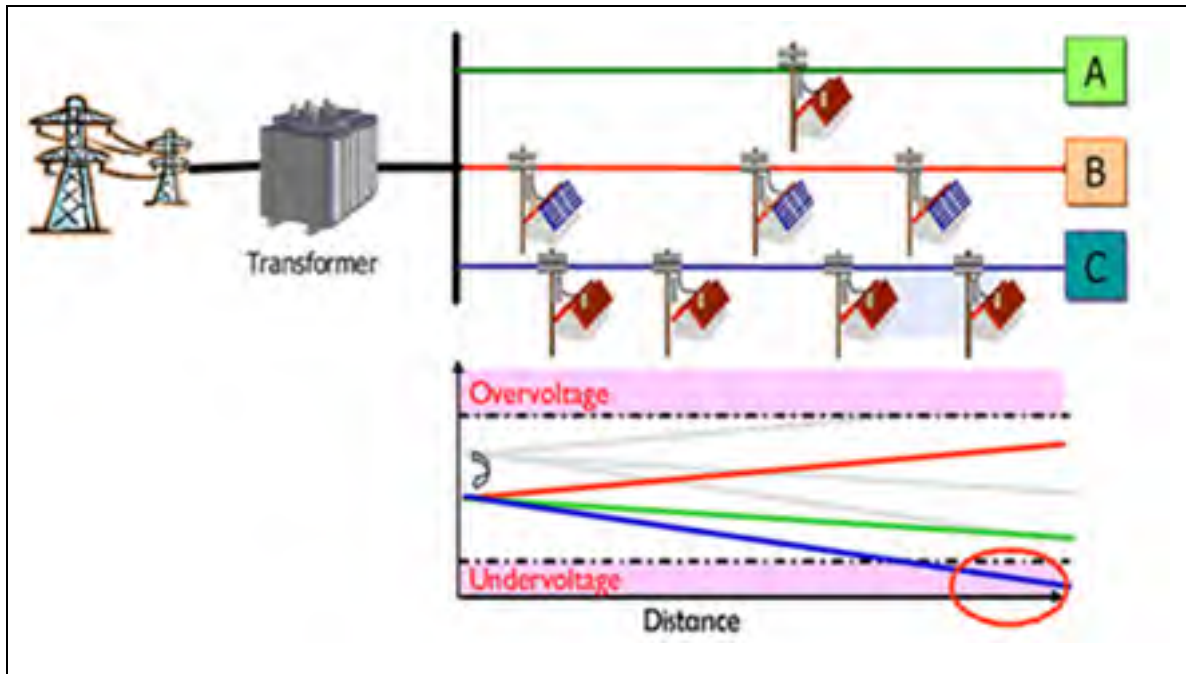
Figure 1.4 Voltage profile at different feeders at presence of PV
Adapted from Ehara (2009)

Active power curtailment (APC) is another popular option for voltage regulation in presence of RES. Although most of electric utilities and countries did not have any PV integration standard, Germany and Japan published their minimum requirement for this purpose (Appen et al., 2013; Ogimoto et al., 2013). In Japan the PV owner must curtail generation when the balance limit of demand – supply exceeded (Ogimoto et al., 2013).

In Germany the owner of small PV system (less than 30 Killowatt peak (kWp)) must decrease the generation output by 70 percent or install a remote control system operated by distribution system operator (DSO). For bigger system, installation of remote control system is mandatory (Appen et al., 2013).

Paper (Tonkoski, Lopes et El-Fouly, 2011b) proposed a droop based APC to prevent over-voltage at distribution LV feeders. Voltage droop control by virtual impedance method is presented in (De Brabandere et al., 2004). In this method the system voltage is measured then output power of PV system controlled based on this value. Because of the intermittency characteristic of RES and daily load variation, the possibility of voltage violation on LV feeders increases. Therefore if the DSO wants to regulate the voltage by the active power curtailment technique, the total power generation of PV system, the total energy delivered to network over one year and the total efficiency of PV system will be decreases. Therefore considering the annual sales of PV power, the financial output of RES become less and less.

According to (Ehara, 2009; Verhoeven, 1998), the reverse power flow is the main cause of voltage rise in distribution feeders. Therefore, some papers for voltage control of feeder focus on controlling the reverse power flow as a main solution. For this purpose, different methods such as demand side management (Asari et Kobayashi, 2012; Hatta, Uemura et Kobayashi, 2010; Inoue et Iwafune, 2010), SVC (Daratha, Das et Sharma, 2013), STATCOM (Aziz et al., 2013), DSTATCOM (Chen et al., 2013; Kun et al., 2012; Lin et al., 2012), storage system (Nykamp et al., 2013; Schoenung et Hassenzahl, 2003) , Electric Vehicle (Byung-Kwan et al., 2013; Kim, Kirtley et Norford, 2013; Tuffner et al., 2012) and SMES (Byung-Kwan et al., 2013) were proposed in recent papers.

If the total or most of RES or PV output can be consumed at the point of production, there will be less voltage violation on feeders. This theory is basis of customer load management. Based on this method the customer load will be managed cooperatively in accordance of RES output. Heat pump water heaters (HPWHs) are one of the instruments that are used for consumer load management (Asari et Kobayashi, 2012; Hatta, Uemura et Kobayashi, 2010; Inoue et Iwafune, 2010).

A heat pump (HP) is a machine that uses the mechanical principal of a refrigeration cycle to transfer heat from a source to other (Hepbasli et Kalinci, 2009). The HP can be used for air conditioning (cooling in summer and heating in winter). Figure 1.5 shows the schematic of a

simplified solar- HPHW system. As it can be seen the solar power produces the electricity needed for heat transfer.
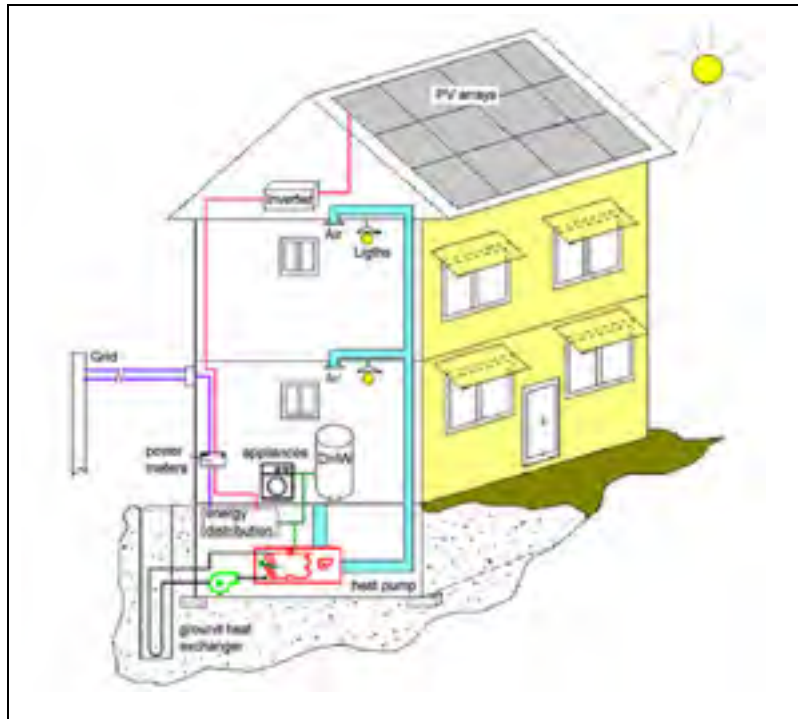
Figure 1.5 Schematic of a simplified solar- HPHW system
Adapted from Hepbasli et Kalinci (2009)

Authors in (Asari et Kobayashi, 2012; Hatta, Uemura et Kobayashi, 2010; Inoue et Iwafune, 2010) proposed using HPWHs for reducing the reverse power flow and consequently decreasing the voltage deviation due to PV production.

The simulation results of (Inoue et Iwafune, 2010), showed that daylight operation of HPWH can decrease the reverse power flow considering the hot water demand of consumer. Hatta et al. (Hatta, Uemura et Kobayashi, 2010) showed HPWH can reduce the size of storage system and the SVC for controlling the feeder voltage. (Asari et Kobayashi, 2012) proposed a distribution line management which minimizes the PV output to feeders by increasing the power demand of consumer. They defined a demand and supply interface (DSIF), which

plans the operation of HPWH, battery storage and PV output. Figure 1.6 shows the schematic diagram of DSIF for controlling reverse power flow of PV generation system.
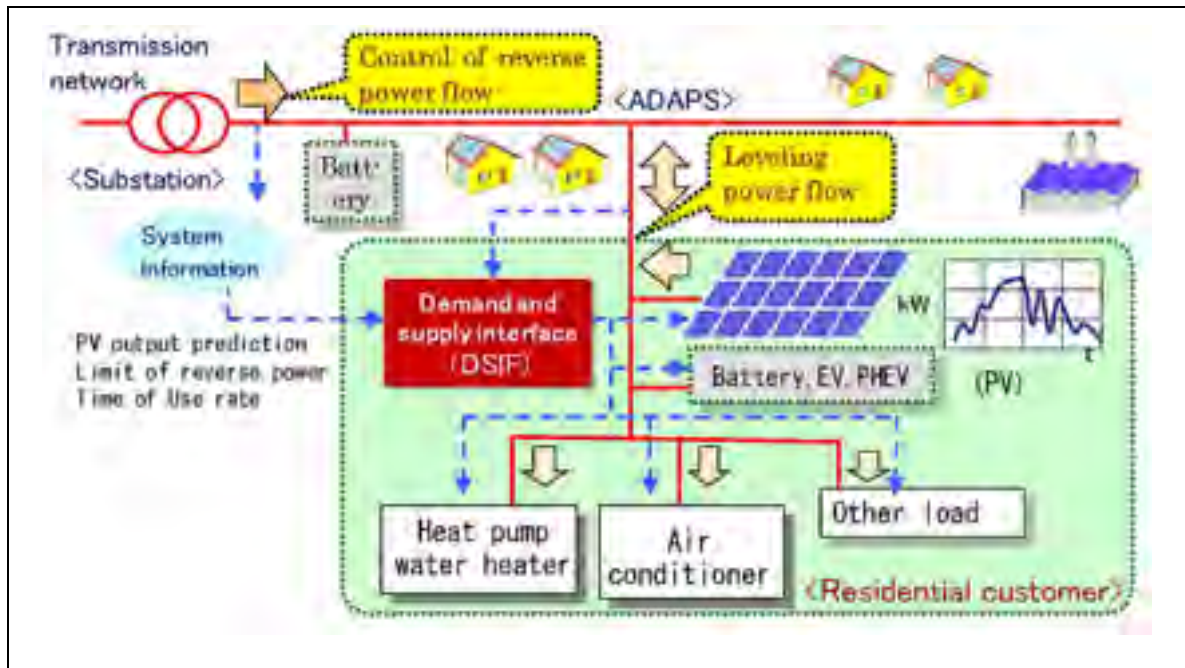
Figure 1.6 Schematic diagram of controlling reverse power flow of PV generation system
Adapted from Asari and Kobayashi (2012)

(Wei-Fu, Shyh-Jier et Chin, 2001) proposed a hybrid photovoltaic and battery energy storage system as demand side management technique. The recent report published by U.S. Department of Energy (Tuffner et al., 2012), proposed utilizing Electric Vehicle in distribution system in order to control the reverse power flow, maintain voltage in its boundaries and to assist higher penetration level of PV generation to distribution system.

Based on IEEE 1547 standard (Basso et DeBlasio, 2004), distributed generation do not currently allow for voltage regulation (they must operate at unity power factor). In spite of that standard, there are a lot of recent papers and reports which propose using reactive capability of inverter based DGs for regulating the voltage at the point of common coupling (PCC) (David Smyth; Farivar et al., 2012; Liu et Bebic, 2008; Tonkoski, Lopes et El-Fouly, 2011b; Turitsyn et al., 2010; Ueda et al., 2008).

Liu et al. in report published by NREL (Liu et Bebic, 2008), investigate the role of PV inverters capabilities in feeder voltage regulation which is beyond the IEEE 1547 requirements. They analyzed different PV penetration levels effect on voltage regulation in distribution system. Their results showed that at a medium PV penetration level (10%), inverter voltage support can help reduce the size of the voltage support capacitors by nearly 40% and at high PV penetration levels (30%–50%), PV inverters might entirely displace voltage support capacitors.

For mitigating of the rapid and fast voltage fluctuation due to high penetration of PV and resulting reverse power flow; (Farivar et al., 2012) proposes using the fast time cycle of inverter for reactive power flow control in comparison of traditional slow timescale Volt/Var control. They solved a radial optimal power flow which minimizes line losses with constraints on voltage magnitudes. (Liu et Bebic, 2008) showed that if we choose the size of inverter 110% of its nominal power, its reactive capability increases near 46%. Considering all the good aspect; in addition of contrasting with DG integration standard (IEEE 1547), the bigger size of inverter and more complex control system are the main disadvantages of using inverter capability for voltage regulation at high penetration of PV.

To sum up, it was shown that the feeder power flow changes not only by the time and feeder loads variation but also by RES integration. In addition, it was shown that the feeder power flow variation has a substantial impact on the feeder voltage control and operation. In the next section the currnet proposed monitoring system in the literature will be pressented. Moreover, the reasons and neccissity of the monitoring devices for distribution feeders will be discussed.

1.3   Literature review in distribution system monitoring

Widespread real-time monitoring of distribution system, because of the high number of feeders and lack of the communication system was impossible for a long time. By decreasing the price of communication system, full deployment of smart meters seems applicable for

implementing the smart grid in distribution system level. Monitoring of a distribution system due to its time varying and unbalanced loading, through smart meters and monitors is one of the basis of smart grid (Tcheou et al., 2014). Different monitoring system approaches and devices have been proposed to assess different conditions of distribution systems. Power quality monitoring system has been used for a long time not only for analyzing power quality issues but also for load modeling (Visconti et al., 2014). (Qiang et al., 2012) proposed a voltage monitoring for micro grid application, to analyze the power quality and reliability indices. Using state estimation technique is one of the most popular solutions proposed in the literature for distribution system monitoring. The authors in (Bernieri, Liguori et Losi, 1995) proposed using the on-line system modelling capability of artificial neural network (ANN) for distribution system state estimation. The application of branch current state estimation method has been proposed in (Baran et Kelley, 1995),(Baran, 2012) for real time monitoring and control of a distribution feeder. Authors in (Ferdowsi et al., 2014) proposed an ANN based monitoring system for better voltage magnitudes estimation of distribution feeder in presence of distributed generation (DG). (Powalko et al., 2009) proposed to use phasor measurement units (PMU) for improved distribution system state estimation.

The renewable energy sources network integration affects the traditional Volt-VAR control, power factor correction and voltage regulation (Bollen et Hassan, 2011). The impacts of high PV penetration on distribution system protection and operation were analyzed in (Baran et al., 2012). Unidirectional power flow was the first design criteria for distribution system planning for decades. Under this assumption the voltage profile is maximum at the feeder head and decreases proportional with loads to the end of the feeder (Kersting, 2012). Depending on the size and location of variable generation and the load size, the power flows may reverse in the feeder [2]. Therefore, the current distributions system vulnerability increases by RES generation. The high RES penetration increases the necessity of deployment of monitoring devices for different purposes.

1.4 Distribution system monitoring necessity

As it was stated in the introduction, contrary to transmission systems, due to high number of feeders and elements, distribution systems suffers lack of sufficient monitoring devices. In this section some challenges which raise the necessity of deployment of monitoring units in distribution network will be presented briefly.

- Distribution systems have been designed for radial and unidirectional power flow. In this design the active and reactive power are transferred from the transmission system to consumers. Therefore, many protection and voltage regulation strategies in distribution networks are based on radial nature. For example, voltage regulators are designed with the flow of power from the higher voltage to the lower voltage. Integration of the RES to distribution systems, however, shows that based on the size and the installation location, the power flow may reverse (Jahangiri et Aliprantis, 2013). For high penetration of RES, traditional unidirectional distribution system will change to bidirectional system which needs a revision of regulation;

- The minimum voltage drop which must be kept within the standard limits was the main concern of distribution system planners for a long time. On the other hand, the feeder overvoltage was not a concern for distribution system design. With RES integration the over-voltage possibilities become one of the main design concerns (Bollen et Hassan, 2011);

- From a practical standpoint the real distribution system has non-uniform load distribution, distributed load location and different wire sizes. The designer considers increased wire size for contingency-support branches during special situations (Short, 2014). Distributed RES integration with intermittent characteristic increases the vulnerability of small wire size feeder to overload conditions;

- In addition, in a unidirectional power flow design philosophy, the designer considers feeder load balancing through opening and closing switches at different locations, as an economical solution regarding the load growth over the time. Due to changing the switch patterns, the distribution network configuration is a dynamic variable (Willis, 2010). The RES generation will increase dynamic characteristic which justifies the capital cost needed to deploy new monitoring techniques;

- Moreover, Volt-VAR control, power factor correction and voltage regulation are important elements for increasing the distribution system efficiency in operation. Reactive power flow on a feeder decreases its active power flow capacity and increases both the voltage drop and loss. In a unidirectional distribution network, even feeders with in-range power factor correction at the substation have portions that are not well corrected (particularly at the feeder's end, where the power factor is much lower) (Short, 2014). The capacitor size needed to correct power factor during peak VAR conditions (during summer due to the high reactive loads of air conditioning system) may seriously over-compensate during off-peak conditions. A survey made by (Willis, 2010) indicated that slightly more than one-third of all switched capacitor banks were not switching properly due to mechanical failure, vandalism or weather conditions.

1.5   Conclusions of literature review and refining the problematic

Based on the equipment failures data and statistics, electric distribution systems, due to high number of feeders have the highest rate of customer supply unavailability (supply interruption) in power systems. In this section, it was argued that the modern distributions system vulnerability increases not only because of infrastructure aging, but also, because of RES generation. It increases the necessity of deployment of monitoring devices for different purposes. Widespread real-time monitoring of distribution system, because of the high

number of feeders and lack of the communication system was impossible for a long time. By decreasing the price of communication system, full deployment of smart meters seems applicable for implementing the smart grid in distribution system level. Monitoring of distribution system due to its time varying and unbalanced loading, through smart meters and monitors is one of the basis of smart grid. In the next chapter it will be shown that the apparent impedance measured on the feeder has great capabilities for on-line monitoring of distribution feeders

CHAPITRE 2

A Monitoring Technique for Reversed Power Flow Detection with High PV Penetration Level

Hashem Mortazavi[1], Hasan Mehrjerdi[2], Maarouf Saad[1], Serge Lefebvre[3], Dalal Asber[3] and Laurent Lenoir[3]

[1]Department of Electrical and Computer Engineering, Ecole de technologie supérieure, 1100 Notre-Dame West, Montréal, Quebec, Canada H3C 1K3
[2]Qatar University, Doha, Qatar
[3]The Research Institute of Hydro-Quebec (IREQ), Power Systems and Mathematics, Varennes, Quebec, Canada

Abstract

The integration of renewable energy resources (RESs) in power systems poses many research challenges. Research shows that the RES output may exceed the consumed power during the day. Consequently, the direction of the power flow on distribution lines can be reversed during some periods. As the voltage regulator is normally designed for unidirectional power flow, this may cause voltage violations on the distribution feeder. Therefore, most utilities try to set a penetration level limit for safe operation. On the other hand, time varying and unbalanced loading are the main characteristics of distribution systems. Moreover, installation of intermittent and non dispatchable PV (photovoltaic) devices increases the control problems of distribution system. This thesis presents an impedance based monitoring method for detection of distribution system current behaviour. It will be shown that by utilizing this monitoring technique not only the small variation of PV penetration level can be easily detected but also some fast transients such as the effect of cloud movement on PV system can be monitored.

This monitoring technique employs only local measurements of bus voltages and line current to measure the apparent impedance seen at the installation point. The practical application of measured impedance as a monitoring technique shows its effectiveness for distribution system monitoring in presence of various PV penetration level.

2.1 Introduction

Deregulation of power system, smart grid, electric vehicle and renewable energy integration pose a lot of challenges to power systems operation. Although a lot of monitoring and protection devices are installed in transmission system due to its complexity, traditional distribution systems suffer lack of monitoring systems due to its high number of feeders and load points.

Distribution systems have been designed for radial and unidirectional power flows. In this design the active and reactive power are transferred from the transmission system to the consumer. Therefore, many protection and regulation strategies in distribution network are based on this radial nature. For example, voltage regulators are designed with the flow of power from the higher voltage to the lower voltage. Integration of the RES in distribution systems however shows that, based on the size and the installation location, the power flow may reverse (Jahangiri et Aliprantis, 2013). For high penetration of RES, traditional unidirectional distribution system will change to a bidirectional system which needs a revision of regulation.

According to (Yang et al., 2012) the reverse power flow is the main cause of voltage rise in distribution feeders. Customer load control is one solution for decreasing reverse power. Reference (Asari et Kobayashi, 2012) proposes that controlling heat pump water heaters (HPWH) at customer side will minimize reverse power flow and voltage violation resulting from high penetration of PV. (Baran et al., 2012) analyzes high PV penetration impacts on distribution system protection and operation. Using flexible AC transmission system (FACTS) and custom power (CP) devices (SVC (Daratha, Das et Sharma, 2013), STATCOM

(Aziz et al., 2013), DSTATCOM (Chen et al., 2013), SMES (Byung-Kwan et al., 2013)), utilizing electric vehicle (Goli et Shireen, 2014), storage system (Marra et al., 2014),(von Appen et al., 2014),(Taheri, Akhrif et Okou, 2013) and active power curtailment technique recommended in (Ogimoto et al., 2013),(Appen et al., 2013),(Tonkoski, Lopes et El-Fouly, 2011a) are the most attractive techniques to mitigate those expected voltage violations.

Monitoring distribution system through smart meters and monitors is one of the basis of smart grid (Tcheou et al., 2014). Different monitoring system approaches and devices have been proposed to assess different system conditions. Power quality monitoring systems have been used for a long time not only for analyzing power quality problems but also for load modeling (Visconti et al., 2014). (Qiang et al., 2012) proposes voltage monitoring of micro grid at number of buses to analyze the power quality and reliability indexes.

Using local data measurement for protection, control and monitoring purpose is an attractive alternate solution to the electric utilities, due to lower installation costs and simplicity of operation. On-line impedance measurement based on local data has been proposed for different applications. The most important application of impedance measurement is in distance relay protection (Shateri et Jamali, 2010). (Vu et al., 1999) proposes using local measured apparent impedance for voltage stability margin estimation. (Cespedes et Jian, 2014) proposes using online grid impedance measurement for adaptive control of grid connected inverters.

Integration of intermittent RES, like solar and wind into a radial and unidirectional power flow distribution system, implies incorporating new monitoring devices that are sensitive to rapid changes of RES generation and power flow direction. In this research, an impedance measuring technique is proposed as a monitoring tool in distribution systems. The performance of impedance seen at number of buses as a monitoring technique is analyzed in presence of RES devices. Due to unbalance loading of distribution system, it will be shown that any proposed monitoring technique shall have the capability for separate three phases

24

monitoring. The speed and stability of proposed monitoring technique is tested by simulation of important generation fluctuation of connected PV system due to clouds movement.

This chapter is organized as follows: in Section 2.2 the basic theory of impedance method for monitoring of distribution feeder with RES will be established. Section 2.3 describes the IEEE 13 node test feeder used as a case study for simulation. Section 2.4 presents the simulation results of testing the proposed method for unit and non-unit power factor operation of PV inverter, fault conditions, load power factor variation and cloud movement.The practical capability of method is validated by analyzing the impact of cloud transients on IEEE 34 node test system. Finally the conclusion is presented in Section 2.6.

2.2 Measured Impedance Theory and Its Application on Reverse Power Flow Detection

2.2.1 Theory of impedance method

Distance relay, typically, is the first choice for transmission line protection. In recent years, it was also proposed as a protection device in distribution system (Shateri et Jamali, 2010),(Chilvers, Jenkins et Crossley, 2005). Distance relays use voltage and current as inputs and calculate the apparent impedance seen at the relay location. This value is a complex number which shows the apparent impedance seen by V/I calculation. A quadrilateral characteristic-distance relay is proposed in (Chilvers, Jenkins et Crossley, 2005) to distinguish the distribution feeder faults in presence of forward and reverse power flow due to DG integration. (Uthitsunthorn et Kulworawanichpong, 2010) proposes using distance relays for distribution feeder protection with renewable power plants to reduce protection coordination complexity due to impedance based setting of distance protection. Although this relay is geared at fast and accurate detection of faults in power system, it was shown that this method has a very good capability to measure and analyze the load conditions (Roberts, Guzman et Schweitzer III, 1993).

When the amount of active and reactive power injected or absorbed varies at distribution system nodes, the node voltage and line current will change. To clarify the effect of load variation and RES integration on apparent impedance seen at any distribution system node, let consider the simple system shown in Figure 2.1.
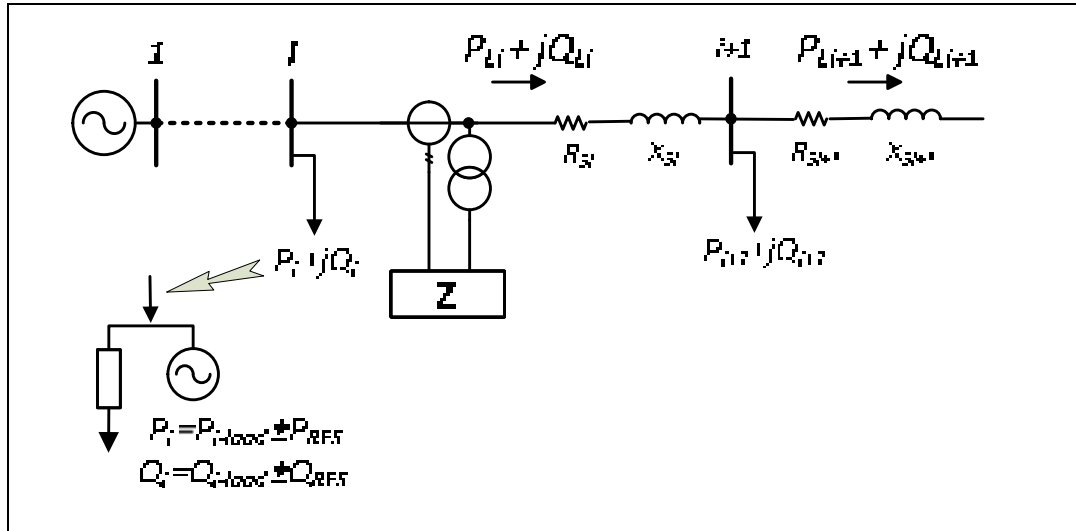
Figure 2.1 Simple system schematic, the impedance measuring unit
connected to sending-end of line connected to bus i

Consider that P_{Li} and Q_{Li} are the total active and reactive power (line power and losses) flowing down from node i, P_i and Q_i are the active and reactive power of load connected to node i, and $R_{si}+jX_{si}$ is the complex line impedance. Voltage drop (ΔV_i) along the feeder between nodes i and $i+1$; $\forall i=1,...,n$, is defined as:

$$\Delta V_i = V_i - V_{i+1} = Z_{si} \times I_i \tag{2.1}$$

$$I_i = \frac{P_{Li} - jQ_{Li}}{V_i^*} \tag{2.2}$$

$$\Delta V_i = (R_{si} + jX_{si}) \times \frac{P_{Li} - jQ_{Li}}{V_i^*} \tag{2.3}$$

$$\Delta V_i = \left[\frac{R_{si} \times P_{Li} + X_{si} \times Q_{Li}}{V_i^*}\right] + j\left[\frac{X_{si} \times P_{Li} - R_{si} \times Q_{Li}}{V_i^*}\right] \tag{2.4}$$

As shown in (2.4), the voltage drop along the feeder has real and imaginary parts. If the voltage of bus $i+1$ is considered as reference point, that $V_{i+1} = |V_{i+1}|\angle 0$ (this voltage is along the positive real axis), then from (2.1) and (2.4) the voltage at node i is obtained by (2.5).

$$V_i = V_{i+1} + \left[\frac{R_{si} \times P_{Li} + X_{si} \times Q_{Li}}{V_i^*}\right] + j \times \left[\frac{X_{si} \times P_{Li} - R_{si} \times Q_{Li}}{V_i^*}\right] \tag{2.5}$$

If the V_R and V_X are defined as (2.6) and (2.7), the voltage at node i can be rewritten as (2.8).

$$V_R = V_{i+1} + \left[\frac{R_{si} \times P_{Li} + X_{si} \times Q_{Li}}{V_i^*}\right] \tag{2.6}$$

$$V_X = \left[\frac{X_{si} \times P_{Li} - R_{si} \times Q_{Li}}{V_i^*}\right] \tag{2.7}$$

$$V_i = V_R + jV_X \tag{2.8}$$

To calculate apparent impedance seen from node i:

$$Z_i = \frac{V_i}{I_i} = \frac{V_R + jV_X}{\frac{P_{Li} - jQ_{Li}}{V_i^*}} \tag{2.9}$$

$$Z_i = V_i^* \times \frac{V_R + jV_X}{P_{Li}^2 + Q_{Li}^2} \times (P_{Li} + jQ_{Li}) \tag{2.10}$$

$$A = \frac{V_i^*}{P_{Li}^2 + Q_{Li}^2} \tag{2.11}$$

$$Z_i = A(V_R + jV_X) \times (P_{Li} + jQ_{Li}) \tag{2.12}$$

$$Z_i = A[(V_R P_{Li} - V_X Q_{Li}) + j(P_{Li} V_X + V_R Q_{Li})] \tag{2.13}$$

For node i, let P_{i-load} and Q_{i-load} be the active and reactive power of load, $P_{Li-loss}$ and $Q_{Li-loss}$ be the active and reactive losses of the line and P_{i-RES}, Q_{Di-RES} denote the active and reactive generation of RES at node i, respectively. If there is no RES connected to that node it is assumed that $P_{RES} = 0, Q_{RES} = 0$. Therefore, we can define the transmitted power through each line of the distribution network as follow:

$$P_{Li} = P_{Li-loss} + P_{(i+1)} + \sum_{i+1}^{n} P_{L(i+1)} \tag{2.14}$$

$$Q_{Li} = Q_{Li-loss} + Q_{(i+1)} + \sum_{i+1}^{n} Q_{L(i+1)} \tag{2.15}$$

$$P_i = P_{i-load} \pm P_{i-RES} \tag{2.16}$$

$$Q_i = Q_{i-load} \pm Q_{i-RES} \tag{2.17}$$

Then by substituting (2.14)-(2.17) in (2.13), it can also be expressed as:

$$Z_i = F(R_{si}, X_{si}, P_{Li}, Q_{Li}, P_{i-RES}, Q_{i-RES}) \tag{2.18}$$

From equation (2.18) it can be seen that the apparent impedance seen from node i is a function of line impedance, transmitted active and reactive power of line and the injected or

absorbed power at the node i and rest of the network. Therefore, the impedance seen at bus i can be used as a monitoring tool for analyzing the actual system situation.

2.2.2 Apparent impedance relationship with power flow direction

As it was stated earlier, voltage and current are two inputs of the method. The calculated positive sequence of voltage and currents are used for positive sequence impedance calculation. In this section, the relationship between the calculated impedance, magnitude and direction of active and reactive power flow through the line will be established.

Consider two consecutive buses i and $i+1$ in Figure 2.1, Z_i is the apparent impedance seen on the i side of the line between those two consecutive buses; P_{Li} and Q_{Li} are the active and reactive powers of the line flowing from side i to $i+1$, respectively; $|V_i|$ is the amplitude of the voltage at bus i.

Therefore the relationships between the measured R and X and the power transmitted through the lines are given below:

$$I_i = (\frac{S_i}{V_i})^* = (\frac{P_{Li} + jQ_{Li}}{V_i})^* \tag{2.19}$$

$$Z_i = \frac{V_i}{I_i} = \frac{V_R + jV_X}{(\frac{P_{Li} + jQ_{Li}}{V_i})^*} \tag{2.20}$$

$$Z_i = \left(\frac{P_{Li} + jQ_{Li}}{P_{Li}^2 + Q_{Li}^2}\right) \times |V_i|^2 \tag{2.21}$$

The real and the imaginary parts of the measured impedance shown in (21) are written as:

$$R_i = \left(\frac{P_{\text{L}i}}{P_{Li}^2 + Q_{Li}^2}\right) \times |V_i|^2 \tag{2.22}$$

$$X_i = \left(\frac{Q_{\text{L}i}}{P_{Li}^2 + Q_{Li}^2}\right) \times |V_i|^2 \tag{2.23}$$

As it can be seen from (2.22) and (2.23), the position of measured apparent impedance in R-X plane depends on the value and direction of active and reactive power. The apparent impedance measured at bus i has reverse relationship with power. The larger the power transferred through the line, the smaller measured R and X.

The sign of R_i in (2.22) and X_i in (2.23) are only related to the sign (direction) of P_{Li} and Q_{Li}, respectively. Then according to (2.14) and (2.15):

$$If \; |P_{i-RES}| > |P_{L(i+1)} + P_{i-load}| \xrightarrow{yields} P_{Li} < 0 \tag{2.24}$$

$$If \; |Q_{i-RES}| \geq |Q_{L(i+1)} + Q_{i-load}| \xrightarrow{yields} Q_{Li} < 0 \tag{2.25}$$

Equations (2.24) and (2.25) show the conditions that the RES generation exceeds the consumption and the final location of the impedance seen at bus i on R-X plane will be at third quarter. For forward Q and reversed P the impedance location will be at the second part of R-X plane.

Based on the direction of active and reactive power flow the R-X diagram can be divided into four parts, Figure 2.2 shows the mapping of power flow direction on R-X diagram. Based on this figure, the impedance located on R axis represented a unity power factor and for X axis the power factor is zero. For the directions of active and reactive power are from node i to $i+1$, the measured impedance will be located at the first quarter of R-X plane.
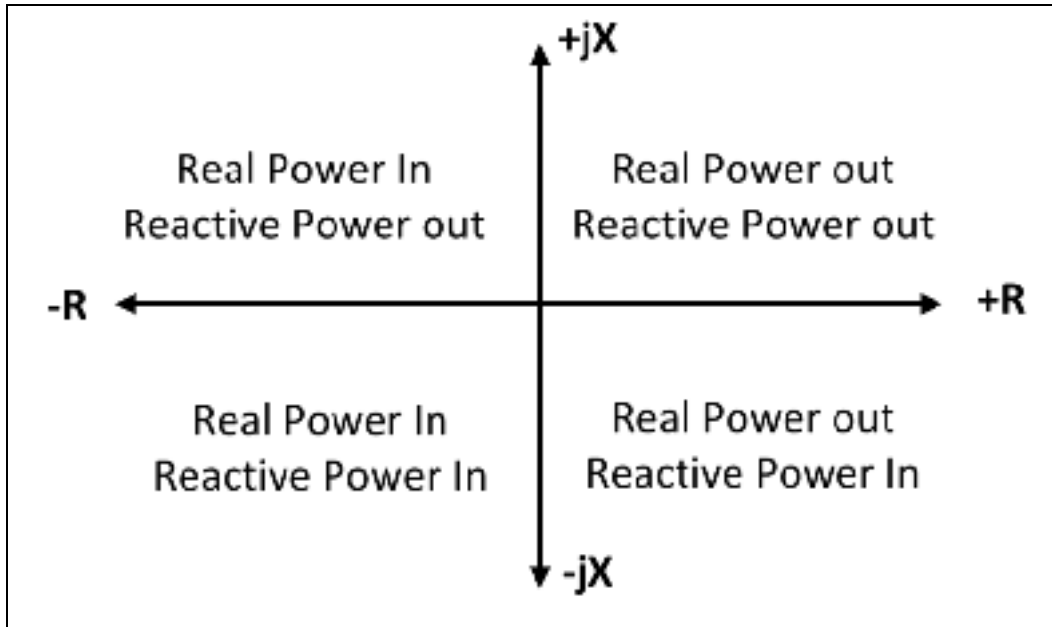
Figure 2.2 Mapping of Power Flow Direction on R-X Diagram
Adapted from Mason (1956)

2.2.3 Impedance measurement

Distance relay is the best tools for impedance measurement in power system. Because the positive sequence component is the only common sequence component in all the types of faults, the measured impedance at distance protection relays are always based on the phase positive sequence impedance. Moreover, the apparent impedance measured by a distance relay will depend on the current and voltage transformers connections too.

The measured impedance is calculated by three one-phase measuring units. The simplest ground distance functions use only a single phase current and a single phase voltage. Consider that V_{AN} is the phase A to ground voltage and I_A is the current flows through the phase A conductor, the apparent impedance seen for phase A is given by (Hase, 2007):

$$Z_A = \frac{V_A}{I_A} \qquad (2.26)$$

The impedance calculated using (2.26) is the positive sequence impedance seen of the line for all system operation condition except fault conditions. Phase-ground distance relay usually employs a zero sequence current compensator for actual system impedance measurement during the fault conditions. Based on (Shateri et Jamali, 2009), all the phase-ground faults detection units measure the same impedance value for the non-fault conditions.

2.3   Case Study

The IEEE 13 Node Test Feeder (Figure 2. 3) is a very small but relatively highly loaded 4.16 kV feeders. This provides a good test for the most common features of distribution analysis software (Kersting, 2012). As this model has unbalanced spot and distributed load, overhead lines and cables, shunt capacitors and a voltage regulator consisting of three single-phase units, it is a good case for testing the impedance method capabilities. The simulations have been performed by OpenDSS (Dugan, 2012) software and Matlab (Guide, 1998). The OpenDSS COM server interfaced with the Matlab program is used for simulation.

Wind, photovoltaic, and biomass are the best choices for RES integration to power system. For large scale power production at transmission level the biomass system and wind turbine are the most obvious solutions. On the other hand, small-scale PV system is more attractive solution for residential installation. For RES integration to distribution system simulation, the PV system is chosen.

This research used the built-in PV system model provided in OpenDSS. Among two options for modeling high penetration of small-scale rooftop PV or large centralized PV, the second one was chosen for the simulation of impedance based monitoring system. Hence to produce various scenarios for simulations, the lumped three phases balanced PV model was added at three different locations, one close to substation source Bus 632, one near the feeder midpoint Bus 671 and one at the end of feeder at Bus 680. For showing the effect of PV location on the proposed monitoring technique at each simulation only one location was used for PV installation.
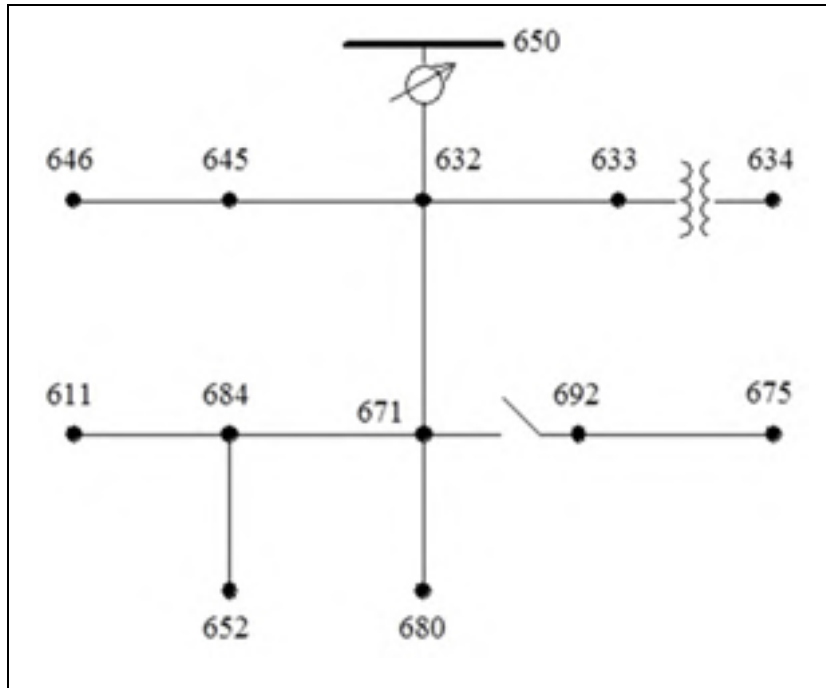
Figure 2.3 Schematic of the IEEE 13 Node Test Feeder

For simulation of different penetration level (PL), Hoke et al (Hoke et al., 2013) showed that the 15% limit for PL as a rule of thumb for most of feeders is very conservative. They showed that in two-thirds of simulated cases, the maximum PL is greater than 90%. In this research, to analyze the full capability of the monitoring technique, the PV output was increased from zero to 1.15 pu of model total load (P=3800 KW) with step size of 0.01 (115 different penetration levels). At each step, a power flow was done by OpenDSS and all voltages, currents, active and reactive power of feeder were saved. In this chapter, except the under-voltage and over-voltage limits, other limiting factors such as feeders current rating, the substation transformer capacity, power quality issues were neglected. The simulation has been performed for both unit and non-unit power factor PV operation. As the original model of IEEE 13 node test feeder does not have a load at bus 680 a 360kW and 270 kVAr load connected to this bus for simulation. A 3-phases 60 kVAr capacitor installed at Bus 680 for voltage regulation.

2.4   Simulation Result and Discussion

2.4.1   Impact of PV penetration Level on measured impedance

To show the impact of PV penetration level (*PL*) the lumped model of PV is connected to bus 680. Figure 2.4 shows the active power flows through feeder 650-632 and bus 632 voltage profile. As it can be seen, by increasing *PL* the active power flow from the source to grid decreases and the voltage increases. It is obvious that by increasing the *PL* the voltage increases, so the tap changer located between bus 650 and bus 632 operates two times to keep the voltage within the standard boundaries.
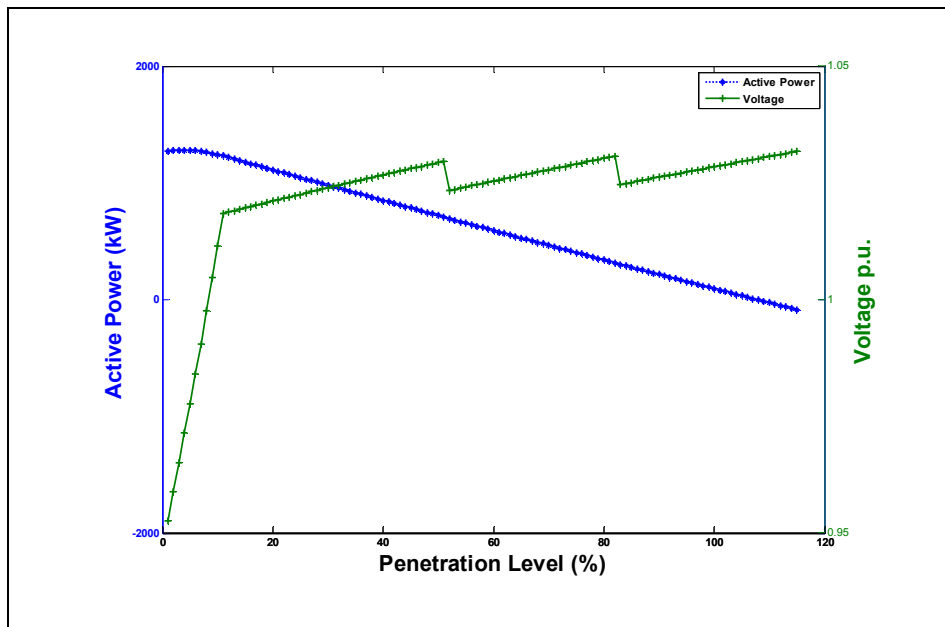
Figure 2.4 Active power flows through feeder 650-632 and Bus 632
voltage profile with active tap changer and PV is connected to bus 680
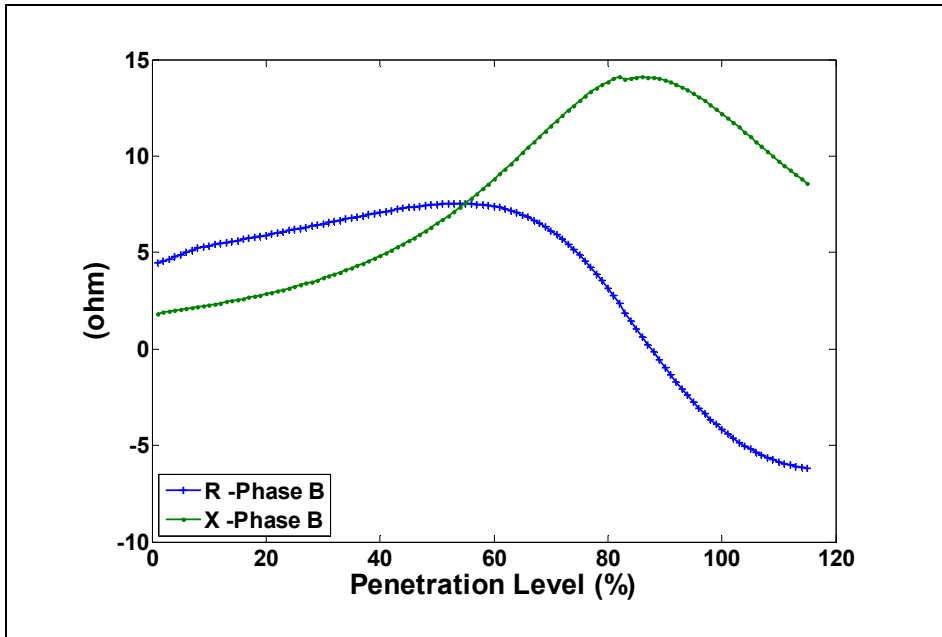
Figure 2.5 Measured R and X vs penetration level at bus 632-phase B
with active tap changer

Figure 2.5 shows the measured R and X for different PLs at bus 632. As it can be seen by increasing PL, the R and X increase till PL=0.58 but after this point although X increases the R decreases. At PL=88% the R becomes zero and after this point the R goes negative corresponding the reversed active power. The reason for the decreasing R is related to the relationship between the measured R and total P and Q flows along the line. Based on equation (2.22) by decreasing the P -due to the increased PV penetration level- the measured R will decrease too.

As it can be seen from Figures 2.4 and 2.5, at the time of tap changing the measured impedance shows a little change. This illustrates that the proposed method is sensitive to small variations of voltage in the system.

Unlike at bus 632, the measured impedance at bus 680 has a different trend. As it can be seen from Figure 2.6 the measured R and X increases by increasing PV penetration level, but, when the active power direction is reversed, the value of R decreases and becomes negative.

This shows that we have reverse active power while the reactive power direction does not change (because the PV only operates at unity power factor). These graphs support the basic theory of proposed method described in part 2.1.2.
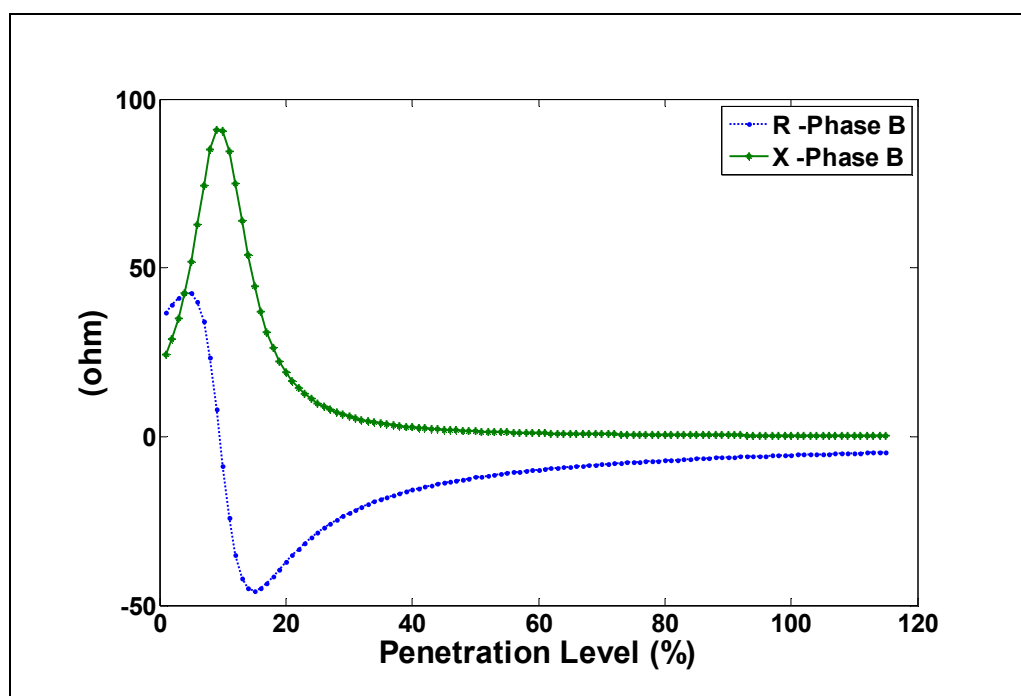
Figure 2.6 Measured R and X vs Penetration Level at bus 680

Figure 2.7 shows the measured impedance plotted on R-X plane three buses for PV connected at bus 680 and PL variation between 0 to 115% of nominal load.

Figure 2.7 shows the measured impedance loci of different measurement units. Figure 2.7-a shows that by increasing *PL* of PV system the reversed active power occurs at PL=108% at bus 632. Meanwhile at bus 671 (Figure 2.7-b) this occurs at PL=93%. In addition for bus 680 (Figure 2.7-c) the reversed active power starts at *PL*=9%.

Figure 2.7 shows that, depending on measurement unit location and PV equipment location, the value and trend of measured impedance has a unique and detectable characteristic. Based on Eq. (2.20), for any type of energized feeder with the voltage and current data available,

the proposed monitoring technique can be used. As stated earlier, the apparent impedance measured at any bus has a direct relationship with PL and reverse with transferred power. The larger the power transferred through the line (equal to low *PL*), the smaller measured R and X and vice versa. For example at bus 632, for PL varying from 20% (equal to high load) to 80% (equal to light load), the impedance locations varies from point (5.904, 2.955) to (3.16, 13.85) on R-X plane.

37

a- Measured impedance at Bus 632- Phase A

b- Measured impedance at Bus 671- Phase A

c- Measured impedance at Bus 680- Phase A
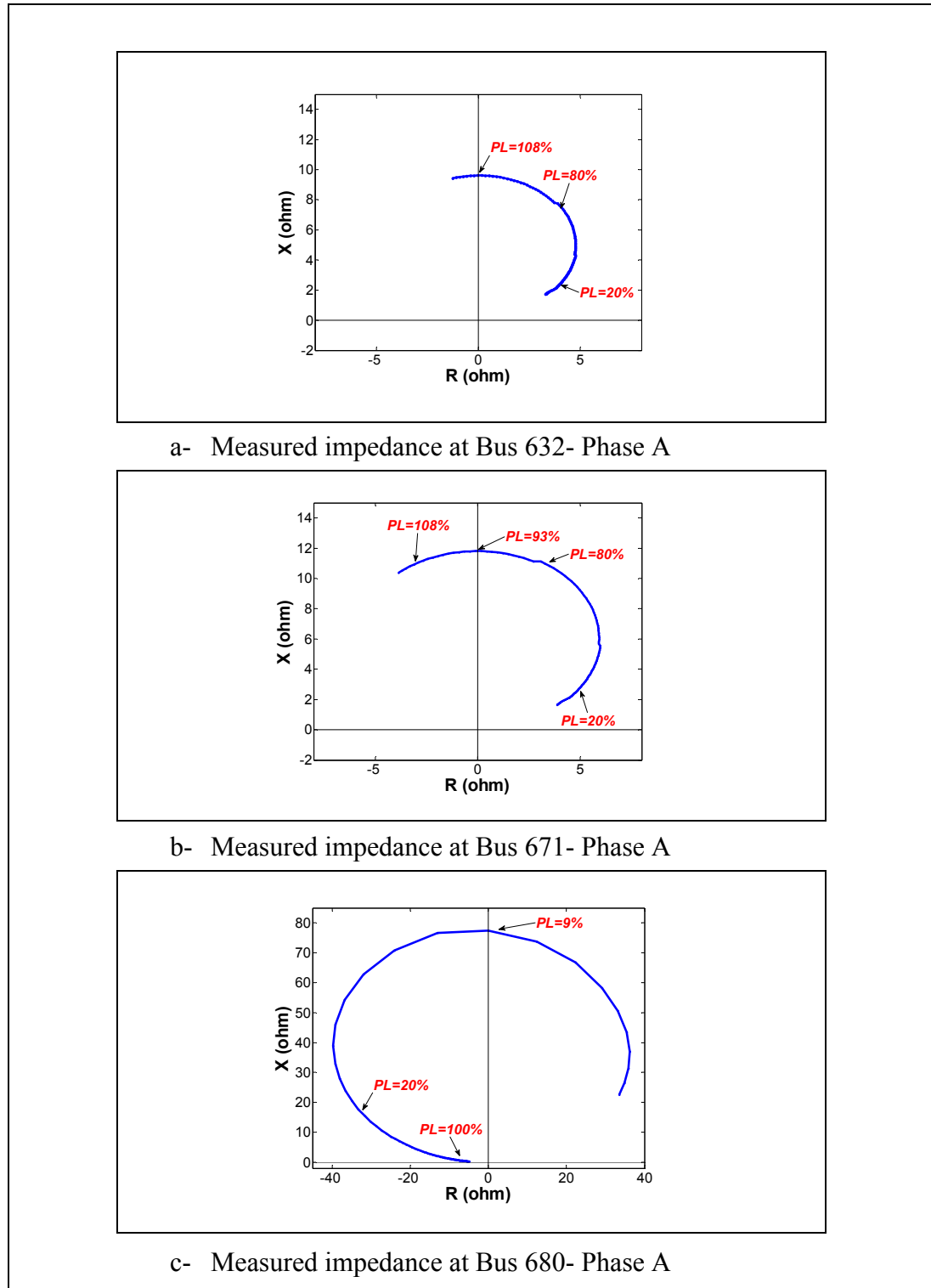
Figure 2.7 Measured impedance at Bus 632, 671 and 680 for PV installed at
bus 680 and penetration level varies from zero to 115%

2.4.2   Impedance variation due to normal load deviation

Continuous load variation is the intrinsic characteristic of distribution system. In the previous section, it was shown that the apparent impedance seen by measuring devices has a distinctive changes due to different PV penetration levels. Figure 2.8 illustrate the typical normalized load patterns applied to the test feeder.
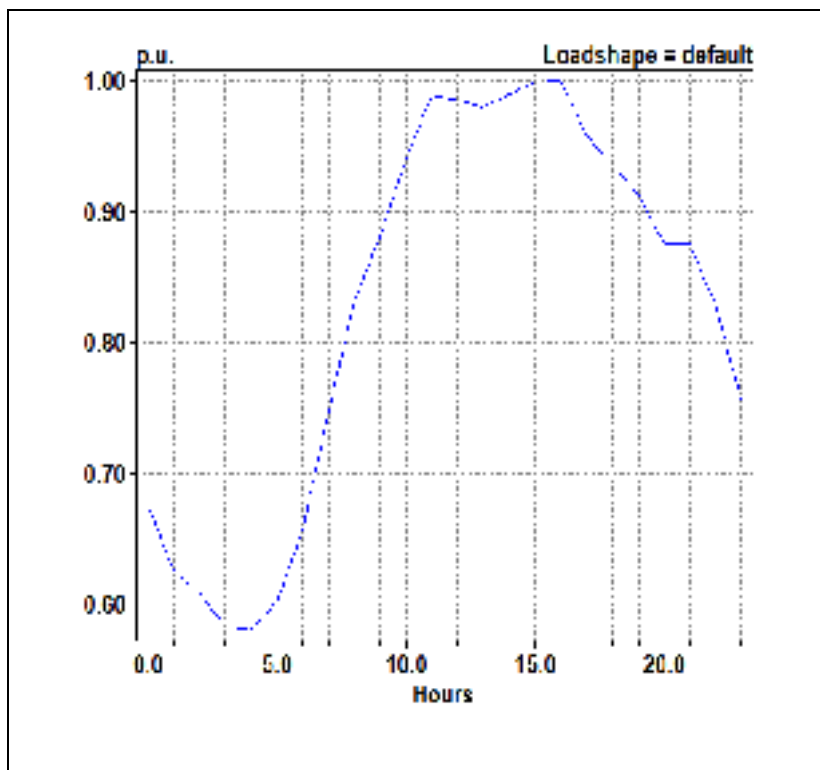
Figure 2.8 The normalized load patterns of residential loads

Figure 2.9 shows the measured impedance trajectories for daily load variation. It is found that the small variation of load shows its impact on the measured impedance. For Example, the measured impedance for phase A changes from 6.785+j2.463 ohm at the lightest load condition (58% of nominal load) to 3.484+j1.782 ohm for the maximum daily load. The difference between the measured impedances are due to the unbalanced loading of distribution system.
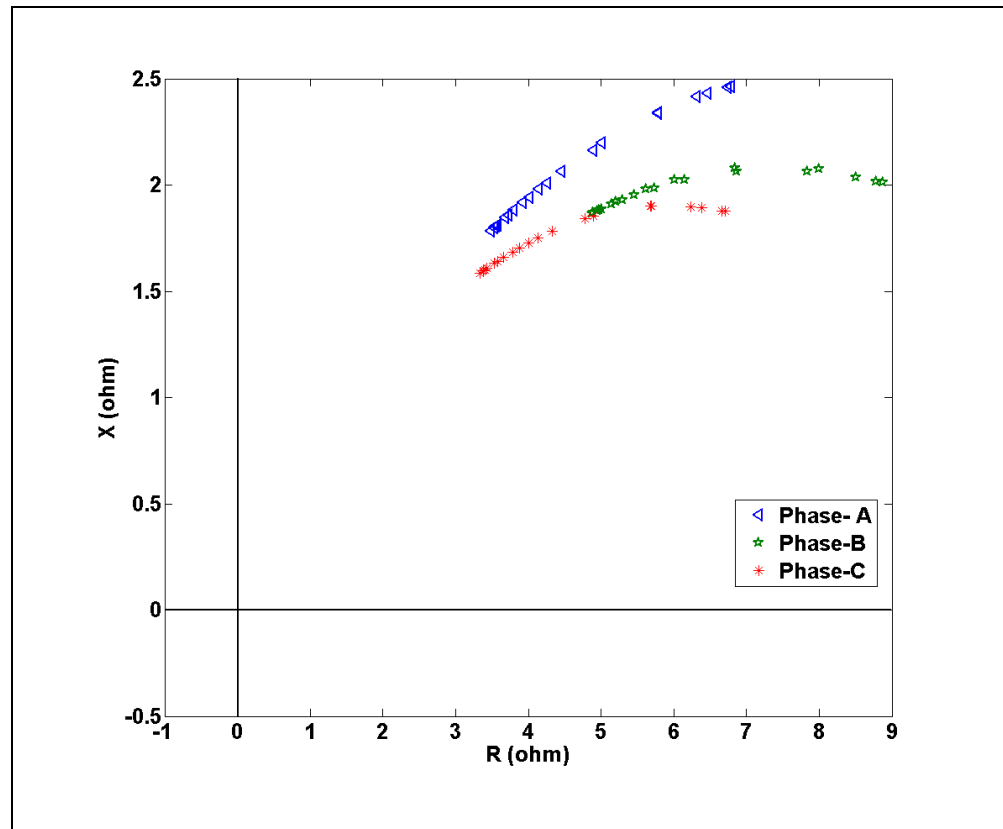
Figure 2.9 Three-Phases measured impedance at Bus 632 for
normal load variation condition

2.4.3   Analyzing the impact of unbalanced distribution system on the measured impedance

Unbalance operation is an intrinsic characteristic of distribution system. It is anticipated that when the voltage and current of the three phases are unbalanced, the resultant measured impedance for each phase is not the same as in the other phases.

For a PV device installed at bus 680 Figure 2.10 shows the loci of measured impedance for each phase at bus 632. It is worth mentioning that reversed power starts at different PL for each phase. While the impedance location for the phase A and C enters the second quarter of R-X plane (for PL=108% and 111% respectively) showing small reversed active power, at the same PL, phase B shows a higher reversed active power. This phenomenon is due to the

unbalanced operation of IEEE 13 node test feeder. It is concluded that for distribution system, any proposed technique shall be capable to monitor each phase separately.

Due to the three phase balanced loads installed at bus 680, it is anticipated that the measured impedance in each phase shall show the same trend. Figure 2.11 shows the impedance trends at bus 680. Although the reversed power occurs at the same PL=9%, the loci of measured impedance are not the same in each phase. Because the feeder 671-680 is fed with unbalanced voltages at bus 671, small differences can be seen on the three phases impedance loci at bus 680.
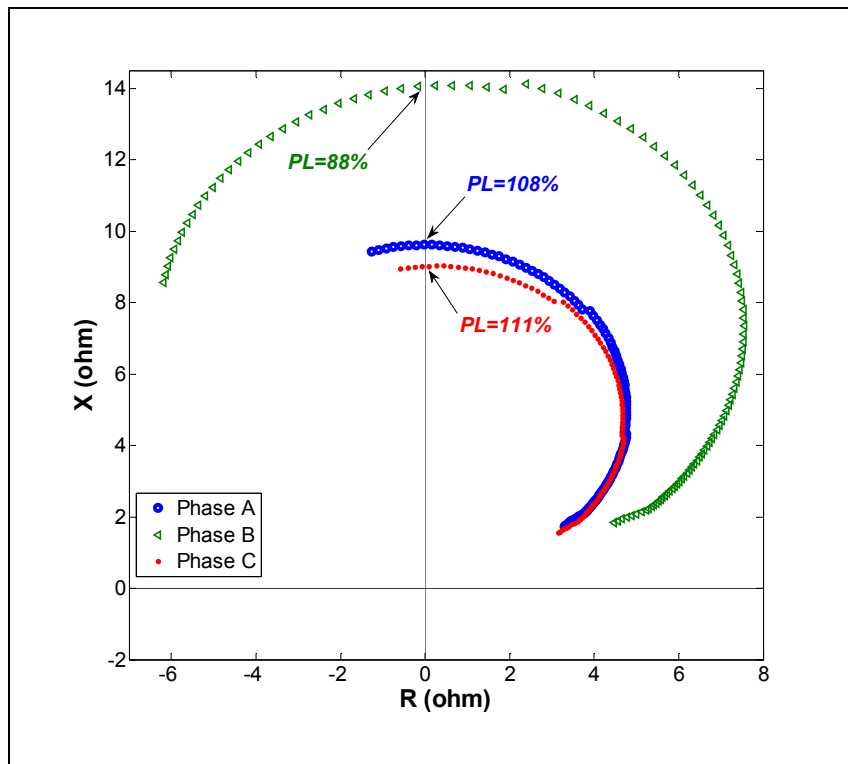
Figure 2.10 Three-Phases measured impedance at Bus 632

Figure 2.12 shows the phase-B impedance trends for the same condition except for the location of PV system which connected to the bus 671. It can be clearly seen that while the

impedance seen from buses 671 and 632 varies a lot with PL variation, the impedance seen from bus 680 contains a small variation due to bus 680 voltage changes.
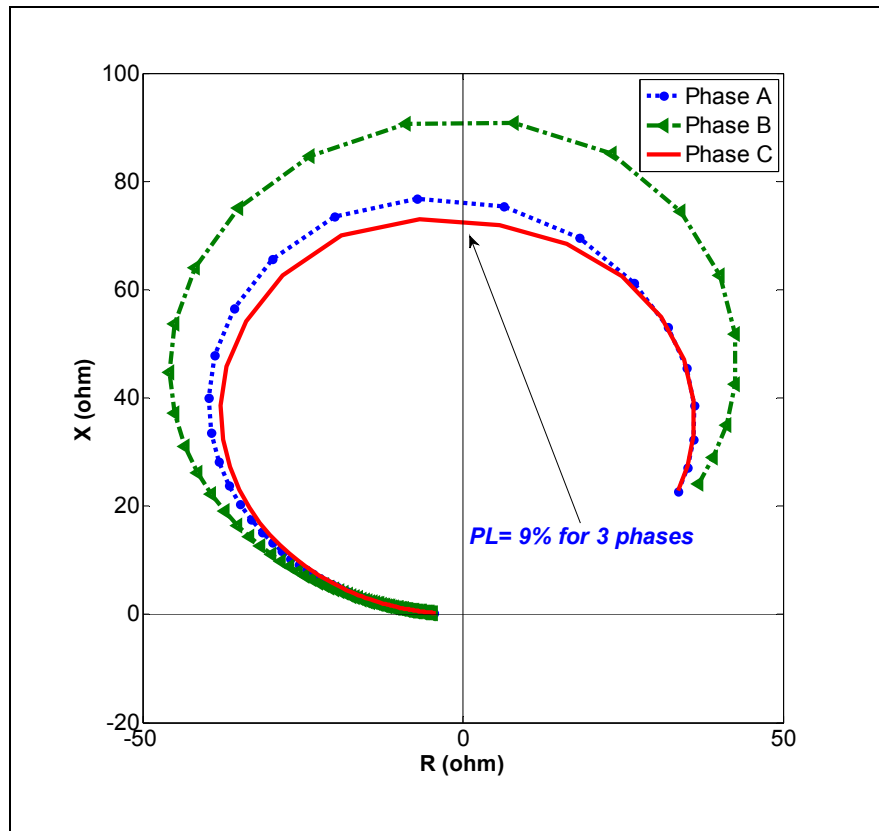
Figure 2.11 Unbalanced voltage effects on 3-Phases
measured impedance at bus 680

Figures 2.10, 2.11 and 2.12 show that the measured impedance has clear reaction for downstream various PV penetrations. Meanwhile, its reaction to upstream PV variation is limited to feeder voltage deviation.
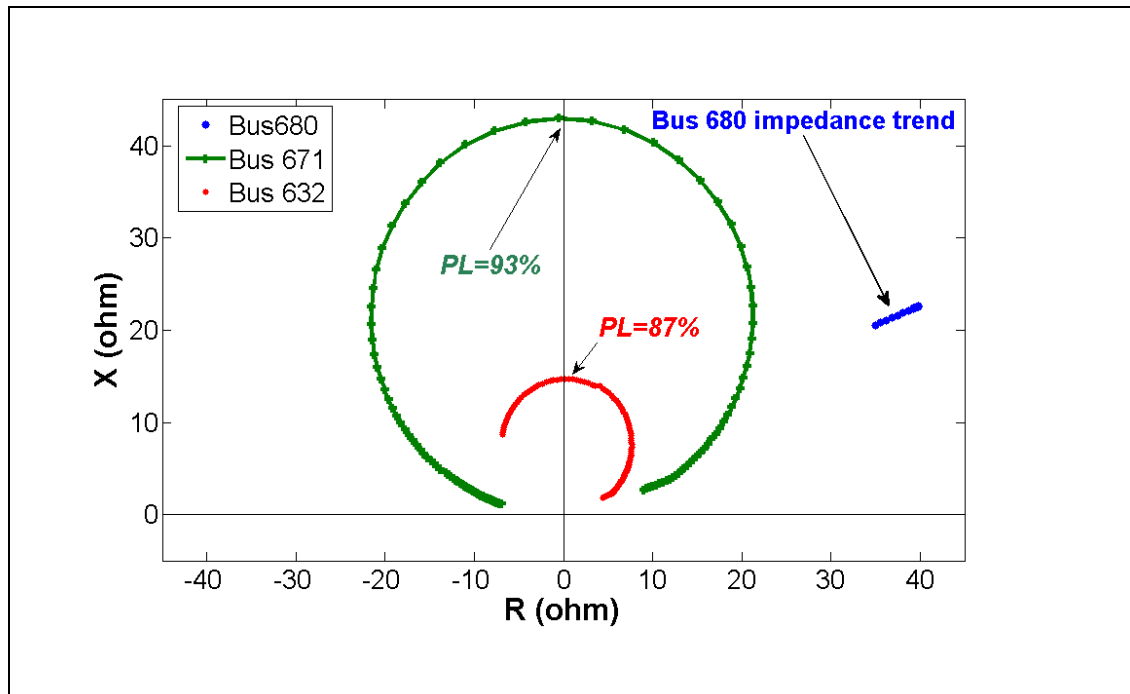
Figure 2.12 Measured impedance at Bus 632, 671 and 680 for PV installed at Bus 671

2.4.4   Impact of load power factor variation

Distribution system loads profiles vary from line to line. The load power factor (pf) varies in accordance with active and reactive power consumed by the load. Figure 2.13 shows the effect of load power factor variation on the measured impedance. For simulation, the same condition of Figure 2. 7 (lumped PV connected to bus 680) is used, except that the power factor of load connected to bus 671 (the biggest load in the test model) is changing form the lagging 0.8684 to unity power factor and then to a 0.8684 leading one. As it was expected for each pf, the impedance trend varies. For unit pf, the reversed active power happens at bigger PL due to increased load active power. On the other hand, for pf=-0.8684, although the reversed active power happened at the same condition of positive pf=0.8684 but the impedance trend moves further against the origin. This happens because the negative pf means the VAr generation. Based on the Eq. (20), any power generation along the line will

decrease the line current, resulting the bigger impedance (any generation connected to line, acts as light load situation).
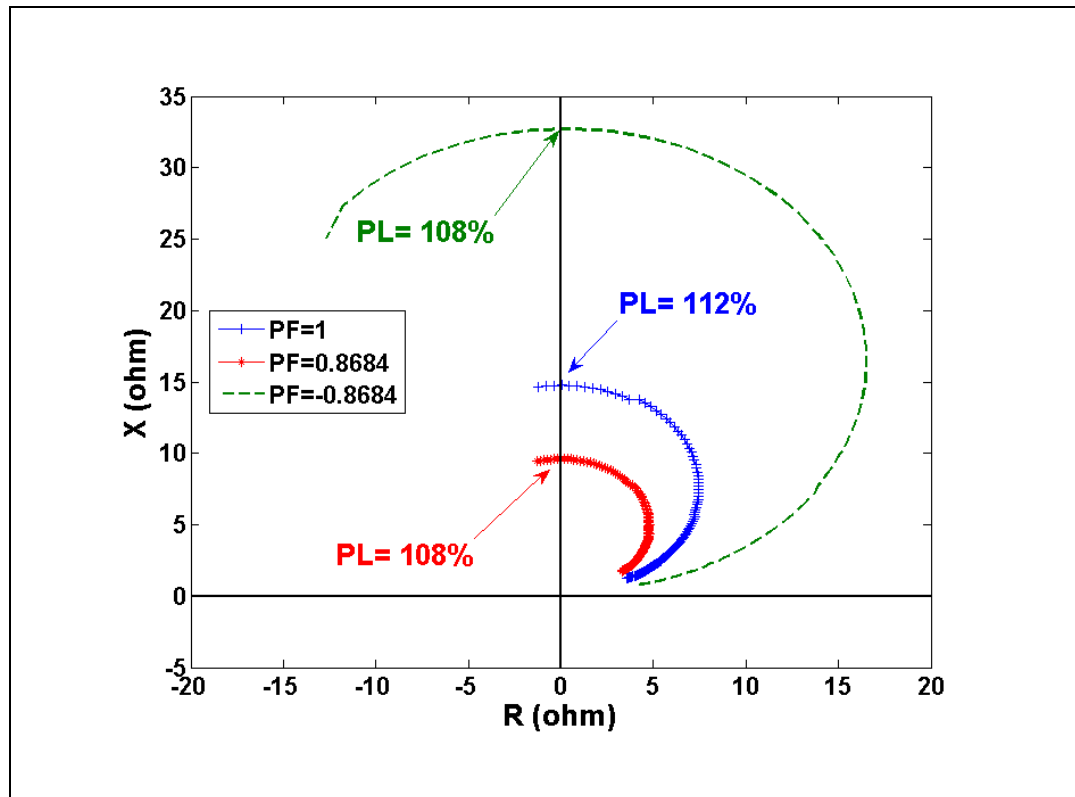
Figure 2.13 Measured impedance at bus 632- Phase A,
for three different load pfs connected to bus 671

2.4.5   Impact of non-unit power factor operation of PV inverter

As it was stated earlier, some DG connection standards such as IEEE 1547 forbid the non-unit power factor operation of distributed generation. Some publications (Vahedi et al., 2013) consider the advantages of using RES inverter capability for voltage support. To analyze the impact of non-unit pf operation of PVs, three situations are simulated with inverter capable to operate at pf=1, 0.95 and 0.9. For example at pf=0.9 with the same size inverter, the maximum active power produced by PV units is limited to 90% of nominal power but at the

same time the system has the capability to produce reactive power around 43% of nominal power to support voltage profile. For this simulation, the PV inverter size does not change. For PV installed at bus 680 and penetration level variation from zero to 115%, Figure 2.14 shows the impact of PV inverter power factor variation on the apparent measured impedance trend. For simplicity, the results of phase A of bus 632 are only shown. It is anticipated that by non-unit operation of PV system and with reactive power generation, some feeders experience not only reverse active power but also reverse reactive power too. As shown in Figure 2.14, by decreasing the pf from 1 to 0.95 (with the same inverter size) the reversed active power happened at bigger PL. For pf=0.90, due to the reactive power generation of PV inverter the impedance trend moves from region 1 to 4 at PL=102% (shows the reversed reactive power with forward active power) and then finally enters to third region at the PL=110%.
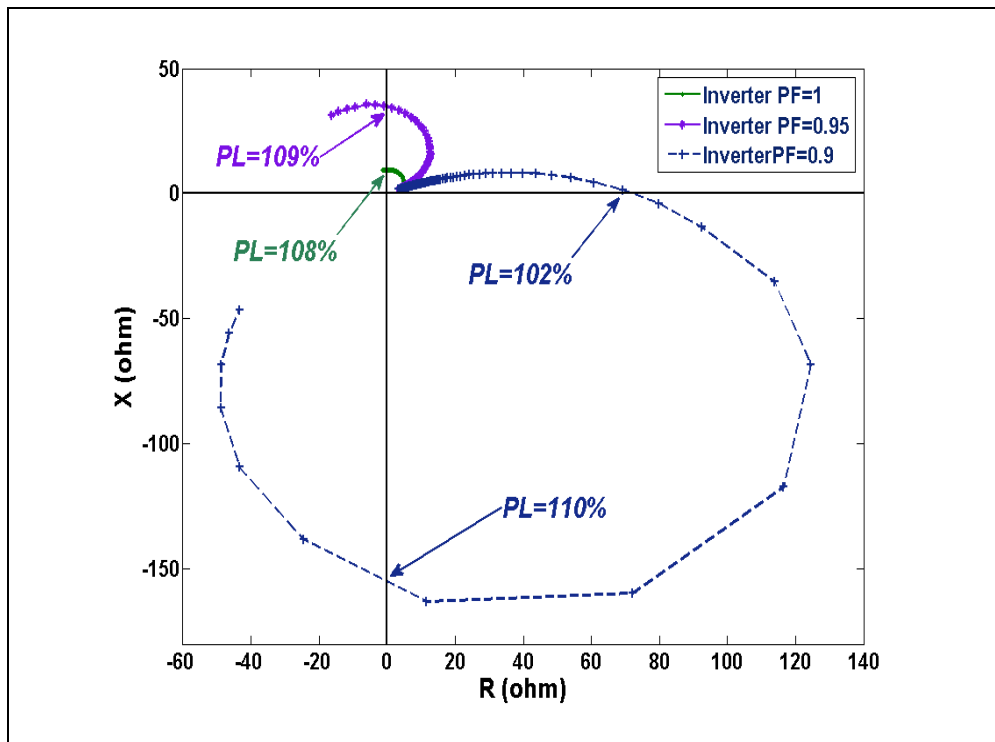
Figure 2.14 Measured impedance at bus 632-phase A for
three different PV inverter output power factors

2.4.6   Investigating the measured impedance trends during fault

RES integration to distribution feeder will change the feeder fault current. Depend on the size and location of RES, the contribution of this generation to fault current varies (*Requirements for the Interconnection of Distributed Generation to the Hydro-Québec Medium-Voltage Distribution System (between 750 V to 44000 V), Hydro-Québec Std, no:E.12-01,2004*). At this condition, non-directional over-current protections will operates for reverse faults, upstream of the protected zone. Therefore some utilities (*Requirements for the Interconnection of Distributed Generation to the Hydro-Québec Medium-Voltage Distribution System (between 750 V to 44000 V), Hydro-Québec Std, no:E.12-01,2004*) (*Distributed Generation Technical Interconnection Requirements - Interconnections at Voltages 50kv And Below, Hydro One Networks Inc Std, no: DT-10-015, Rev. 3, 2013*), at their interconnection standard of DG to distribution system, recommend to install a distance relay. For example, Hydro- Quebec does not accept over current relay as the main protection and recommend to install a distance relay for conditions such as: outage of one of DG installed in the feeder, intermittent DG generation characteristic and etc.

In this section the impact of fault on the feeder is investigated on the measured impedance trend. In normal operation of feeder, the measured apparent impedance is the combination of the feeder impedance and the equivalent impedance of total connected loads. Considering the compensation impact of capacitor bank on feeder power factor, the load impedance normally is very close to real axis. During the fault condition, the measured impedance has a significant decrease (for example at phase A, from $(3.966+j7.12)$ Ω to $(0.08+j0.2)$ Ω) and it moves toward the origin. The final location of the measured impedance is determined by the type of fault and the fault impedance. The value of the apparent impedance during the fault is very close to the actual impedance of feeder between the measuring point and fault point plus the fault impedance.

Figure 2.15 shows the trend of measured impedance at bus 632 for a three phases to ground short circuit occurred at bus 671. A non-directional impedance relay is defined with the 80%

of line 632-671 impedance as setting. This protection is shown by red circle in Figure 2.15. A thorough investigation shows that the measured fault impedance value is settled down in the defined protection zone.
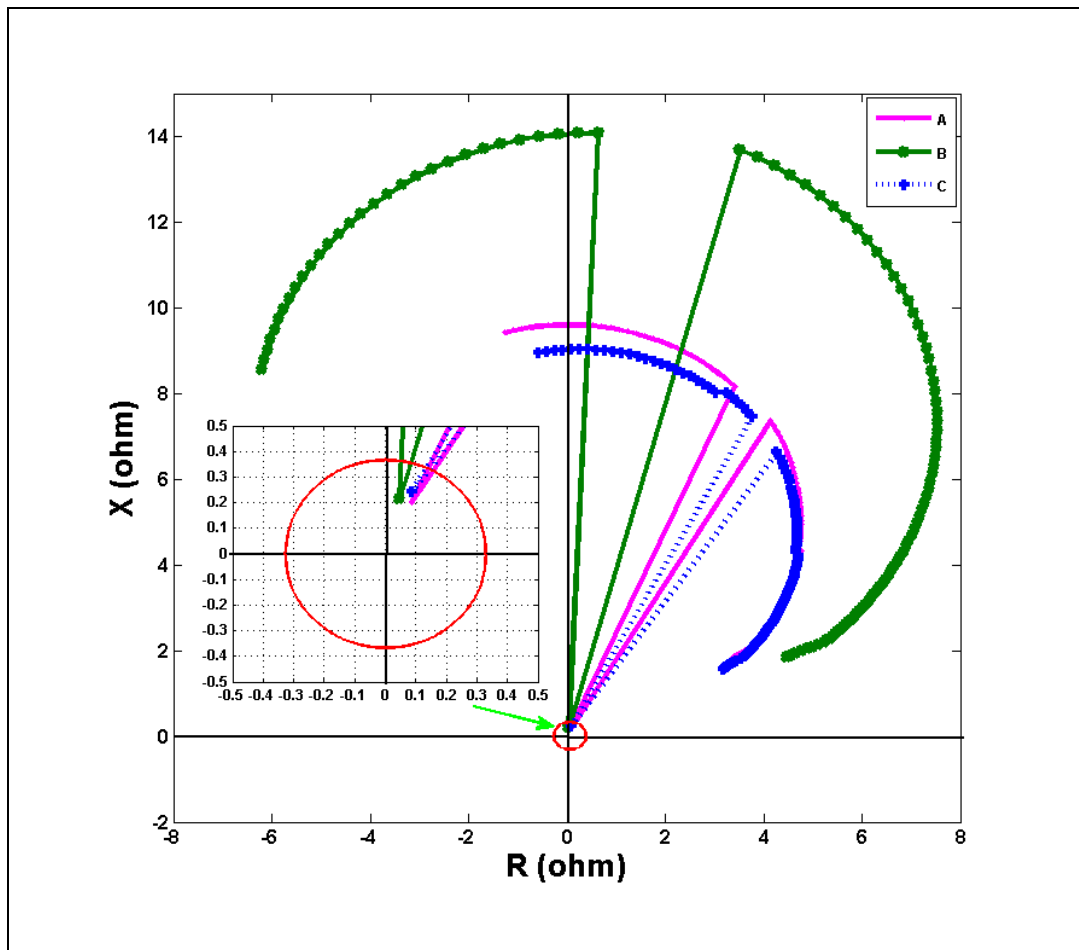
Figure 2.15 Measured impedance at bus 632 for 3phase to ground fault at bus 671. The small red circle is a non-directional impedance relay

Furthermore to substantial decreases of impedance during the fault, by increasing the PL of RES, the resultant impedance will be increased. Considering the Eq. (2.9), by increasing the RES penetration, the current flow through the line decreases and the measured impedance will be increased. According to the distance relay literature and the result of this section, it is shown that the fault zone is completely different than normal operation of measured impedance.

2.4.7 Analyzing the capability of proposed method for fast transients

Normally distribution system loads are unbalanced and time varying (Kersting, 2012). By integration of RES like wind and solar, the distribution system faces intermittent and fast transients like in distributed generation.

For PV systems, the solar irradiation energy varies slowly over time from sun rise to sunset with a pre-known patterns correlated with the longitude and latitude of installation site. The faster transient involved with solar generation is related to cloud movements. The PV system generation fluctuation is a function of many factors. The centralized or distributed PV system, the total installed capacity, local weather pattern and the PV panel type are the major factors which determine the transient characteristic of PV system output (Dugan et McDermott, 2011).

The cloud movement causes a fast transient on PV generation, and is one of the biggest challenges for increasing the PV installation. Basically after a cloud movement over the installation site, the PV generation decreases dramatically. Afterward a solar ramp will increase the output of PV system. For distributed rooftop PV, these types of transients have less challenge for distribution system operation due to the little possibilities of simultaneous ramp up and down of all PV units. The PV plant size, its layout, wind speed and cloud movement direction are dominant factors affecting the generation and consequently the feeder voltage profile (Dugan et McDermott, 2011). In other hand, for PV farm where all the PV panels are installed in a small area, the impact of cloud transients is substantial on operation and control of distribution system (Godfrey et al., 2010).

In this part of the chapter, the impedance method capability will be analyzed by fast transient of cloud movement. Figure 2.16 shows the 2900 seconds simulation of cloud movement on PV system generation (Dugan et McDermott, 2011). The time interval between each sample is one second. As it was stated earlier, among two options of modeling high penetration of small-scale distributed rooftop PV or large centralized PV, the second one was chosen for the

simulation of impedance based monitoring system. Therefore, due to smaller installation area of centralized PV system, the cloud movement transient impact will be severe.
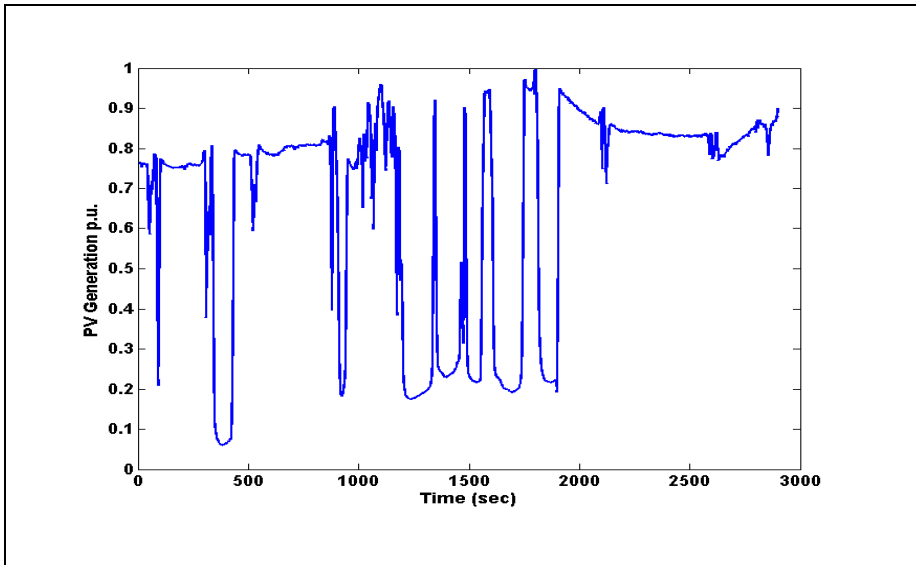
Figure 2.16 Cloud transients impact on PV output
Adapted from Dugan and McDermott (2011)
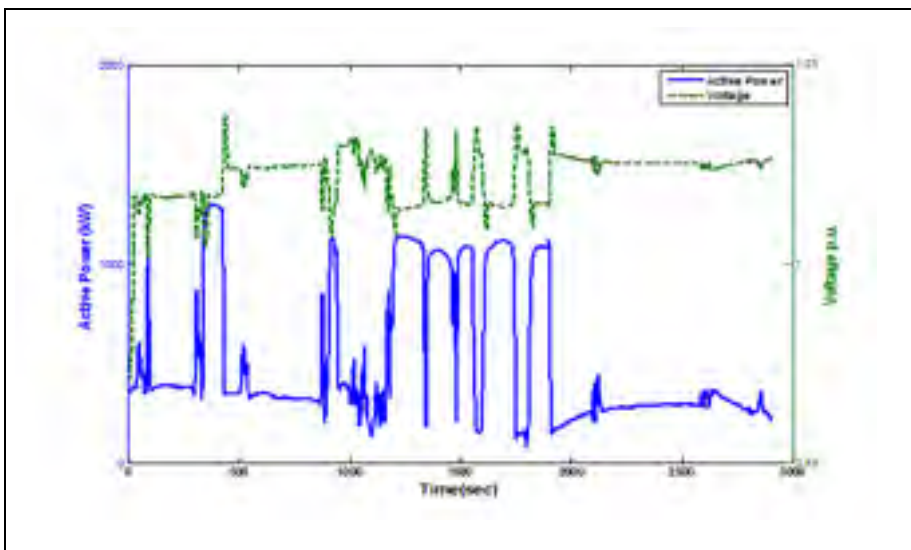
Figure 2.17 The Voltage and active power variation at bus 632
for PV installed at bus 680 while cloud passing transients

For the PV system installed at bus 680, Figure 2.17 shows the impact of cloud transients on the active power and voltage of bus 632 (connected to the substation bus). In some cases the PV system output ramp down from 1 p.u. to 0.4 p.u. in less than 15 seconds (for example check between 1800 to 1820 seconds at Figure 2.16).

In comparison with Figure 2.4, these fast transients cause high fluctuation in power flow and consequently high operation of tap changers. Due to the time constant of tap changer operation, the consumer electric devices experience some short term low voltage (when the cloud blocks the sun) and over-voltage (when the cloud passes away). Figures 2.18 and 2.19 show the impact of cloud movement transients on measured R and X at bus 632. As it can be seen the impedance method can react to fast transients in distribution system operation due to its simplicity of calculations.

Figure 2.20 shows the measured impedance at bus 632 on the three phases for the cloud transients. Although the high spatial diversity of R and X associated cloud movement, the mapped R and X on the impedance plane shows a special and detectable trend for each phase. In next section it will be shown that by defining different operation area on the R-X plane this monitoring technique can be used as a practical tool for better operation of distribution system.

2.5   A practical application of impedance method

To show a practical application of the impedance based monitoring system, the IEEE 34 Node Test Feeder is chosen. This test feeder is an actual feeder located in Arizona(Kersting, 2012)-(Christakou et al., 2013). This unbalanced feeder has both spot and distributed load. For PV integration nine distributed 200 kW PV units are connected to feeder in different locations as shown in Figure 2.21. Four impedance measuring units are connected to buses 802, 816, 852 and 834. The location and direction of measuring units are shown in the Figure 2.21 by the red arrow.

Considering the worst case operation of PV units, the cloud movement pattern shown in Figure 2.16 is used as the PV unit sun irradiation input. Figure 2.22 shows the apparent impedance trend measured at those four locations in response to the cloud movement. For simplicity, only the phase-measured impedances are shown. While the impedance trend shows the reversed active power for bus 852, the bus 834 shows the reversed active and reactive power. This phenomena happens due to the two capacitors installed at the buses 848 (450 kVAr) and 844 (300 kVAr).

However, considering the speed and the type of events, some rules and alarm settings can be defined in the impedance-based method to send alarms or actions to the distribution system operator or to controlling devices installed at distribution system. For example, in some utilities it is forbidden for distribution system to feed the transmission system. To implement this limitation, a flag was defined in the monitoring system to generate an alarm. For normal operation the flag is zero and for reversed power detection at the measuring point the flag changes from zero to one and an alarm is issued.
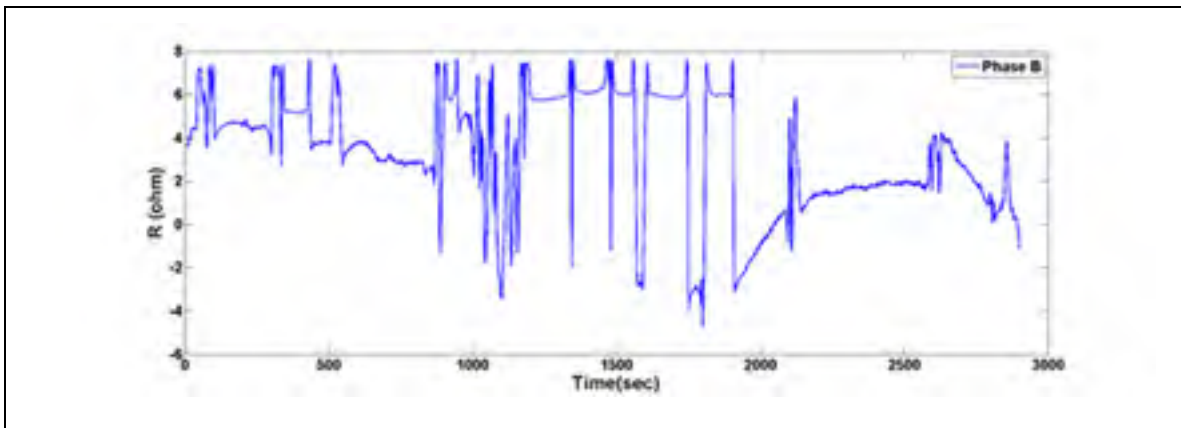
Figure 2.18 Cloud transients impact on measured R at bus 632
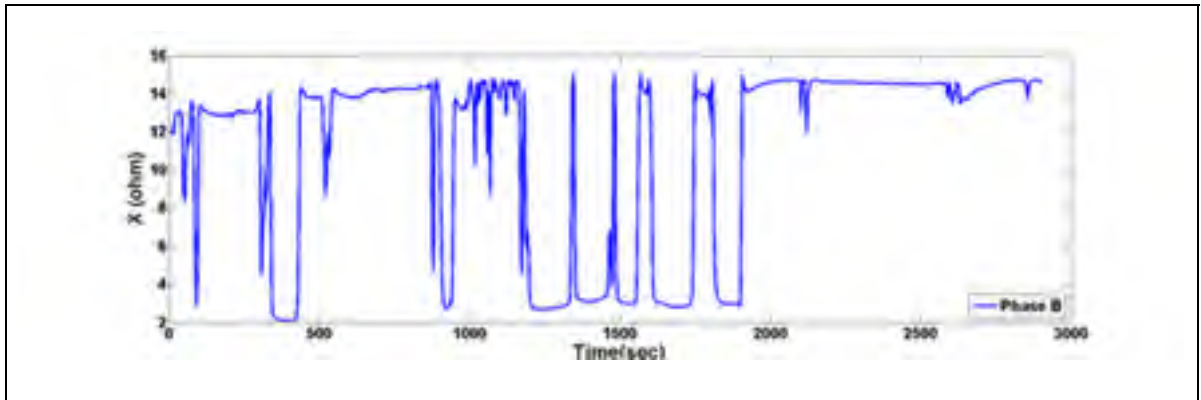
Figure 2.19 Cloud transients impact on measured X at bus 632
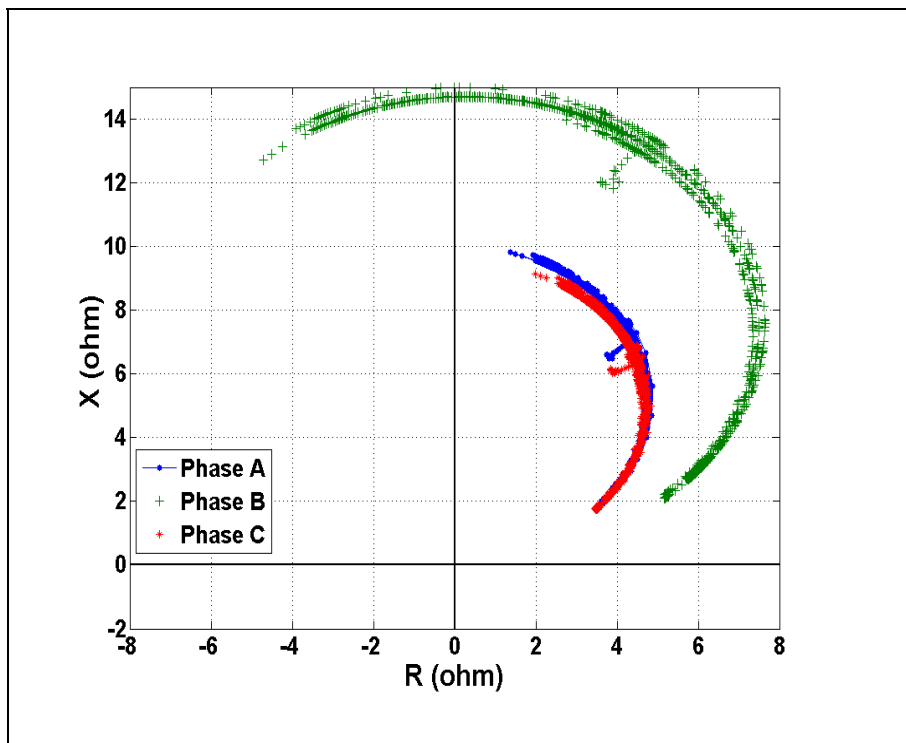
Figure 2.20 Cloud transients impact on measured impedance at Bus 632

52
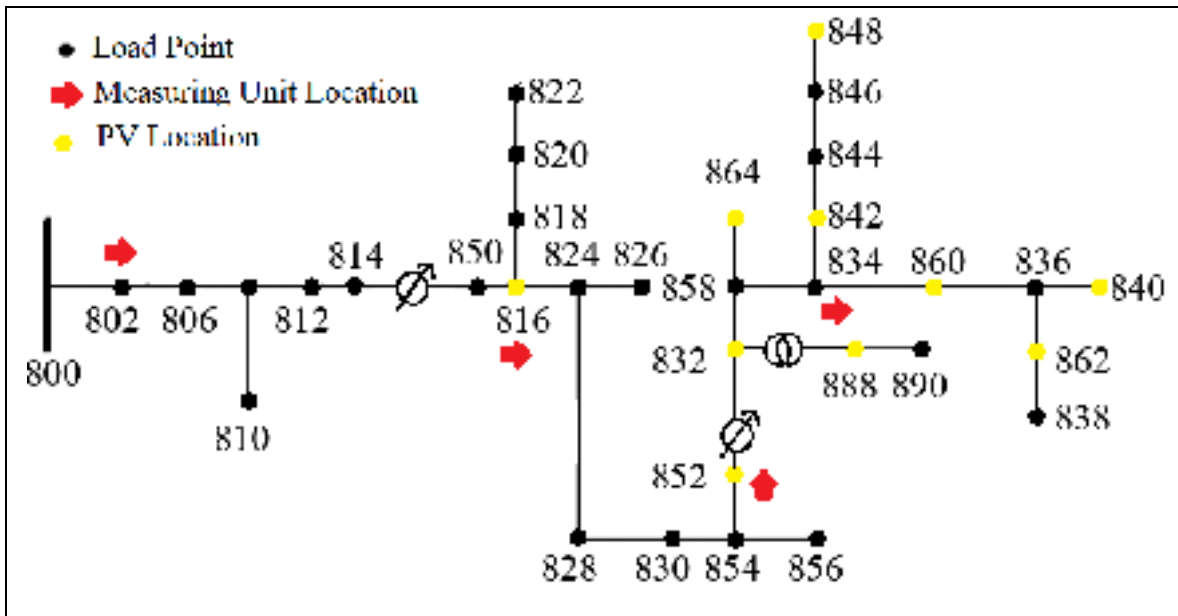
Figure 2.21 IEEE 34 Node Test Feeder. Nine 200 kW PV unit installed at yellow buses.
The location and direction of four impedance measuring units are shown by red arrow
Adapted from Shafiee, Fotuhi-Firuzabad et al. (2013)

Figure 2.23 shows the defined alarm output for reverse power detection at four measuring points. As it can be seen from figures 2.22 and 2.23 at bus 852 and 834 the phase *A* undergoes some reversed active power due to transient of cloud passing. Therefore, the alarm is issued repeatedly, whenever reversed active power happens. On the other hand, for buses 802 and 816, no alarms are issued.

As it was stated earlier, due to two capacitor installed at buses 848 and 844 for power factor correction, power flow analysis shows the permanent reversed reactive power at bus 834. Therefore a flag is defined for reversed reactive power detection. This limitation is shown in Figure 2.22 by light green line.
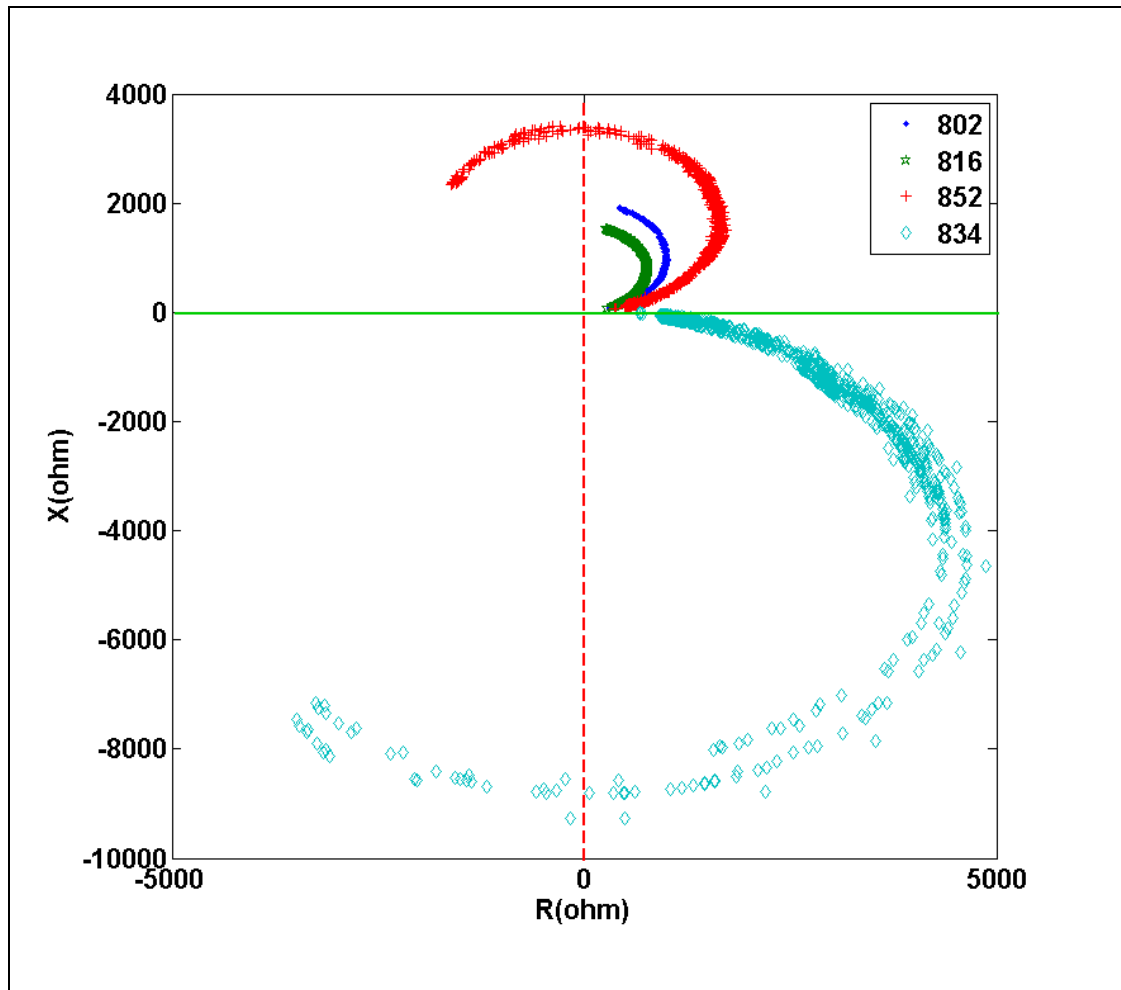
Figure 2.22 Cloud transients impact on measured impedance (for phase A)
at four Buses. The red line shows the reverse active power starting point.
The light green line shows the reverse reactive power starting point

Figure 2.24 shows alarms issued for both reversed active and reactive power, the result is shown for phase C. Due to unbalanced characteristic of IEEE 34 node, unlike the phase A as shown in Figure 2.22, the phase C undergoes reverse power (both active and reactive) not only at buses 834 and 852 but also for buses 802 and 816. For instance, bus 802-phase C shows reversed active power for short period of times, on the other hand, endures reverse reactive power for most of the times.

54
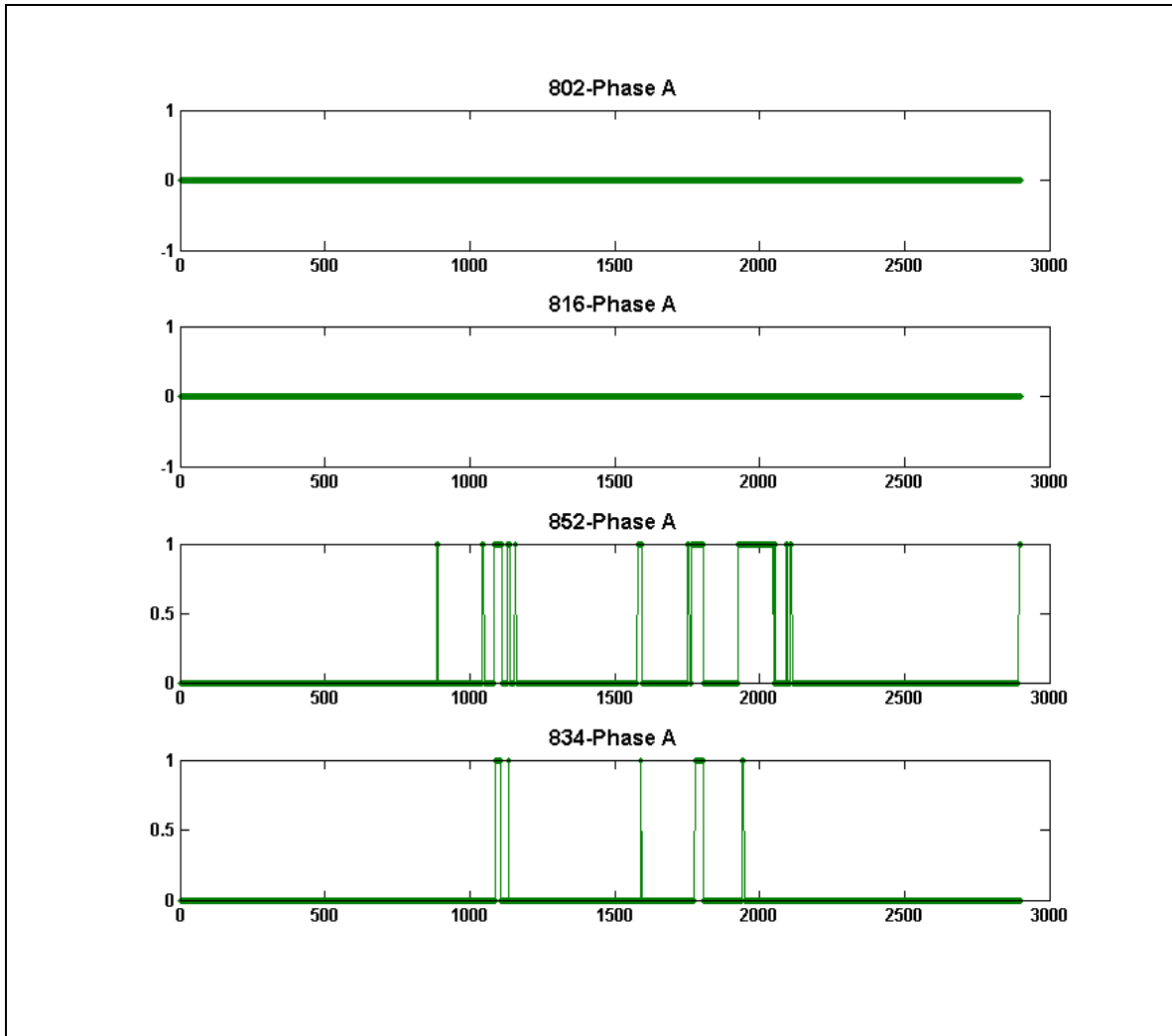
Figure 2.23 Alarm issued for reversed active power at different buses (Phase A)

This chapter has outlined a monitoring application of apparent impedance measurement. It was shown that the apparent impedance has considerable capability to use as a monitoring technique for reverse power flow detection at any condition. Because, based on Eqs (2.22) and (2.23), any point (r, x) on the *R-X* coordinates plane is in one-to-one correspondence with a point (p, q) in the *P-Q* coordinates plane. Meanwhile the application of the method after a substantial changes in the grid like islanding need to be investigated. After Islanding, the power flow direction in the micro-grid may be changed. The application of the proposed method for islanded micro-grid is the same as protection device application. Therefore, the

optimal location and setting for the measuring unit will be affected by islanding. Work is continuing in order to put the method to practical use. The defined alarm and action output of this monitoring technique can be combined with current voltage controller of the feeder for better voltage regulation in presence of RES.
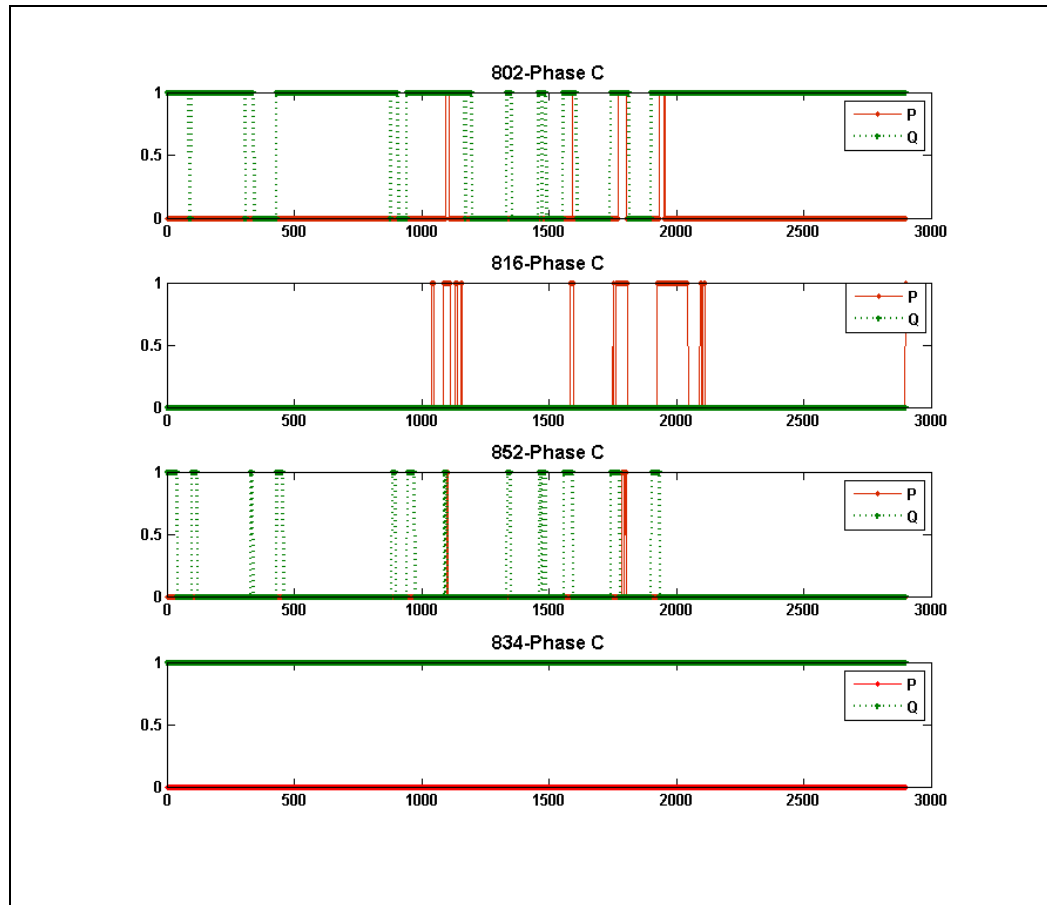
Figure 2.24 Alarm issued for reversed active and reactive power
at different buses (Phase C)

2.6   Conclusion

In this chapter, an impedance-based monitoring technique for evaluation of current situations of distribution system has been presented.

The main contribution of the work is based on measured impedance that has high capability for detecting different states of distribution system in presence of various PV penetration levels.

The results indicate that any proposed monitoring technique shall have the capability of monitoring for balanced and unbalanced system. The dynamic capability of the proposed method has been tested by monitoring the fast transient phenomena such as cloud movement on centralized PV units under unbalanced system conditions of the IEEE 34-bus three-phase distribution network.

A practical application of the proposed method is simulated to show the capabilities of measured impedance to monitor and control of distribution system in presence of various penetration levels of PV. Authors are working on using this method for voltage control improvement of distribution system with high PV integration

CHAPITRE 3

An Impedance Based Method For Distribution System Monitoring

Hashem Mortazavi[1], Hasan Mehrjerdi[2], Maarouf Saad[1], Serge Lefebvre[3], Dalal Asber[3] and Laurent Lenoir[3]

[1]Department of Electrical and Computer Engineering, Ecole de technologie supérieure, 1100 Notre-Dame West, Montréal, Quebec, Canada H3C 1K3
[2]Qatar University, Doha, Qatar
[3]The Research Institute of Hydro-Quebec (IREQ), Power Systems and Mathematics, Varennes, Quebec, Canada

Abstract

This chapter presents a new approach in monitoring of a power distribution system. It uses the bus voltage and injected current to extract the apparent impedance seen from the measuring unit location. Then the apparent impedance variation is used for monitoring of different electrical quantities of the feeder such as feeder power factor, the minimum and maximum of active and reactive power flow. This chapter also presents the mathematics for defining monitoring zone on the R-X plane to detect those parameters variations. The proposed method was tested with the unbalanced distribution system feeder loading, distributed and lumped model of solar and wind power generations. OpenDSS and Matlab are used to test the effectiveness of the method with the IEEE 8500 node test feeder. The dynamic performance of the proposed method is studied for on-line monitoring of the reactive power capability requirement of a Canadian utility for a wind farm integrated to the system. The results show that the monitoring method based on the apparent impedance has a good capability to detect different operation conditions. In addition, the simplicity of the proposed method allows easy application of it in smart grid and traditional distribution system.

3.1   Introduction

Based on the equipment failures data and statistics, electric distribution systems, due to high number of feeders have the highest rate of customer supply unavailability (supply interruption) in power systems (Billinton, Allan et Allan, 1984). Network automation, newer protection philosophy, deployment of monitoring technique, coordinated Volt-VAR control, fast fault detection technique, improving the feeder load balancing and voltage regulation are the main technique to improve the customer service quality and distribution system reliability.

Widespread real-time monitoring of distribution system, because of the high number of feeders and lack of the communication system was impossible for a long time. By decreasing the price of communication system, full deployment of smart meters seems applicable for implementing the smart grid in distribution system level. Monitoring of distribution system due to its time varying and unbalanced loading, through smart meters and monitors is one of the basis of smart grid (Tcheou et al., 2014). Different monitoring system approaches and devices have been proposed to assess different conditions of distribution systems. Power quality monitoring system has been used for a long time not only for analyzing power quality issues but also for load modeling (Visconti et al., 2014). (Qiang et al., 2012) proposed a voltage monitoring for micro grid application, to analyze the power quality and reliability indexes. Using state estimation technique is one of the most popular solutions proposed in the literature for distribution system monitoring. The authors in (Bernieri, Liguori et Losi, 1995) propose using the on-line system modelling capability of artificial neural network (ANN) for distribution system state estimation. The application of branch current state estimation method has been proposed in (Baran et Kelley, 1995),(Baran, 2012) for real time monitoring and control of a distribution feeder. Authors in (Ferdowsi et al., 2014) proposed an ANN based monitoring system for better voltage magnitudes estimation of distribution feeder in presence of distributed generation (DG). Powalko et al. in (Powalko et al., 2009), proposed to use phasor measurement units (PMU) for improved distribution system state estimation.

The renewable energy sources network integration affects the traditional Volt-VAR control, power factor correction and voltage regulation (Bollen et Hassan, 2011). High PV penetration impacts on distribution system protection and operation were analyzed in (Baran et al., 2012). Unidirectional power flow was the first design criteria for distribution system planning for decades. Under this assumption the voltage profile is maximum at the feeder head and decreases proportional with loads to the end of the feeder (Kersting, 2012).

Depending on the size and location of variable generation and the load size the power flows may reverse in the feeder.Therefore, the current distributions system vulnerability increases by RES generation. The high RES penetration, increases the necessity of deployment of monitoring devices for different purposes.

Mortazavi et al. proposed an impedance based monitoring technique for reverse power flow detection in (Mortazavi et al., 2015a). It was shown that the apparent impedance is sensitive to small load variation. Its changes correspond to distributed generation variations and it has a very good capability for reverse power flow detection on each phase, separately.

In addition, the dynamic application of impedance monitoring technique was validated for fast transient conditions such as cloud movement impacts on solar farm. Based on the interconnection standard, by RES integration to distribution system, utilities need to install distance relay as the main feeder protection device. In (H. Mortazavi, 2015.), authors propose using the distance relay not only as a protection device, but also as a monitoring tool at presence of renewable energies.

There are very few publications regarding monitoring of MV and LV feeders in distribution systems despite many smart meter applications for the residential and commercial consumers. It was shown that by RES integration to distribution system the distribution system changes from a passive network to an active network with dynamic characteristics (Bollen et Hassan, 2011) . This chapter proposes the idea of an integrated feeder power flow monitoring technique based on impedance measurement. This chapter presents the

mathematics needed for mapping monitoring zone from *P-Q* plane onto the *R-X* plane. It used to detect power factor variations and active and reactive power flows beyond the pre-defined limits. In addition, it will be shown that based on the proposed transformation, any complex monitoring zone in the *P-Q* plane can be transferred to the *R-X* plane. The dynamic performance of the proposed method is studied with the unbalanced IEEE 8500 node test feeder, for on-line monitoring of the reactive power capability requirement proposed by the Alberta Electric System Operator (AESO) (Ellis et al., 2012) for a wind farm integrated to the system.This chapter is organized as follows: in Section 3.2 the necessity of distribution system monitoring will be explained. Section 3.3 describes the mathematic relationship between the active and reactive power flows and the measured impedance trajectories. Section 3.4 presents the IEEE 8500 node test feeder as case study and the simulation results will be presented in Sections 3.5 and 3.6. Finally the conclusion is presented in Section 3.7.

3.2   Distribution system monitoring necessity

As it was stated in introduction, contrary to transmission systems, due to high number of feeders and elements, distribution systems suffers lack of sufficient monitoring devices. In this section some challenges which raise the necessity of deployment of monitoring units in distribution network will be presented briefly.

* Distribution systems have been designed for radial and unidirectional power flow. In this design the active and reactive power are transferred from the transmission system to consumers. Therefore, many protection and voltage regulation strategies in distribution networks are based on this radial nature. For example, voltage regulators are designed with the flow of power from the higher voltage to the lower voltage. Integration of the RES to distribution systems, however, shows that based on the size and the installation location, the power flow may reverse (Jahangiri et Aliprantis, 2013). For high penetration of RES, traditional unidirectional distribution system will change to a bidirectional system which needs a revision of regulation;

- The minimum voltage drop which must be kept within standard limits, was the main concern of distribution system planner for a long time. On the other hand, the feeder overvoltage was not a concern for distribution system design. With RES integration the over-voltage possibilities become one of the main design concerns (Bollen et Hassan, 2011);

- From a practical standpoint the real distribution system has non-uniform load distribution, distributed load location and different wire size. The designer considers increased wire size for contingency-support branches during special situations (Short, 2014). Distributed RES integration with intermittent characteristic, increases the vulnerability of small wire size feeder to overload conditions;

- In addition, in a unidirectional power flow design philosophy, the designer consider feeder load balancing, through opening and closing switches at different locations, as an economical solution regarding the load growth over the time. Due to changing the switch patterns, the distribution network configuration is a dynamic variable (Willis, 2010). The RES generation will increase this dynamic characteristic which justifies the capital cost needed to deploy new monitoring techniques;

- Moreover, Volt-VAR control, power factor correction and voltage regulation are important elements for increasing the distribution system efficiency in operation. Reactive power flow on a feeder, decreases its active power flow capacity and increases both the voltage drop and loss. In a unidirectional distribution network, even feeders with in-range power factor correction at the substation have portions that are not corrected well (particularly at the feeder's end, where the power factor is much lower) (Short, 2014). The capacitor size needed to correct power factor during peak VAR conditions (during summer due to the high reactive loads of air conditioning system) may seriously over-compensate during off-peak conditions. A survey made by H. L. Willis (Willis, 2010) indicated that slightly more than one-third of all switched capacitor banks were not switching properly due to mechanical failure, vandalism, or weather conditions.

In this section, it was argued that the modern distributions system vulnerability increases not only because of infrastructure aging, but also, because of RES generation. It increases the necessity of deployment of monitoring devices for different purposes. In the next section it will be shown that the apparent impedance measured on the feeder has great capabilities for on-line monitoring of distribution feeders.

3.3   Measured impedance trajectory and power flow

In the last section, it was mentioned that there are different situations in distribution systems which need more attention in order to improve network operation. The capability of the impedance based method for reverse power flow detection was shown in (Mortazavi et al., 2015a). In this chapter it will be shown that the apparent impedance has a good potential for monitoring of feeder power factor, in addition to reverse and forward active and reactive power flow.

3.3.1   Impedance measurement

The apparent impedance seen from any point on a feeder is calculated by three single phase measuring units. Each unit uses only a single phase current and a single phase voltage. Considering that V_{AN} is the phase A to ground voltage and I_A is the current flows through the phase A conductor, the apparent impedance seen for phase A is given by (Hase, 2007):

$$Z_A = \frac{V_{AN}}{I_A} \tag{3.1}$$

The impedance calculated using (3.1) is the positive sequence impedance for all system operation condition except fault conditions (Hase, 2007). In practical application, the feeder grounding must be checked and in order of accurate V_{AN} and I_A measurement, maybe grounding transformers are needed to be installed (IEEE Guide for the Application of Neutral Grounding in Electrical Utility Systems--Part IV: Distribution, 2015).

3.3.2 Mapping between P-Q and Z plane

The mapping concept will be used to develop the relationship between the measured impedance and power flow quantities. To do so, for an impedance measuring unit , located at sending-end of Figure 3.1 (bus 1) the apparent impedance measured by an impedance measuring unit is calculated by (Mortazavi et al., 2015a):

$$|\bar{Z}| = \frac{|\bar{V}|}{|\bar{I}|} = \left(\frac{P + jQ}{P^2 + Q^2}\right) \times |V|^2 = \frac{|V|^2 \times \bar{S}}{|\bar{S}|^2} \tag{3.2}$$
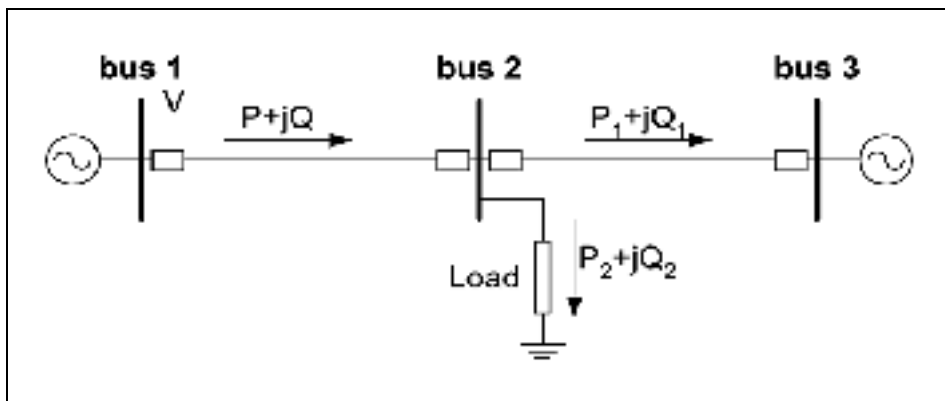
Figure 3.1 Simple two source system power flow
Adapted from Kim, Heo et Aggarwal (2005)

Where, $\bar{Z}$ is the apparent impedance obtained by measuring unit installed at *bus 1*, $\bar{I}$ is the line current flow from *bus 1* to *bus 2*, measured by a phase CT (current transformer), $\bar{V}$ is the measured line to ground voltage of *bus 1* by a one phase VT (voltage transformer), $\bar{S}$ is the apparent power, and P, Q are the active and reactive powers transmitted from *bus 1* to *bus 2*, respectively.

Eq. (3.2) shows the relationships between the measured apparent impedance at bus 1 and the active and reactive power transmitted through the line, and it can be used for mapping between the *P-Q* plane and *R-X* plane. The measured $\bar{Z}$ is a complex value and has real and the imaginary part which are written as (Mortazavi et al., 2015a):

$$R = \left(\frac{|\bar{V}|^2}{P^2 + Q^2}\right) \times P \tag{3.3}$$

$$X = \left(\frac{|\bar{V}|^2}{P^2 + Q^2}\right) \times Q \tag{3.4}$$

The sum of squared of (3.3) and (3.4) are written as:

$$R^2 + X^2 = \frac{|\bar{V}|^4}{P^2 + Q^2} \tag{3.5}$$

For fixed apparent power, Eq. (3.5) is a circle with fixed radius: $\frac{|\bar{V}|^2}{\sqrt{P^2+Q^2}}$ and center coordinate of $(0,0)$. The measured impedance loci for fixed apparent power condition are shown in Figure 3.2. The load power factor variations determine the impedance loci direction in R-X plane. For variable load power factor, the 'd_1' direction in circle 'C_1' shows the impedance loci while the load power factor decreases (or the load power factor angle φ increases). For fixed load power factor, the impedance locus is illustrated by line 'a' in Figure 3.2.

The 'd_2' direction in line 'a' shows the impedance loci for fixed load power factor, while the transmitted apparent impedance increases. For variable power factor the apparent impedance loci moves in a circle loci. The circle 'C_1' shows the impedance loci for this condition. The radius of the circles is inversely proportional to apparent power magnitude. By increasing apparent power magnitude the circle radius decreases and vice versa. Therefore, the circle "C_2" represents the heavier load condition in comparison with the circle "C_1".

Table 3.1 Explanation of R and X sign

Condition	Sign of R	Sign of X
Power Flow from Bus *1* to *2*	Positive	
Power Flow from Bus *2* to *1*	Negative	
Lagging Reactive Power from Bus *1* to 2		Positive
Lagging Reactive Power from Bus 2 to *1*		Negative
Leading Reactive Power from Bus *1* to 2		Negative
Leading Reactive Power from Bus *2* to *1*		Positive
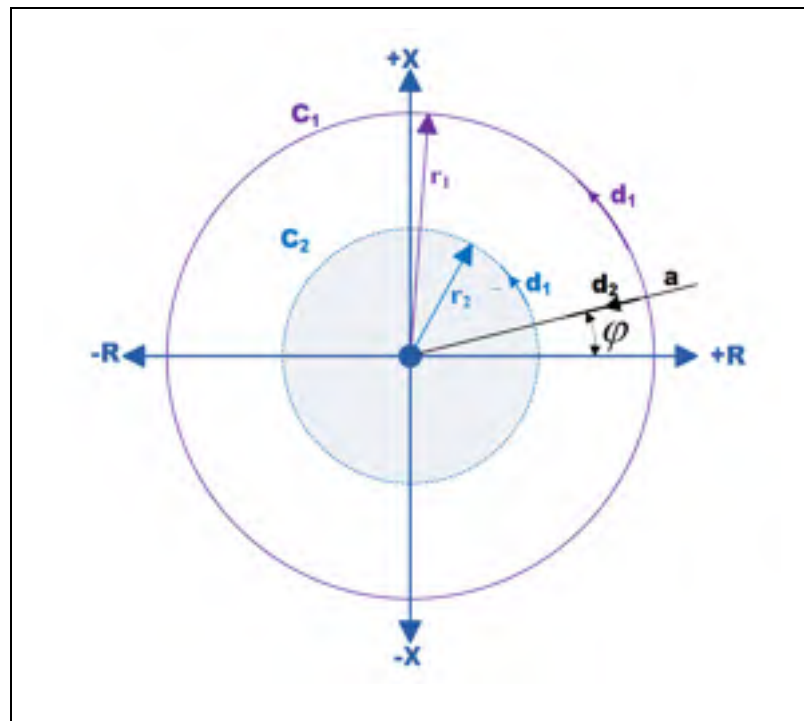
Figure 3.2 Measured impedance trajectories for active and
reactive power variation while the apparent power is fixed

Moreover, Eqs. (3.3) and (3.4) show that the location of calculated apparent impedance in R-X plane depends on the value and direction of transmitted active and reactive power from bus 1 to bus 2. The sign of R in (3.3) and X in (3.4) are only related to the sign (direction) of P and Q, respectively. Table. I explains the relationship of R and X sign of calculated impedance with the actual active and reactive power flow direction (Mason, 1956). As each

point R-X corresponds one-to-one to a point in P-Q plane, therefore, the R-X plane has the capability to react to every change in the P-Q plane.

3.3.3 Special Cases

In the last section the general equation for mapping the *P-Q* plane to *R-X* plane was derived. There are several special considerations in distribution system design and operation. In this section basic mathematic will be presented for special cases such as conversion of fixed active or reactive power limit to the *R-X* plane. Later these special cases will be used to analyze more complex situations.

Considering the Figure 3.1, $\overline{V}$ is the measured line to ground voltage at bus 1, and P, Q are the active and reactive powers transmitted from bus 1 to bus 2, respectively. Eq. (3.6) is used for calculating the voltage drop along the feeder (Bollen et Hassan, 2011).

$$\Delta V = \frac{[R \times P + X \times Q]}{V^2} \qquad (3.6)$$

Eq. (3.6) indicates that the voltage drop is related to line power flows. In distribution system design each feeder has a predefined voltage drop for minimum and maximum feeder load which must be in standard region. With RES integration the voltage drop varies depending on the RES generation, its location and feeder consumption. The compensated voltage drop is the main cause of feeder over-voltage. Reference (Bollen et Hassan, 2011) showed that the negative voltage drop not only occurs at reversed power flow but may also happen at low forward power flow. Utilities use low forward power relays in order to control (or prevent) power flow on some special lines in the network (Tholomier, Yip et Lloyd, 2009).

3.3.3.1 Minimum forward reactive power flow limitation

In distribution system design the minimum and maximum reactive power transferred through the feeder are used for capacitor banks size selection and their optimal location (Willis, 2010). As it is shown in Figure 3.3, Q_0 is considered as the minimum designed reactive power flow on the line. To find the mapping of the hatched region for $Q>Q_0$, where $Q_0>0$, in *R-X* plane, first the line will be mapped on the R-X plane then the mapping of $Q>Q_0$ region will be found.
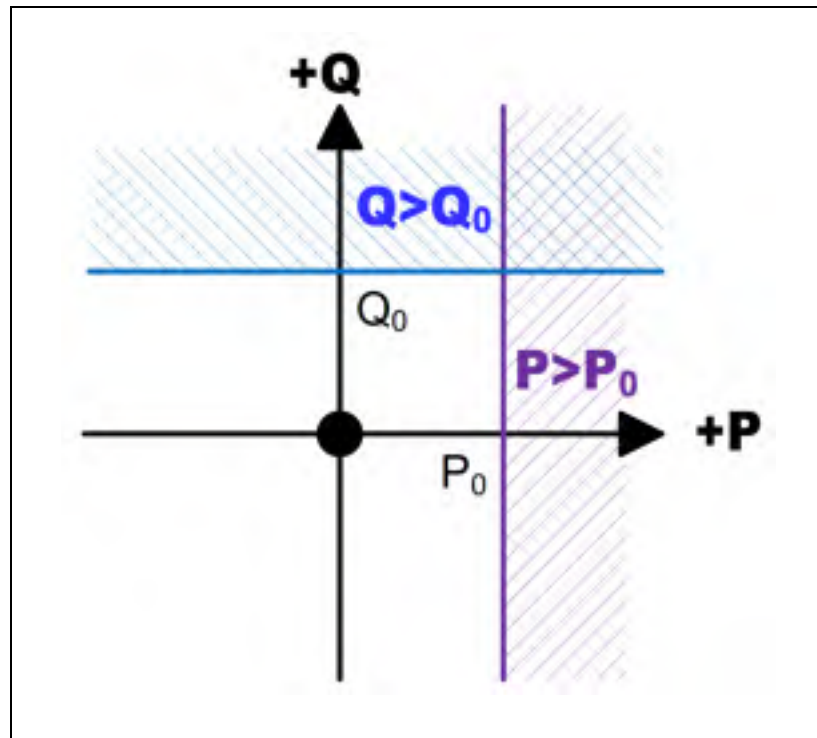
Figure 3.3 Defined minimum active and reactive power
regions on the P-Q plane

Note that the straight line Q_0 in Figure 3.3 has a finite length. By substituting (3.4) into (3.5) results in:

$$R^2 + X^2 = X \times \frac{|\bar{V}|^2}{Q_0}$$
(3.7)

Eq. (3.7) can be re-arranged as:

$$R^2 + (X - \frac{|\bar{V}|^2}{2Q_0})^2 = \frac{|\bar{V}|^4}{4Q_0^2} \tag{3.8}$$

For fixed reactive power, Eq. (3.8) is a circle with radius: $\frac{|\bar{V}|^2}{2Q_0}$ and center coordinates of $\left(0, \frac{|\bar{V}|^2}{2Q_0}\right)$. As the line Q_0 is not infinite the final mapping is an arc instead of a complete circle (missing the original of R-X plane).

This circle is illustrated in Figure 3.4 as curve 'C_1' and traces the trajectory of the measured impedance, which moves in the 'd_1' direction as the real power increases. For $Q > Q_0$, the (3.8) is written as:

$$R^2 + (X - \frac{|\bar{V}|^2}{2Q_0})^2 \leq \frac{|\bar{V}|^4}{4Q_0{}^2} \tag{3.9}$$

Eq. (3.9) shows the final region as all the points inside the circle 'C_1'. In the same manner, the transforming region of $Q < Q_0$ is all the points outside of circle 'C_1'.

3.3.3.2   Minimum active power flow limitation

Consider P_0 as the minimum designed active power flow on the line. To find the mapping of hatched region for $P > P_0$ where $P_0 > 0$ in R-X plane, substituting (3.3) into (3.5) results in:

$$R^2 + X^2 = R \times \frac{|\bar{V}|^2}{P_0} \tag{3.10}$$

This can be re-arranged as follows:

$$(R - \frac{|\bar{V}|^2}{2P_0})^2 + X^2 = \frac{|\bar{V}|^4}{4P_0{}^2} \tag{3.11}$$

For fixed active power, Eq. (3.11) is a circle with radius: $\frac{|\bar{V}|^2}{2P_0}$ and center coordinates of $\left(\frac{|\bar{V}|^2}{2P_0}, 0\right)$. In Figure 3.4 this circle is illustrated as 'C$_2$'. Based on (3.11) when the transmitted reactive power increases the impedance locus moves in 'd$_2$' direction. The region of the R-X plane corresponding to (3.11) and for $P > P_0$ is the region inside the circle 'C$_2$'.
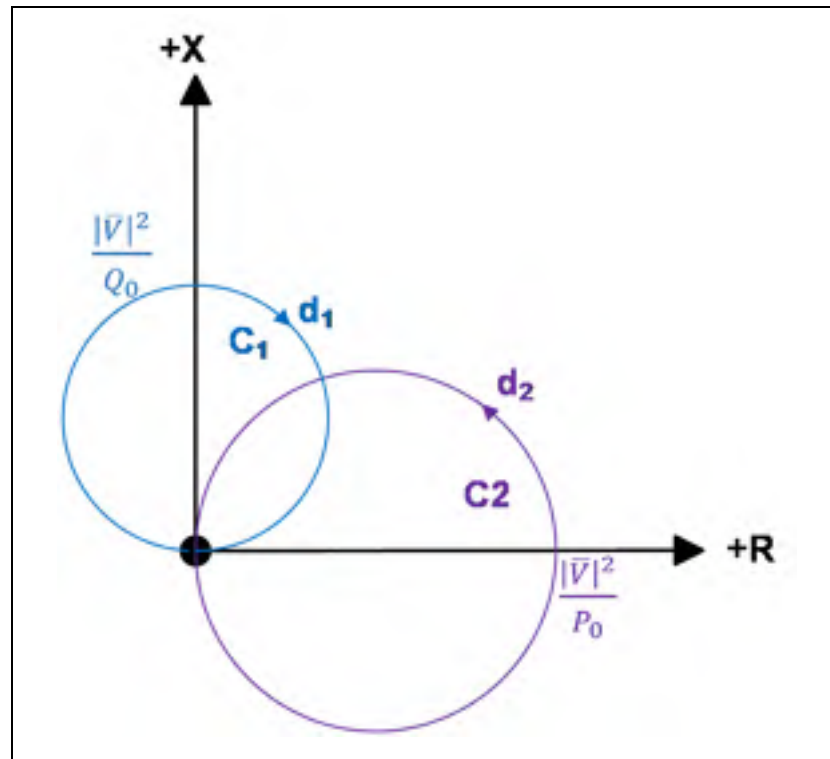
Figure 3.4 Measured impedance trajectories for active and reactive power variation

3.3.3.3   Fixed power factor

Distribution system operator usually prefers unit power factor or close to unity, because of the corresponding reduction of the line losses due to less reactive power flow. The tendency to increase the level of penetration of renewable energy sources, and the effect of those variable sources on the feeder power flow and voltage regulation urges the utilities to put

some limitation at the point of interconnection (*POI*). For example FERC predetermined the reactive capability requirement up to 0.95 lag to lead at the POI for wind power generation in FERC Order 661-A(FERC Order No. 661-A, December 12, 2005.).

Fixed power factor operation of feeder is a line in *P-Q* plane. For mapping that from *P-Q* plane to *R-X* plane, (3.4) divided by (3.3) results in:

$$\frac{X}{R} = \frac{Q}{P} = \tan\varphi \tag{3.12}$$

Where φ is defined as the power factor angle of the line. Eq. (3.12) shows that mapping a straight line passing through the origin in *P-Q* plane is a straight line passes through the origin in *R-X* plane.

3.4   Case Study

To show the capability of impedance based monitoring technique, the IEEE 8500 Node Test Feeder (Figure 3.5) is chosen. As presented in (Arritt et Dugan, 2010), the 8500 node test feeder is a relatively large network that has 2516 medium voltage nodes, all type of line configurations such as single, two and three-phase MV and LV lines. It has four voltage regulators, one installed at substation and three distributed along the feeder. The circuit also contains three controlled and one uncontrolled capacitors banks. The settings of the voltage control devices were set at their nominal values in the simulations. When the reactive power flow in the line is 50% of the capacitor size, the capacitor controller switches it ON and when the flow is 75% of the capacitor size in the reverse direction switches it OFF. As this model is a large, heavy loaded, consisting of three-phase and one-phase overhead lines and cables, it is a good case for testing the impedance method monitoring capabilities.The GridPV toolbox(Reno et Coogan, 2014) is used as a COM server interfaced between OpenDSS (Dugan, 2012) and the Matlab (Guide, 1998) for system simulation.

For RES simulation, there are different choices such as solar PV, wind turbine, biomass and small hydro turbines. In this research, both the PV system and wind turbine model provided in OpenDSS are used as the RES model. Both the lumped and distributed model of PV system are installed at different locations to analyze the generation location impact on the measured apparent impedance.

Hoke et al. in (Hoke et al., 2013) showed that the 15-20% limit for PL studies is very conservative for most of feeders in distribution network. They showed that in more than 66% of the simulated cases, the maximum PL is greater than 90%. Therefore for simulation of different penetration level (PL) impact analysis, the PV generation was increased from zero to 1.15 pu of the nominal size of PV unit. At each step, the PV output increased one percent and then a power flow was run with OpenDSS. Power flow solutions (voltages, currents, active and reactive power of feeder) were sent to MATLAB through the COM server interface. Then those data were analyzed by GridPV toolbox and user written scripts. The simulation results are shown for unit power factor operation of PV systems, otherwise it will be mentioned.

3.5   Simulation Result and Discussion

3.5.1   Reverse power flow detection

Based on Eq. (3.2) the measured impedance can be used as a tool for reverse power flow detection. For a radial distribution system design, the reverse power flow causes over-voltages in some part of a feeder. According to the Eqs (3.3) and (3.4) the measured R and X signs have a direct relationship with active and reactive power signs, respectively. To simulate the reverse power flow, 14 distributed PV units with different sizes in range of 100, 200 and 300 kW with total generation of 3700 kW are installed at different locations based on the nominal load of the line.

72
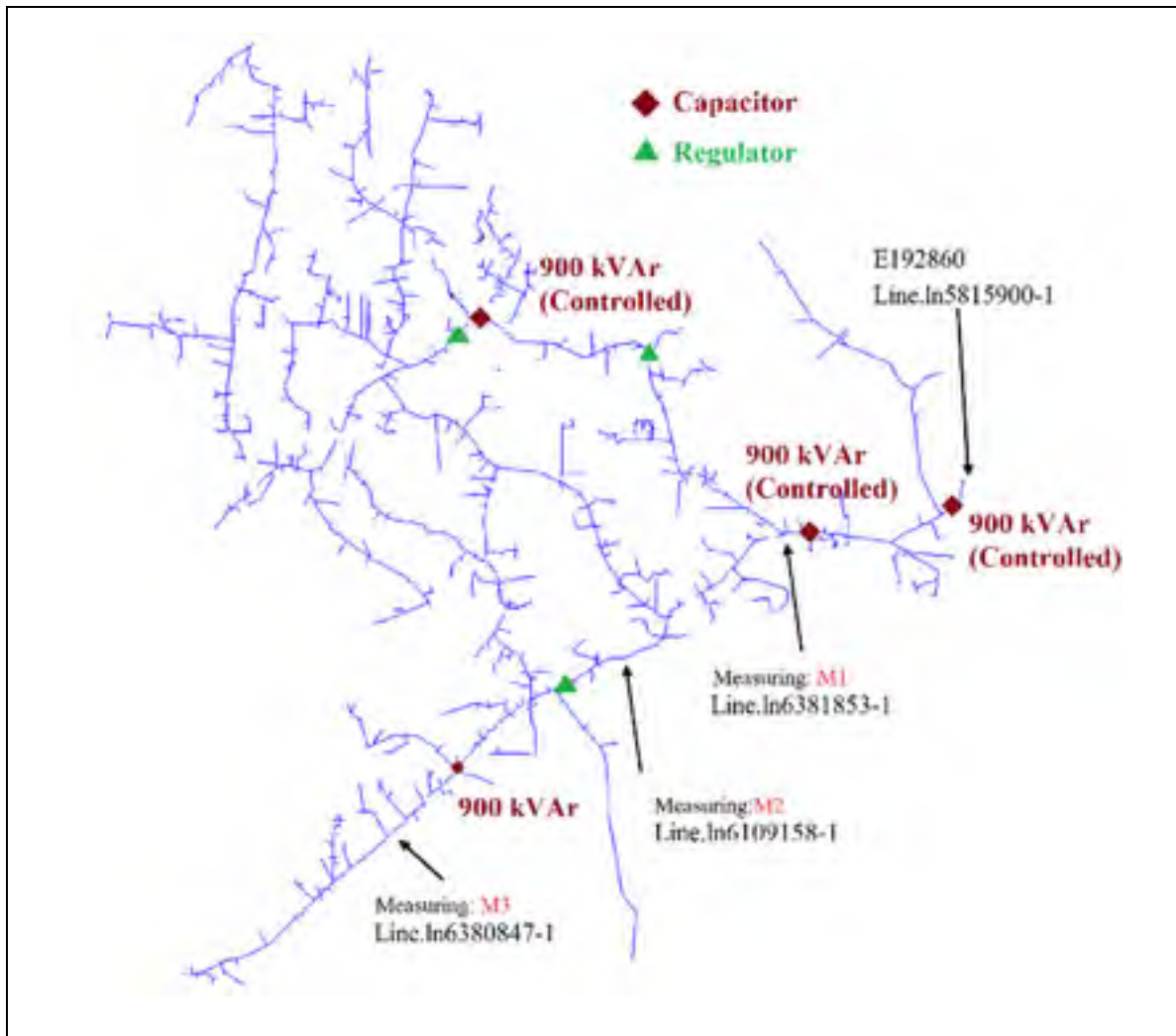
Figure 3.5 Schematic of the IEEE 8500 Node Test Feeder
Adapted from Arritt and Dugan (2010)

Figure 3.6 shows the exact value of active and reactive power for each feeder according to the distance from the substation. As it can be seen, the reverse active power happens at some locations (only on phase-A and phase-C around 7 km from the substation). Regarding reactive power flow, Figure 3.6 shows numerous reverse reactive power at different locations due to presence of switched and unswitched capacitor bank distributed along the feeder.

Figure 3.7 shows the apparent impedance loci measured at three different measuring units' location. The measuring unit locations are chosen according the (Arritt et Dugan, 2010). The apparent impedance measuring units' location are shown in Figure 3.5.
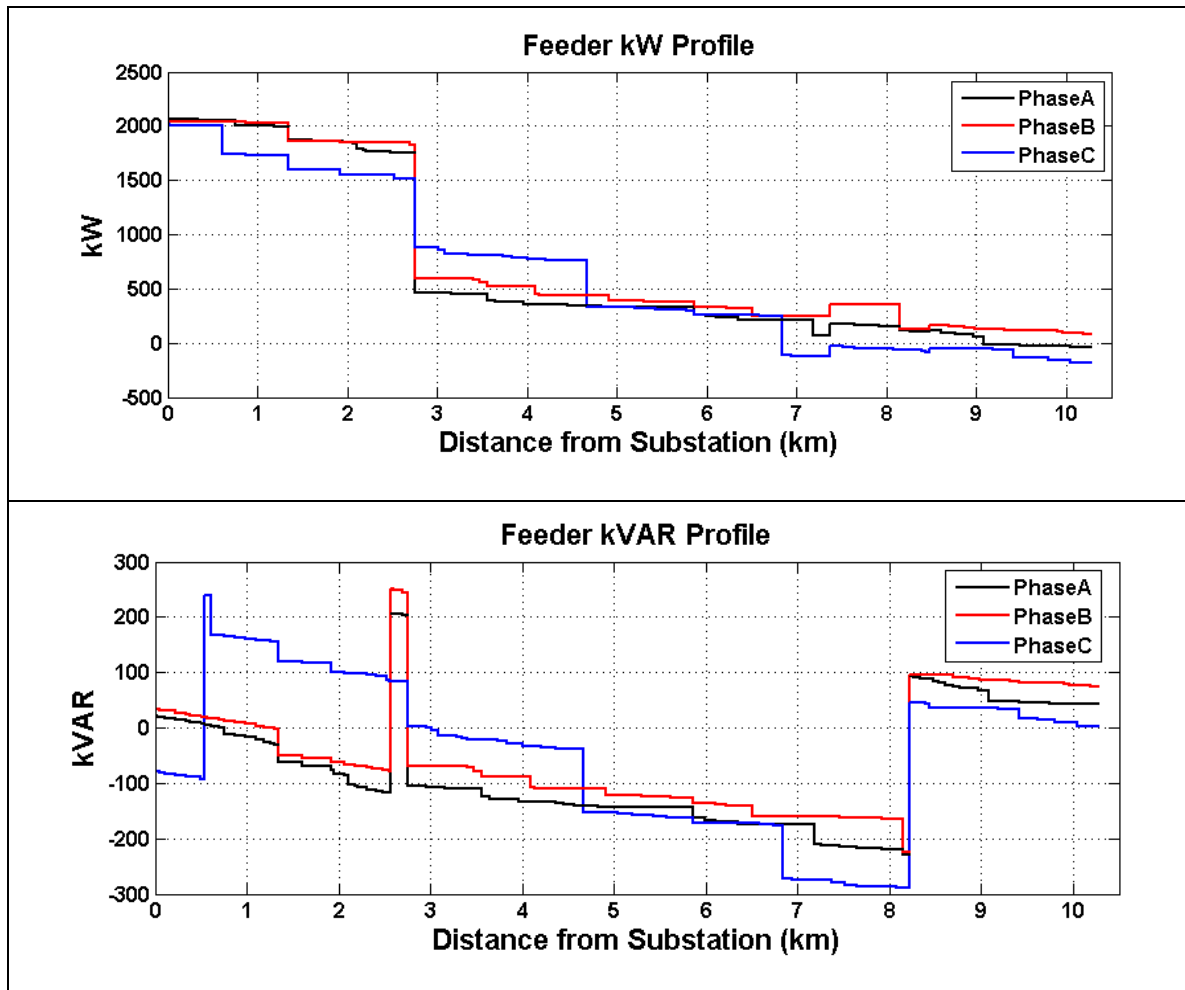
Figure 3.6 All feeder active and reactive power based on the distance from substation

Figure 3.7-a shows the measured impedance in each phase at measuring point M1 (installed at bus L2955077). Sudden changes in the measured impedance loci are related to substation and feeder voltage regulator tap changer variation.

While Figure 3.7-a shows the forward active and reactive power flow on the line LN6381853- 1, Figure 3.7-b shows the reversed reactive power flow with forward active power flow on the line LN6109158-1 due to a 900 kVAr capacitor bank installed downstream the measuring point M2 (bus:L2936279).

For measuring unit M3, unlike the phase-B in Figure 3.7-c the phases A and C show the reversed power happens at different PL. For the phase A, at PL=108% the R becomes zero and after this point the R goes negative corresponding the reversed active power. The reason for the decreasing R is related to the relationship between the measured R and total P and Q flows along the line. Based on equation (3.3) by decreasing the P -due to the increased PV penetration level - the measured R will decrease too. While the impedance location for the phase A is entered to the second quarter of R-X plane (for PL=108%) showing small reversed active power, the phase C shows a higher reversed active power started at PL=73%. This phenomenon happens due to the unbalanced operation of IEEE 8500 node test feeder. Based on the Eq.s (3.3) and (3.4), the apparent impedance measured at any location, has a direct relationship with RES penetration level and reverse relationship with transferred power. The larger the power transferred through the line (equal to low RES penetration level), the smaller measured R and X and vice versa.

Unbalance operation is an intrinsic characteristic of distribution system. This unbalance operation has different causes such as, feeder unbalanced load, time varying and nonlinear loads and feeders configuration. Therefore, it is anticipated that when the voltage and current of the three phases are unbalanced the resultant calculated impedance for each phase is not the same as other two phases. This unbalanced operation of distribution system was shown in the Figure 3. 7. The three-phase calculated impedances at those metering locations, not only have not the same values, but also shows different patterns for PL variations. For example, unlike the phase B as shown in Figure 3.7-c, the phase A and C undergo reverse power active power at different PLs. Therefore, due to unbalance operation of distribution system, any proposed monitoring technique shall have the capability for separate three phases monitoring.
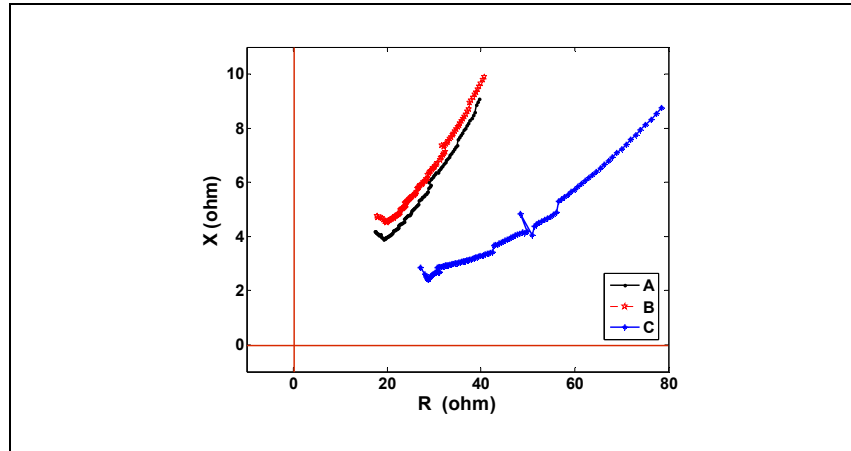
a- Measured impedance at measuring point M1- three phases.
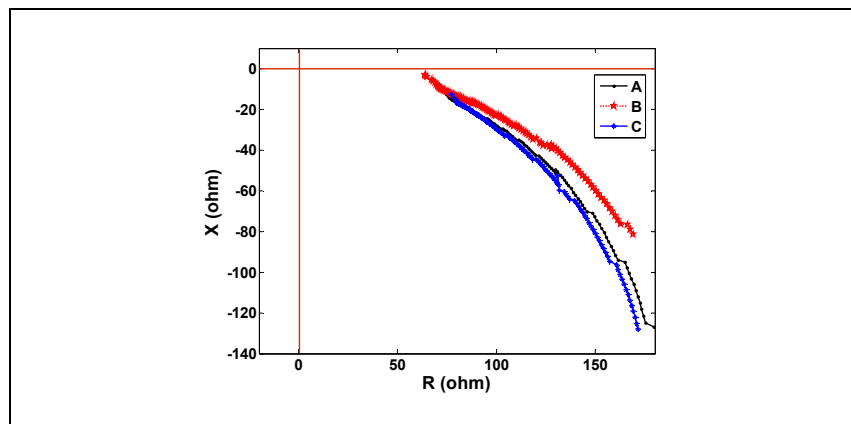
b- Measured impedance at measuring point M2- three phases.
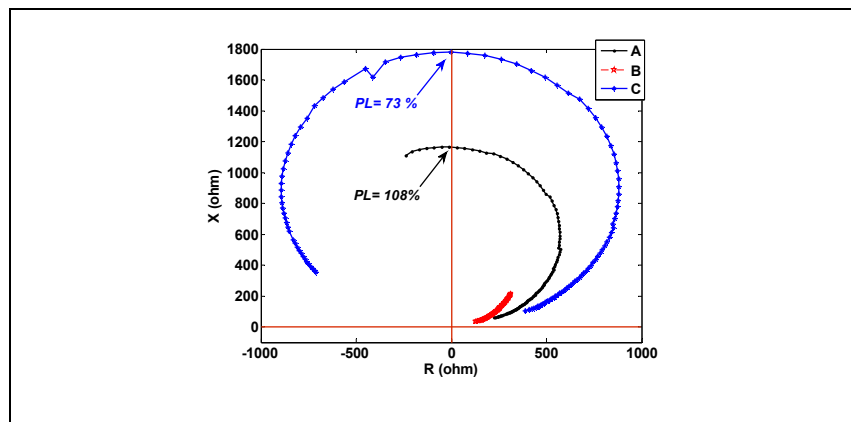
c- Measured impedance at measuring point M3- three phases.

Figure 3.7 Measured impedance at different measuring points

Figure 3.8 shows the IEEE 8500 node test feeder power flow direction produced by GridPv toolbox at a snapshot of system (at the PL=100%). While the number of monitoring points are limited in a real distribution system, Figures 3.7 and 3.8 show that the reversed power happens not only at different locations, but also may be happens at one or two phases only.
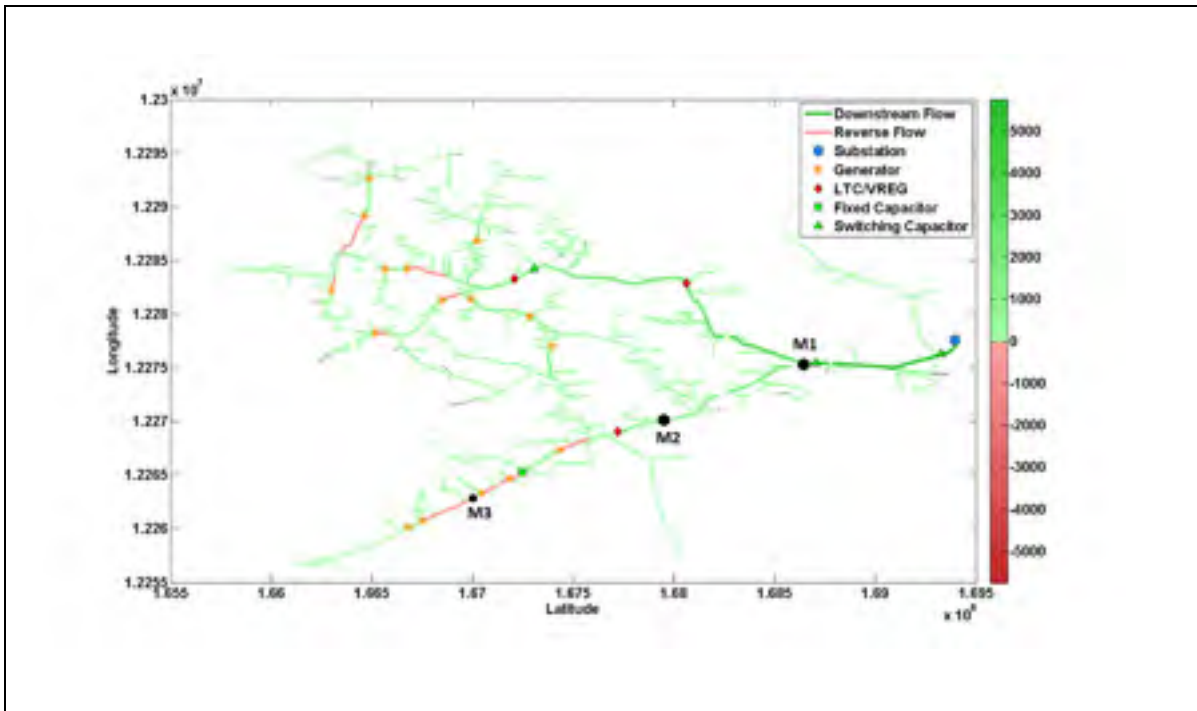
Figure 3.8 IEEE 8500 node test feeder power flow direction for PL=100%.
The red colors shows the reversed power flow part of feeder.
The PV units' location are shown by Orange stars

3.5.2   Monitoring the feeder PF

In general, maintaining the feeder power factor as close as possible to unity is a goal in distribution system design as long as the voltage level lies within the allowable range. However, maintaining a unity power factor could result in high number of operations of voltage regulating equipment which will decrease the equipment maintenance period and make it uneconomical. Therefore a range of power factor variation is always defined. For

example, based on the Hydro-Quebec interconnection guideline, the customer load at the connection point must have a power factor of 95% or higher for large-power customers and 90% or higher for medium- and small-power customers.

Figure 3.9-a shows a snapshot of the IEEE 8500 feeder power factor for the maximum PV penetration level, for the same condition of the last section (14 distributed PV units). Figure 3.9-b is a part of Figure 3.9-a zoomed in, and this snapshot clearly shows that some feeders suffer from low power factor. This mostly happens near the RES point of connections. According to the Eqs (3.12), the simple explanation of this phenomenon is the variation of ratio of active power to apparent power, transmitted through feeder, due to the PV generation. In this simulation all the 14 PV units operates at unity power factor.

For acknowledgment by the distribution system operator, a set of feeder over-excitation and under-excitation alarms were defined for each monitor based on the Eq. (3.12). The set points are defined for pf = ±0.90 for each monitor. For values detected beyond those limits, an alarm will be issued. Figure 3. 10 shows the output of alarm system for PV penetration level variation. It can be clearly seen that only monitor M3 detects over excitation condition only on the phase- A (alarm starts at PL= 82%) and the phase-C (alarm starts at PL= 56%). The comparison of Figures 3.7 and 3.10 shows that although the measuring point M2 shows the continuous under-excited condition (reversed reactive power only) for all the phases of that feeder, at any conditions the feeder power factor goes beyond the pre-defined settings (maintain its power factor between 0.90 and unity).

Comparison of Figure 3.8 and Figure 3.9 emphasizes the necessity of installation of the monitoring units for critical feeder and points of high RES integration, because the feeder electric parameters may go beyond the distribution system designer limits.

78

a- IEEE 8500 node test feeder.

b- The zoomed in part of the IEEE 8500 node test feeder.
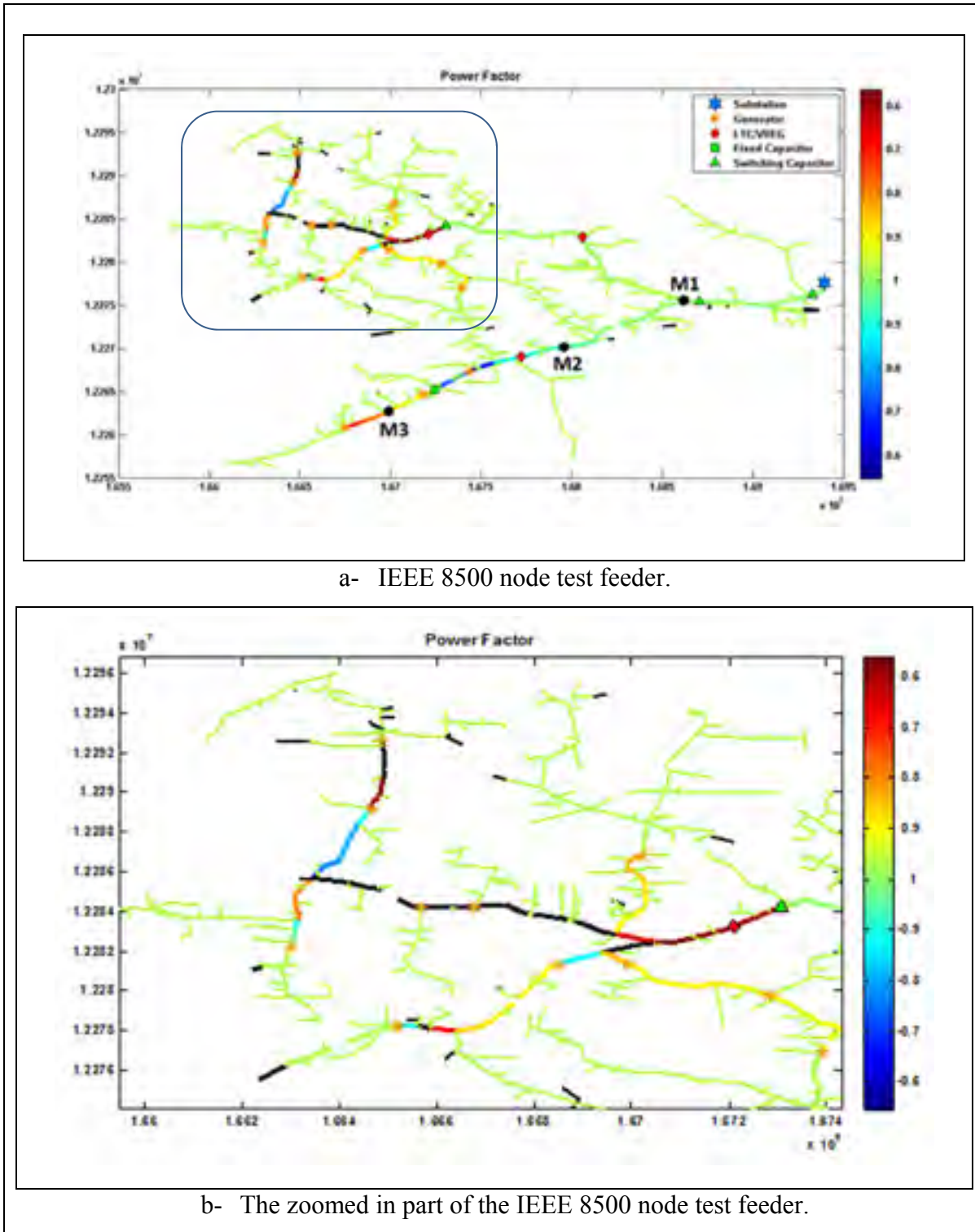
Figure 3.9 IEEE 8500 node test feeder power factor variation. The blue spectrum feeder
shows the lagging (capacitive) pf>1 and the red spectrum shows the leading (inductive) pf<1.
The PV units' location are shown by Orange stars

3.6   Practical implementation of monitoring method

In order of reliable operation of power system, the generating units must comply with certain reactive power requirement depending on the network they are connected. Although many of existing interconnection regulations have been based on traditional generating units' capabilities, the increasing rate of RES integration forces the power system regulators to consider variable type of generation in their standards and practical procedures. IEEE 1547 standards, as a base regulation for RES integration in North America, banned operating in voltage or reactive power control mode for distribution level connection of PV and wind turbine.
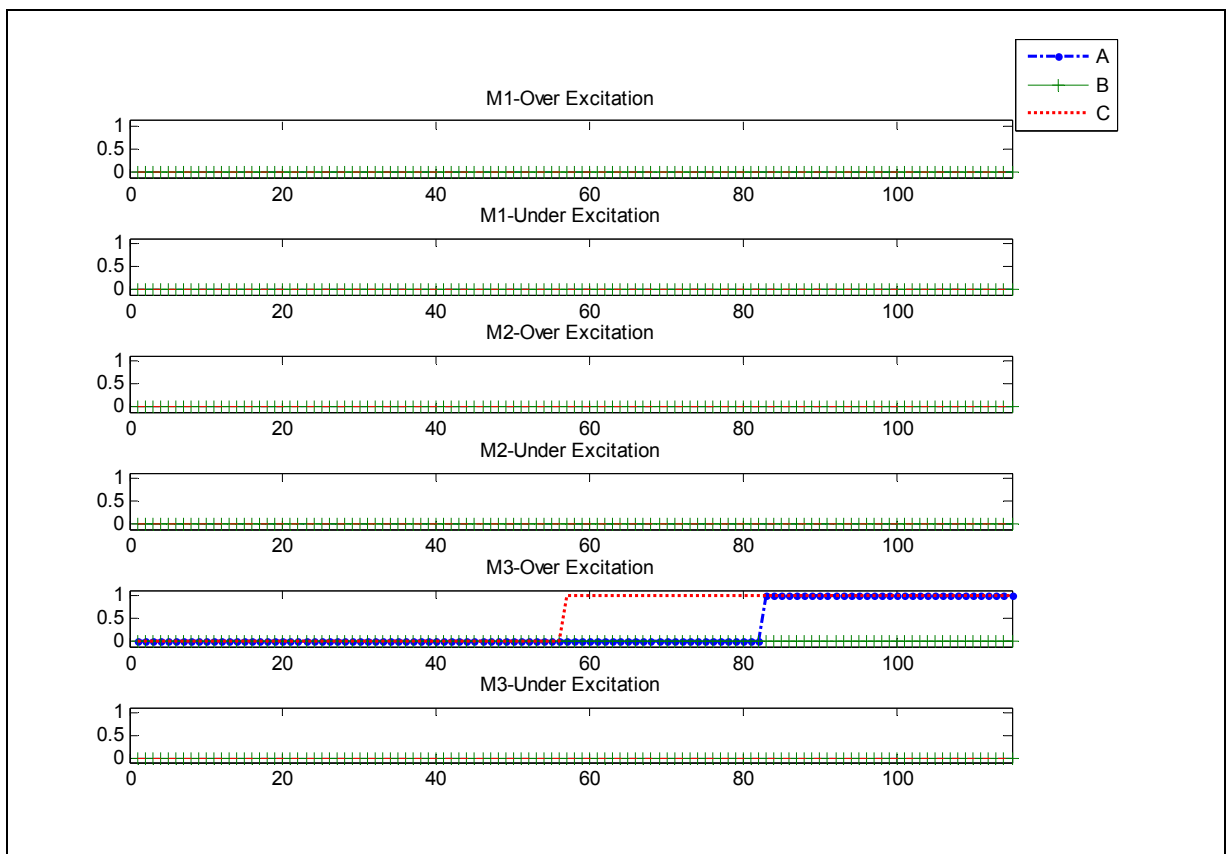
Figure 3.10 Alarm issued for detecting over excited and under excited
condition detected at three measuring point

On the other hand, variable generation units based on inverter technology are technically capable of providing steady-state and dynamic reactive power support to the grid. Therefore, FERC Order 661-A, demands the transmission operator to perform a system impact study, whether there is a need for a dynamic reactive capability, for wind farms, up to the 0.95 leading/lagging power factor range (Ellis et al., 2012). Meanwhile, some transmission service providers define certain reactive power requirements for wind power integration to their system. For example the Alberta Electric System Operator (AESO) defines the "Wind Power Facility Technical Requirements" (WPFTR) for integration of wind power facilities. Figure 3.11 shows the reactive power capability requirement defined by AESO (Ellis et al., 2012), (El Itani et Joós, 2012).
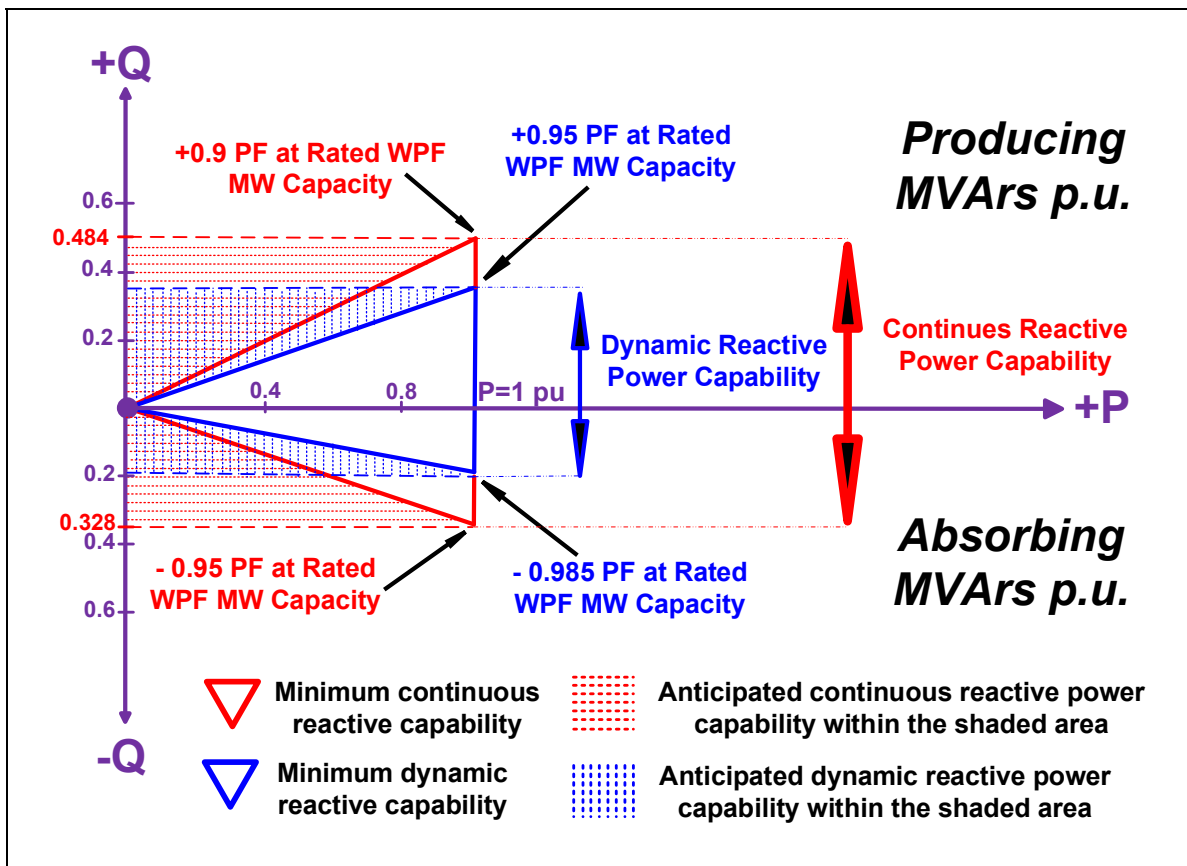
Figure 3.11 Reactive power capability requirement for AESO
Adapted from Ellis, Nelson et al. (2012)

Although some utilities prefer static reactive power requirement, the AESO specifies both a dynamic range and a total range of reactive operation for wind farm integration. For example, AESO specifies a dynamic range of 0.95 lag to 0.985 lead and a total range of 0.95 lead, 0.90 lag, indicating a need for smooth and rapid operation between 0.95 lag to 0.985 lead, but allowing for some time delay for lagging power factors below 0.95.
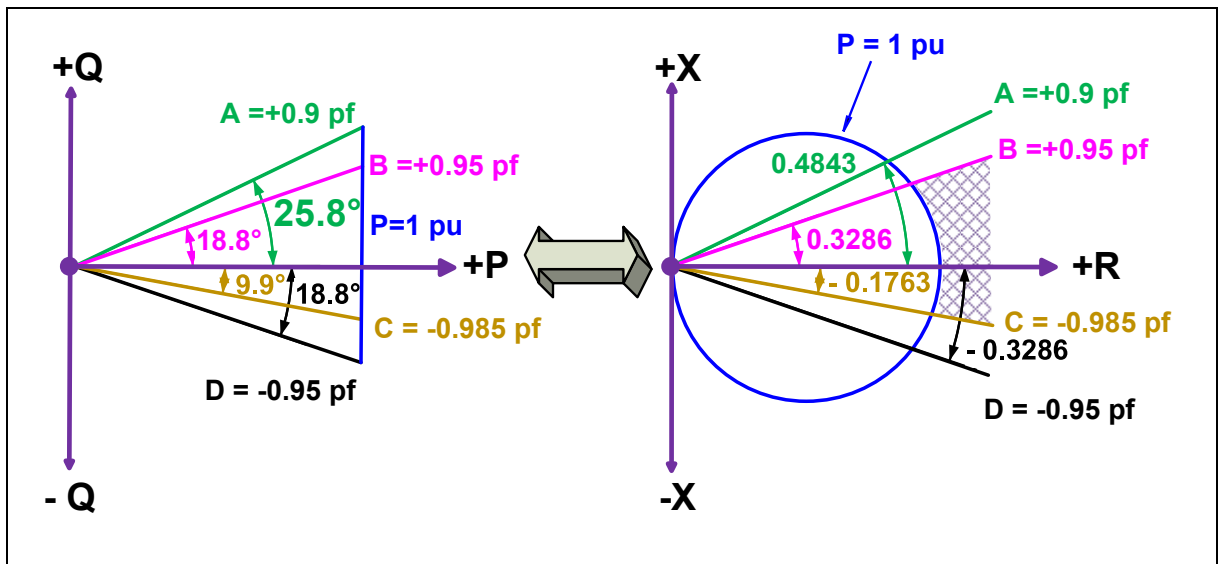
Figure 3.12 AESO reactive requirement curve mapped to R-X plane. The hatched area shows the mapped area correspond to dynamic range operation while P≤ 1pu

To show the practical application of the impedance based monitoring system, the static and dynamic range of reactive power requirements curve will be mapped to *R-X* plane and then based on those defined criteria the monitoring system setting will be calculated. Figure 3.12 shows mapping of the AESO defined area for reactive power requirement from *P-Q* plane into the *R-X* plane. It worth mentioning that, the hatched area in *R-X* plane in the Figure 3.12, shows the mapped area correspond to dynamic range operation while P≤ 1pu conditions in *P-Q* plane. In another words, for the conditions that the transferred power increases from the pre-defined nominal power of the line (P_0=1 pu) the mapped impedance will be settled down inside the circle.

For practical implementation of monitoring technique for AESO reactive requirement, the IEEE 8500 test feeder is modified as follows. The aggregated model of a 500 kW wind farm operating at pf=0.9 feeding to a large commercial load of 250 kW with pf=0.85 will be used in this section. In order to perform this, a 1 km, three phase line connected to bus m1026357 is added to IEEE 8500 node test feeder. The line parameters and wire size are the same as the main feeder data. Then the wind turbine and load are connected to end of this line. The nominal voltage of the line is 12.47 kV.

Three one-phase impedance measuring units (current and voltage transformers) installed at the bus *m1026357* for each phase. In order to define the monitoring system direction, the polarity of the measuring units, designed in a way that the impedance measuring units monitor the point of interconnection (*POI*) from the wind farm perspective. Hence the measuring units monitor the line power flow.

As it was stated earlier the wind farm feeds the local load and the surplus power is sent to the grid. Therefore, the impedance measuring unit focuses on the changes of the total line power flow, not the changes of individual load or wind farm. Therefore, the resulting net power flow (wind power generation minus load) on each phase is monitored based on the AESO chart. The data used to in this section for wind turbine generation are 1-second wind power time series for 2900 consecutive seconds is shown in Figure 3.13 (Dugan, 2012).

Figure 3.14 shows the apparent impedance trends measured at *POI*, plotted on the mapped AESO reactive power requirement chart. While the impedance trend shows the reversed active and reactive power flow through the line for some time intervals, it can be seen that the impedance trend passes through the fixed PF lines. As the load value is fixed, this phenomena happens due to active and reactive power generation of wind turbine. Due to balanced loading, the impedance trends for the three phases are close to each other. Two different line nominal active power limits are defined for monitoring charts (P_n=50 kW (Blue circle) and P_n=70 kW (Brown circle) for each phase). It means that when the net active power flow of the line increases the limit of each phases, the measured impedance will pass

through the corresponding circle. Note that for power flow beyond the power limit, the impedance settled down inside the circle and vice versa. Like section 3.5.2 different alarms can be defined for distribution system operator awareness, based on the defined regulation.
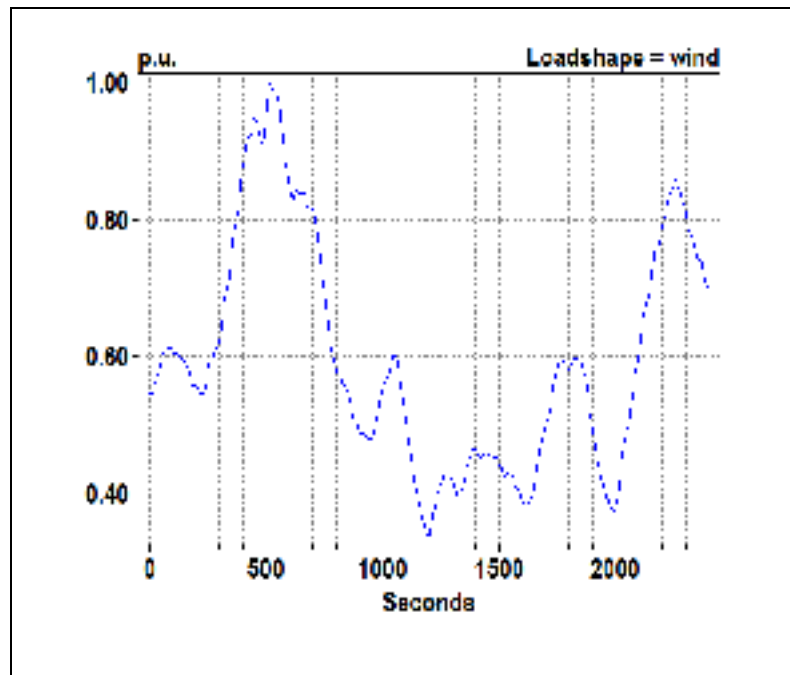
Figure 3.13 Wind power profile example
Adapted from Dugan (2012)

As it can be seen from Figure 3.14, for a typical wind turbine power generation such as the Figure 3.13, the reactive power requirement chart is violated more than once.
Therefore, for high penetration level of renewable energy integration, installation of real time monitoring devices such as the proposed method is recommended to ensure the reliable operation of distribution system.
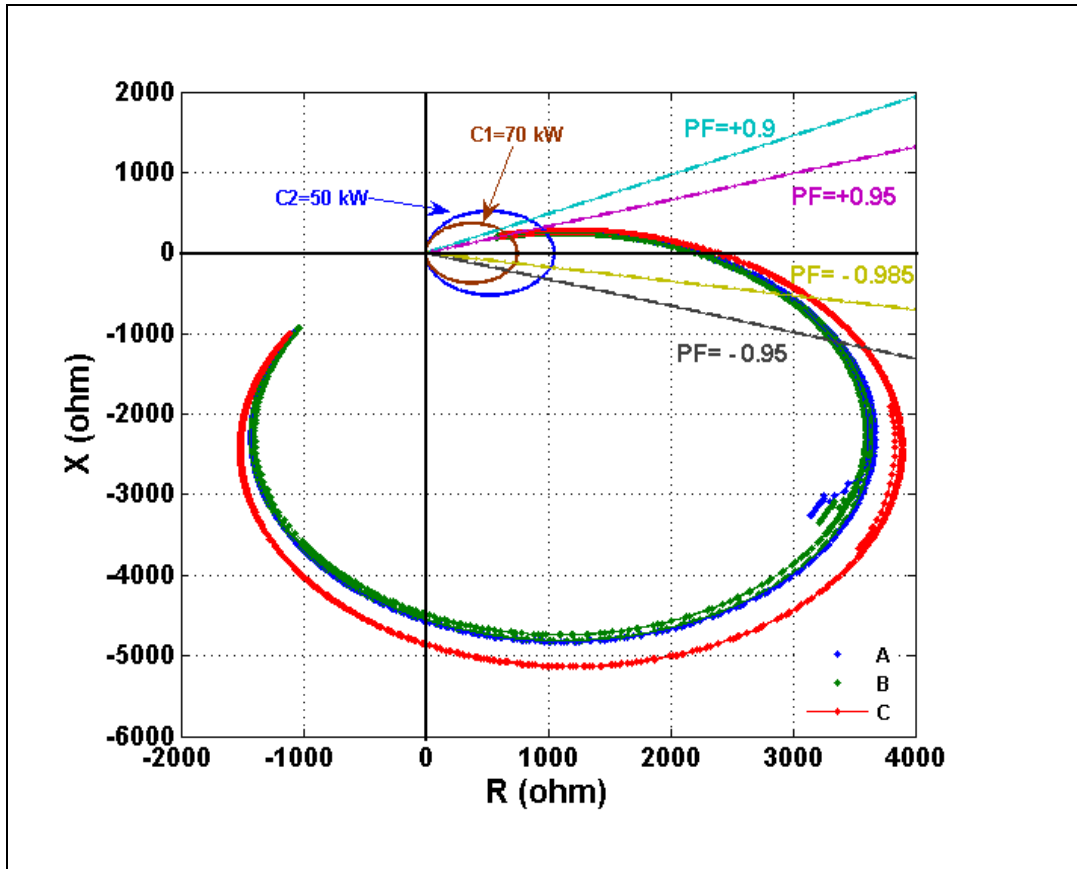
Figure 3.14 The output of three phase impedance measuring unit plot
on the AESO reactive power requirement chart

3.7   Conclusion

For a long time, the distribution system was designed based on the radial power flow assumptions. By integration of variable and intermittent RES to the distribution system, some assumptions (such as: radial power flow, little chance of over-voltage happening and etc.) which were used as a basis for distribution system design are not true anymore.

This chapter shows the necessity of online monitoring system for important feeders in distribution system. It was shown that the apparent impedance measured on the feeder has great capabilities for on line monitoring of distribution feeder.

This chapter establishes the steady-state mathematical model for defining the monitoring zone in *R-X* plane as the main contribution. It was shown that the apparent impedance has a good potential for monitoring of feeder power factor, reverse and forward active and reactive power flow. In addition, it was shown that complex power curve can be transferred to R-X plane to monitor the reactive power requirement regulation issued by utilities for RES integration.

Authors are working on using this method for reactive power management in distribution system with high RES integration.

CHAPITRE 4

A Modified Load Encroachment Technique for
Power Factor Monitoring

Hashem Mortazavi[1], Hasan Mehrjerdi[2], Maarouf Saad[1], Serge Lefebvre[3] and Dalal Asber[3]

[1]Department of Electrical and Computer Engineering, Ecole de technologie supérieure,
1100 Notre-Dame West, Montréal, Quebec, Canada H3C 1K3
[2]Qatar University, Doha, Qatar
[3]The Research Institute of Hydro-Quebec (IREQ), Power Systems and Mathematics,
Varennes, Quebec, Canada

Abstract

This chapter presents a new approach in application of distance relay in power distribution system. During the heavy load conditions, the load encroachment of impedance into the distance relay protection zones is a well-known reason for distance relay mal-operation. Therefore, all the modern digital distance relays are equipped with the load encroachment scheme which prevents the mal-operation of relay during the heavy load conditions. This chapter proposes the idea of using the load encroachment scheme of distance relay for monitoring purpose in presence of RES integration. Furthermore, it will be presented that based on the defined monitoring zones some alarms can be defined. In other words, an integrated feeder protection and power factor monitoring technique based on the impedance measurement will be proposed. The OpenDSS and Matlab software are used to test the effectiveness of the method with the IEEE 8500 node test feeder. The proposed method is

88

tested with the unbalanced distribution system feeder loading and distributed model of solar generations. The dynamic performance of the proposed method is studied for on-line power factor monitoring of the feeder with the fast sun irradiation dynamic.The results show the necessity of power factor monitoring in distribution system with RES integration. In addition, the simplicity of the proposed method allows its easy application in the digital distance relay.

4.1   Introduction

Integration of variable and intermittent source of electricity to the power system such as wind, solar and biomass to traditional power system not only improves the feeder voltage profile, decreases power loss and peak load shaving, but also raises a lot of challenges for the systems protection, control and operation.

According to the literature, radial and unidirectional feeder power flow is the first assumption for distribution system design. In this assumption the voltage profile is maximum at the sending-end of feeder and decreases proportional with loads to the receiving-end of the feeder (Kersting, 2012). By integration of variable and intermittent renewable energy source and feeder load profile, the power flow may reverse in the feeder. Therefore, considering the feeder load distribution and RES intermittent generation, unidirectional feeder will change to a bidirectional feeder for an unspecified of time, which impacts not only on the feeder voltage regulation, but also on the feeder protection philosophy.

More than 70% of the faults on the overhead lines are of the single phase to ground type (Shateri et Jamali, 2009). Traditionally, overcurrent relay has been used as the main protection on the distribution system for instantaneous and timed tripping of the feeder breaker. Moreover protective relay coordination based on the current is relatively easy in radial networks. The addition of RES into distribution systems can result in increased requirements for the feeder protection scheme. The integrated RES to the system, contributes to the fault current in addition to the grid current (Baran et El-Markaby, 2005). Therefore, the

fault current measured by the protective relay is greater than the original fault current from the main source. Depending on the size, type, installation locations, and number of the RESs their impacts on the fault currents vary. High RES integration impacts on distribution system protection and operation was analyzed in (Baran et al., 2012). In addition, most of the DGs are connected to the distribution network through the power electronic inverters. Solutions to the impact of DG on protection devices have been presented in (Rajaei et al., 2014),(El-Khattam et Sidhu, 2008) where the authors suggest a novel fault current management technique for radial distribution systems. In (Saleh et al., 2015) to (Coffele, Booth et Dysko, 2015) authors propose adaptive scheme for coordination between over current relays in distribution system with high penetration of distributed generation. Authors in (Nikolaidis, Papanikolaou et Safigianni, 2015) proposes a communication-based directional overcurrent protection scheme for radial distribution lines with DG.

One of the most popular solutions proposed in the literature to solve the over current protection problem is using the impedance base protection of distribution feeder in presence of RESs and DGs. Distance relay was proposed as the main feeder protection relay in distribution system (Singh et Telukunta, 2014), (*Requirements for the Interconnection of Distributed Generation to the Hydro-Québec Medium-Voltage Distribution System (between 750 V to 44000 V), Hydro-Québec Std, no:E.12-01,2004*)(Uthitsunthorn et Kulworawanichpong, 2010). For accurate fault detection in distribution system with DG integration, a quadrilateral characteristic-distance relay is proposed to mitigate the reverse power flow side effects (Chilvers, Jenkins et Crossley, 2005). In (Singh et Telukunta, 2014) an adaptive Fuzzy rule based distance relay scheme is proposed as a solution for distance relay under reaching due to infeed currents from RES generation. In addition to protection capability of distance relay, in (Roberts, Guzman et Schweitzer III, 1993) it was shown that apparent measured impedance has a very good capability to measure and analyze the load conditions.

Since addition of RES generation to distribution system provide additional sources for feeding fault current; the traditional non-directional over-current protections will operates for

reverse faults, upstream of the protected zone. Therefore some utilities (*Requirements for the Interconnection of Distributed Generation to the Hydro-Québec Medium-Voltage Distribution System (between 750 V to 44000 V), Hydro-Québec Std, no:E.12-01,2004*), (*Distributed Generation Technical Interconnection Requirements - Interconnections at Voltages 50kv And Below, Hydro One Networks Inc Std, no: DT-10-015, Rev. 3, 2013*) recommend using of a distance relay as the main feeder protection in their DG interconnection standard at distribution level. For instance, Hydro-Quebec recommend a distance relay installation on the feeder instead of an over current relay for conditions such as: possibility of outage of one of installed DG in the feeder, intermittent DG generation characteristic and etc.

Meanwhile, the load encroachment of impedance into the distance relay protection zones is a well-known reason for distance relay mal-operation (Fenghai, Kostic et Zhiying, 2015). Traditionally, load encroachment affects the zone 3 of the conventional distance relay. Thus, For heavily loaded lines, the load encroachment scheme is used for improving the accuracy of the distance protection (Sinclair et al., 2014). In addition, distribution system is a time varying system with unbalanced load. Addition of intermittent generation units such as RES increases the importance of distribution system monitoring. Different monitoring system approaches have been proposed to evaluate current conditions of distribution system. In (Valverde, Saric et Terzija, 2013), for accurate state estimation of distribution network, correlated input variables were used to propose a stochastic monitoring technique. For real time analysis and voltage monitoring, Casali and et al. in (Casali, 2013) propose using phasors measurement unit in distribution system at presence of PV.

For reverse power flow detection at high PV penetration level, Mortazavi et al proposed an impedance based monitoring technique in (Mortazavi et al., 2015a). It was shown that the apparent impedance, not only is sensitive to small load variation, but also, changes corresponds to PV units generation fluctuations. The dynamic capability of proposed impedance based monitoring technique was validated by monitoring the impact of cloud movement on lumped and distributed PV units.

This chapter proposes a practical application of using the load encroachment scheme of distance relay for monitoring the feeder power flow in addition to its protection task. Several paper published in the recent years for application of distance relay in distribution system protection (Shateri et Jamali, 2009),(Baran et al., 2012) ,(Chilvers, Jenkins et Crossley, 2005), (Sinclair et al., 2014),(Fenghai, Kostic et Zhiying, 2015). Considering those solutions for protection application of distance relay, for the first time this chapter proposes monitoring capability of distance relay in distribution network. Some alarms have been proposed based on the impedance trend movement through the pre-defined monitoring zone due to RES generation variations.

This chapter is organized as follows: in Section 4.2 the basic theory of distance relay and its relationship with power flow will be explained. Section 4.3 describes the proposed load encroachment monitoring technique. IEEE 8500 node test feeder used as a case study for simulation is described in Section 4.4. The simulation results for load variation and distributed PV installation impacts on apparent impedance seen by distance relay is described in Section 4.5. Finally the conclusion is presented in Section 4.6.

4.2   Impedance relay Theory and Its relationship with Load Encroachment Monitoring Technique

4.2.1   Impedance measurement

Impedance relaying technique is the best tool for line protection in power system. The principle of this technique measures the line impedance at a fundamental frequency. Voltage and current data are used for this purpose and they generally contain the fundamental frequency signal added with harmonics and DC offset. In distance relay protection philosophy, the measured impedance between the relay location and the fault point, determines if a fault is internal or external to a protection zone. In the proposed application the apparent impedance is used as a pattern recognition tool in order of distribution system monitoring.

The Z_A, Z_B, and Z_C are the measured apparent impedance of the line at the relay location using (4.1):

$$Z_A = \frac{\bar{V}_A}{I_A}, \ Z_B = \frac{\bar{V}_B}{I_B}, \ Z_C = \frac{\bar{V}_C}{I_C} \tag{4.1}$$

Where $\bar{V}_A, \bar{V}_B$ and $\bar{V}_C$, are the voltages at the relay location and I_A, I_B, and I_C, are the currents through the relay.

The impedance calculated using (4.1) is the positive sequence impedance seen of the line for all system operation condition except the fault conditions. For accurate phase to ground distance protection of line, a zero sequence current compensator is employed for actual system impedance measurement during the fault conditions. Based on (Shateri et Jamali, 2009), all the phase-ground faults detection units measure the same impedance value for the non-fault conditions.

4.2.2   Current infeed due to DG integration

The integration of DG (and RES) has a significant impact on feeder currents and its protection consequently. Consider a simple radial distribution feeder connected to substation by a transmission line of impedance $Z_{th.}$ As shown in Figure 4.1, V_G is the sending-end voltage of feeder. Consider Z_{L1} as the total impedance of the feeder. The DG point of interconnection (*POI*) is located at the distance of d from the sending-end of feeder. The impedance relay under consideration is located at sending-end of feeder and has V_G and I_G as its inputs.
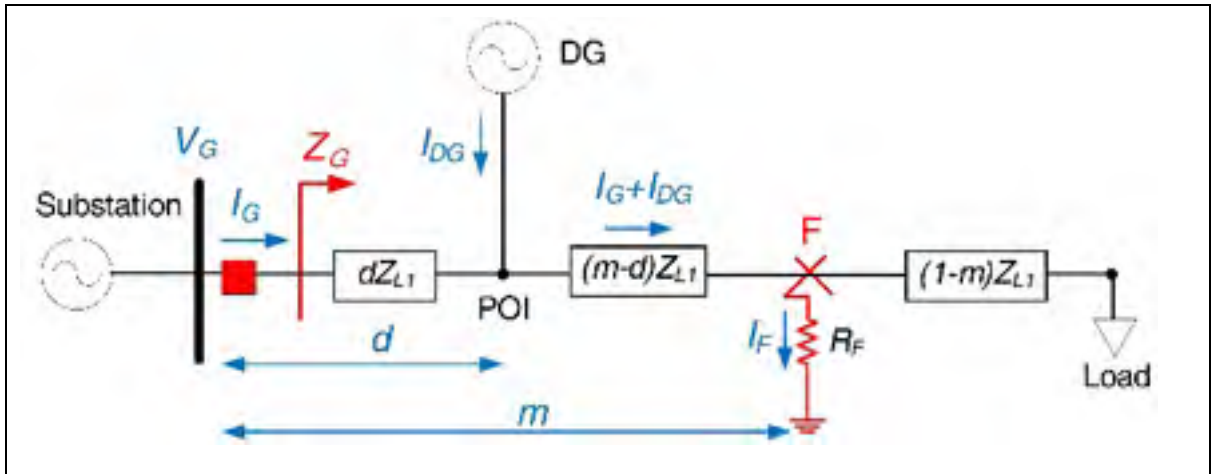
Figure 4.1 Simple distribution feeder with a DG and fault located downstream
Adapted from DG Das, Santoso et al. (2014)

Consider the case of a three-phase fault with a fault resistance of R_F at the distance m from the sending-end of the circuit as it is shown in Figure 4. 1. The fault current at the sending-end of the feeder with no DG generation can be calculated as follows:

$$I_{F-NoDG} = \frac{V_{sys}}{mZ_{L1} + R_F + Z_{sys}}$$

(4.1)

Where

Z_{L1} is the total impedance of the feeder.

R_F is the fault resistance.

V_{sys} is the Thevenin equivalent voltage of the source.

Z_{sys} is the Thevenin equivalent impedance of the source.

When the DG generation is added (by neglecting the load), if Z_{DG} is considered as the impedance from the DG to point of interconnection, the total fault current is as follow:

$$I_F = \frac{V_{sys}}{(m - d)Z_{L1} + R_F + \dfrac{Z_{L1} \times Z_{DG}}{dZ_{L1} + Z_{DG} + Z_{sys}}}$$

(4.2)

With a DG integration to the distribution grid, distribution feeders are no longer radial. Comparison between (4.1) and (4.2) shows that the addition of generation unit (DG or RES) increases the fault current, but reduces the fault current contribution from the substation.

In this condition, by occurring a fault downstream of the DG unit *POI*, Eq. (4.2) shows that, DG contribute to the total fault current and will modify the apparent impedance seen from the substation, consecutively. For these situations, the overcurrent protection have a reach that varies with changes in the upstream feeder current, the DG generation and fault impedance. This situation get worse when RES with intermittent generation integrates to the feeder. Based on the literature and some DG interconnection guidelines (*Distributed Generation Technical Interconnection Requirements - Interconnections at Voltages 50kv And Below, Hydro One Networks Inc Std, no: DT-10-015, Rev. 3, 2013 ; Requirements for the Interconnection of Distributed Generation to the Hydro-Québec Medium-Voltage Distribution System (between 750 V to 44000 V), Hydro-Québec Std, no:E.12-01,2004*),, installation of directional overcurrent relay or impedance type of protection is recommended to block tripping from DG infeed during adjacent feeder fault conditions.

According to (*Requirements for the Interconnection of Distributed Generation to the Hydro-Québec Medium-Voltage Distribution System (between 750 V to 44000 V), Hydro-Québec Std, no:E.12-01,2004; (*Sinclair, Finney et al. 2014), *Distributed Generation Technical Interconnection Requirements - Interconnections at Voltages 50kv And Below, Hydro One Networks Inc Std, no: DT-10-015, Rev. 3, 2013 *), distance relays can provide a more reliable and secure protection scheme. Distance relay are impedance based and provide a fixed reach, while overcurrent protection has a variable reach especially with intermittent RES integration (Sinclair et al., 2014). In order to analyze the impact of the DG generation and fault current on impedance based protection scheme, the voltage drop is calculated by:

$$V_G = dZ_{L1}I_G + (m - d)Z_{L1} \times (I_G + I_{DG}) + R_F I_F \tag{4.3}$$

In (4.3), V_G and I_G are the voltage and current inputs of impedance measuring unit located at the substation. The measured apparent impedance seen from substation Z_G, as it was shown in Figure 4.1, is calculated by:

$$Z_G = \frac{V_G}{I_G} = mZ_{L1} + (m - d)Z_{L1}(\frac{I_{DG}}{I_G}) + R_F(\frac{I_F}{I_G}) \qquad (4.4)$$

The effect of intermediate in-feed to the measured impedance can be seen from the equation (4.4). According to (4.4), the apparent impedance seen by the measuring unit is function of impedance to the fault point (mZ_{L1}), fault resistance and DG current infeed for short circuit condition. It can be seen that Z_G increases by $(\frac{I_{DG}}{I_G})$. The larger the DG in-feed is the bigger is the impedance seen by impedance measuring unit. In this condition, the impedance measured is larger than the actual impedance. The error is proportional to the ratio of DG currents I_{DG} and feeder source current I_G. In normal feeder operation (non-fault condition), the DG current has impacts on the measured impedance, and cannot be neglected. Eqs. (4.2), (4.4) show that the negative effect of DG on the protective relay accuracy becomes more severe by increasing the distance from the main source to the fault point.

However, solutions to the impact of DG on distance relay have been presented in (Chilvers, Jenkins et Crossley, 2005),(Das, Santoso et Maitra, 2014),(Sinclair et al., 2014),(Singh et Telukunta, 2014),(Voima et Kauhaniemi, 2014). Therefore, in this paper, it is assumed that the impact of DG and RES integration on distance relay in distribution network is solved. Therefore, the main focus will be on the monitoring application of distance relay in presence of RES integration.

4.2.3 Distance relay load encroachment scheme

Increasing the loading of the transmission line or shifting the power flow from one line to another, under stressed operating conditions, may cause the measured apparent impedance of the line to enter the protection zones of a distance relay. This phenomenon is referred as load

encroachment. The effect of load on the operation of distance relays is well known and is studied in several papers. The load encroachment of impedance into the distance relay protection zones is a well-known reason for distance relay mal-operation (Fenghai, Kostic et Zhiying, 2015). Traditionally, load encroachment affects the zone 3 of the conventional distance relay. Thus, correct zone selection and proper setting are important for the three-phase fault discrimination from load encroachment.

Figure 4.2 shows the Mho characteristic trip zone of a distance relay and the load encroachment region for normal line loading. For heavily loaded lines, the load encroachment scheme is used for improving the accuracy of the phase distance or phase overcurrent protection (Sinclair et al., 2014). In load encroachment scheme the apparent impedance seen from the sending-end of the feeder is measured. If the measured apparent impedance drop within the load encroachment region shown in Figure 4.2, the load-encroachment scheme blocks tripping of the phase distance relay due to the heavy loading.
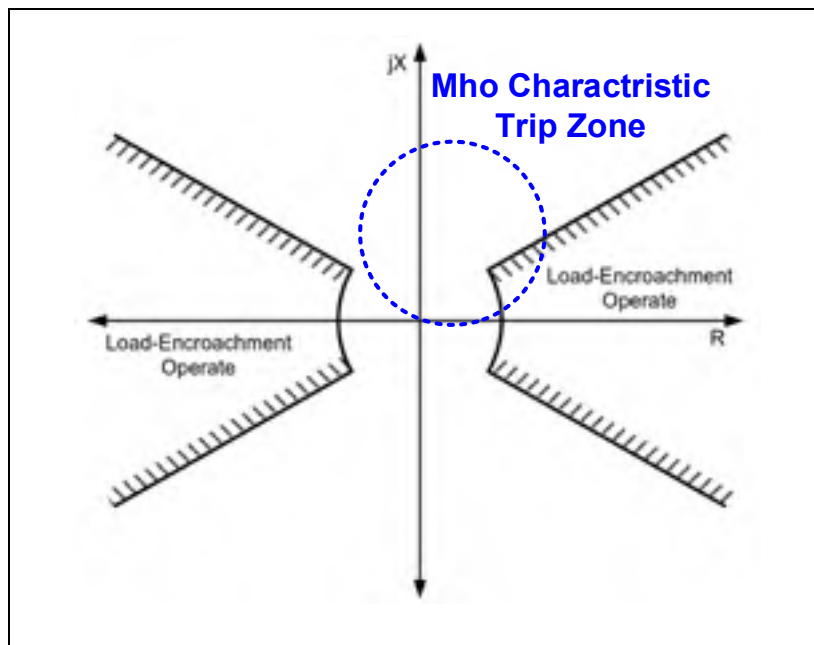
Figure 4.2 Load-encroachment characteristic
Adapted from Sinclair, Finney et al. (2014)

4.2.4   Relationship between R-X plane and P-Q plane

Let us consider a simple feeder as shown in Figure 4.1. The distance relay measuring unit installed at the sending-end of feeder and measures the current flow through the line (I_G) and bus voltage (V_G) and then the apparent impedance seen by distance relay is calculated by the complex ratio of the voltage to the current. Consider that P_G and Q_G are the active and reactive power flowing down from measuring point. Apparent impedance seen from node G is calculated:

$$I_G = \left(\frac{S_G}{V_G}\right)^* = \left(\frac{P_G + jQ_G}{V_G}\right)^* \tag{4.5}$$

$$Z_G = \frac{V_G}{I_G} = \frac{V_G}{\left(\frac{P_G + jQ_G}{V_G}\right)^*} \tag{4.6}$$

$$Z_G = \left(\frac{P_G + jQ_G}{P_G^2 + Q_G^2}\right) \times |V_G|^2 \tag{4.7}$$

Eq. (4.7) shows the relationships between the measured apparent impedance at bus G and the active and reactive power transmitted through the line at the measuring point. The measured Z_G is a complex value and has real and imaginary parts.

$$R_G = \left(\frac{|V_G|^2}{P_G^2 + Q_G^2}\right) \times P_G \tag{4.8}$$

$$X_G = \left(\frac{|V_G|^2}{P_G^2 + Q_G^2}\right) \times Q_G \tag{4.9}$$

Eqs. (4.8), (4.9) show that the R-X plane is a mapping of P-Q plane by a positive mapping factor such as $\left(\frac{|V_G|^2}{P_G^2 + Q_G^2}\right)$. Each point on R-X plane corresponds one-to-one to a point in P-Q

plane. Therefore, the R-X plane reacts simultaneously to every change in the P-Q plane. Since the mapping factor is always a positive quantity there is a sign consistency between the two planes. Therefore, the sign of R_G in (4.8) and X_G in (4.9) are only related to the sign (direction) of P_G and Q_G, respectively (Mason, 1956). In addition, the apparent impedance seen by the measuring unit is inversely proportional to the apparent power flowing on the line. If the apparent power doubles up, the impedance seen by relay will reduce by 50%.

4.3   Load Encroachment Monitoring Technique

RES integration to network not only has effect on the feeder protection sensitivity and accuracy, but also has effect on the conventional voltage regulation , Volt-VAR control and power factor correction (Bollen et Hassan, 2011). There are very few publications regarding monitoring of MV and LV feeder in distribution system despite many smart meter application for the residential and commercial consumer. It was shown that by RES integration to distribution system the distribution system protection philosophy changes from a conventional over current based protection to using modern distance relay. Moreover, it was shown that the distance relay prone to mal-operates due to load encroachment phenomena.

This chapter proposes the idea of using the load encroachment scheme of distance relay for monitoring purpose in presence of RES integration. Furthermore, it will be presented that based on the defined monitoring zones some alarms can be defined. In other words, an integrated feeder protection and monitoring technique based on the impedance measurement will be proposed.

At the first step the load encroachment scheme will be used to monitor the feeder power factor variation. To perform this, the mathematics are needed for mapping power factor monitoring zone from *P-Q* plane onto the *R-X* plane that will be presented in the next sections.

4.3.1 Analyzing the power factor variation reasons

Distribution system traditionally has been designed for radial and unidirectional power flow. For example, in voltage regulation philosophy the flow of power is considered from sending-end of feeder (the higher voltage) to the receiving end of feeder (lower voltage). Integration of the RES to distribution systems, however, shows that based on the size and the installation location, the power flow may reverse (Jahangiri et Aliprantis, 2013). Therefore, for high penetration of RES, traditional unidirectional distribution system will change to a bidirectional system.

Based on IEEE 1459-2010 standard (IEEE Standard Definitions for the Measurement of Electric Power Quantities Under Sinusoidal, Nonsinusoidal, Balanced, or Unbalanced Conditions, 2010), the power factor defines as follow:

$$\mathrm{PF} = \frac{\mathrm{P}}{\mathrm{S}} = \frac{\mathrm{P}}{\sqrt{\mathrm{P}^2 + \mathrm{Q}^2}} \qquad (4.10)$$

Eq. (4.10) shows, regardless of the source of power generation in the distribution system (substation or RES), any changes in the feeder power flow causes the PF fluctuation.

Furthermore, feeders with in-range power factor correction at the substation have portions that are not well corrected (particularly at the feeder's end, where the power factor is much lower) (Short, 2014). In addition, the calculated capacitor bank size to correct power factor, may become over-compensated during peak VAR conditions. Meanwhile Willis in (Willis, 2010) shows that more than one-third of all switched capacitors in one utility did not have proper operations due to mechanical failure and weather conditions.

Moreover, reactive power flow in a feeder increases both the voltage drop and loss. In a well-designed, unidirectional distribution network, due to non-uniform load distribution and distributed load the feeder power factor is not constant and changes along the feeder.

However, the RES integration to feeder will increase the possibility of feeder PF violated beyond the designed value. Therefore, the necessity of monitoring the feeder PF and taking action to keep it in the range is increased by RES integration.

4.3.2 Fixed power factor line mapping from P-Q plane to R-X plane

In order of implementing the power factor monitoring in a distance relay, the mapping concept will be used to develop the relationship between the measured impedance and power flow quantities. To do so, for an impedance measuring unit, located at sending-end of Figure 4.1 (V_G and I_G as its inputs) the apparent impedance measured by an impedance measuring unit is calculated by Eq.s (4.8) and (4.9).

Practically, close to unit power factor operation of distribution system is desirable. However, it was shown by (4.10) that the feeder power factor is a local parameter and can be easily changed by power flow variations. Therefore, electric utilities tend to define some regulation for interconnection requirements for power factor variation range due to the RES integration at the *POI*.

For example, based on the Hydro-Quebec interconnection guideline (*Requirements for the Interconnection of Distributed Generation to the Hydro-Québec Medium-Voltage Distribution System (between 750 V to 44000 V), Hydro-Québec Std, no:E.12-01,2004*), the customer load at the point of interconnection must have a power factor range of 95% or higher for large-power customers, and range of 90% or higher for medium- and small-power customers. In FERC Order 661-A (FERC Order No. 661-A, December 12, 2005.), the reactive capability requirement recommended for wind farm generation is up to 0.95 lag to lead at the POI.

Fixed power factor operation of feeder is a line in *P-Q* plane. For mapping that line from *P-Q* plane to *R-X* plane, (4.9) divided by (4.8) results in:

$$\frac{X_G}{R_G} = \frac{Q_G}{P_G} = \tan \varphi \qquad (4.11)$$

Where φ is defined as the power factor angle of the feeder. Eq. (4.11) shows that mapping a straight line passing through the origin in *P-Q* plane is a straight line passes through the origin in *R-X* plane.

4.3.3   Modified Load Encroachment Monitoring Technique

All the modern digital distance relay equipped with the load encroachment function. The setting calculations of the load-encroachment characteristics are easy, because they can be directly related to the maximum load conditions. Once the maximum load conditions of the feeder and the range of power factors of the load are defined the load-impedance areas can be found.
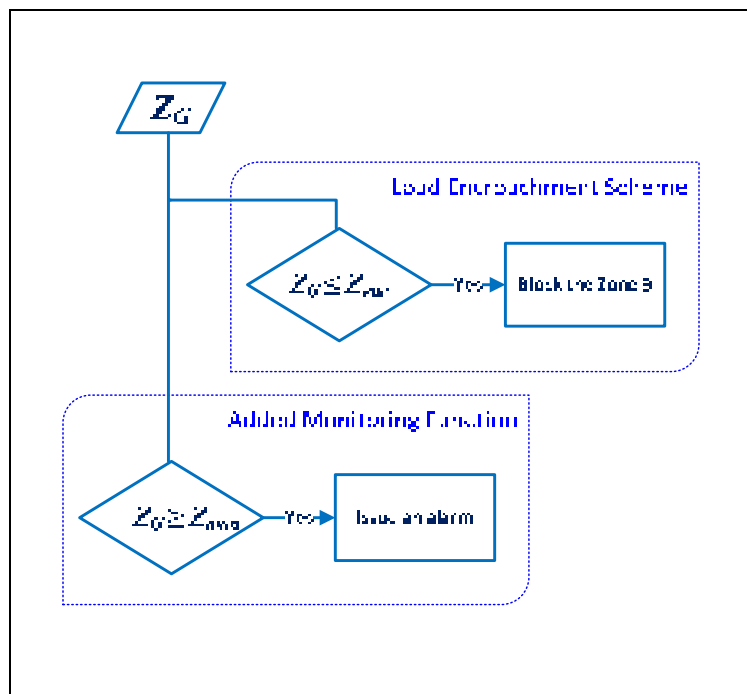
Figure 4.3 The modified load encroachment scheme

The flow chart in Figure 4.3 shows how the proposed load encroachment scheme of the system shown in Figure 4.1 operates using the new algorithm. First the values of apparent impedance seen by distance relay Z_G is measured. After the measurement process the traditional load encroachment scheme compare the Z_G with the defined load encroachment zone (Z_{enc}) and if it is found to be inside of its practical range then blocking of zone 3 should take place otherwise zone 3 is unblocked. The same process will be applied for the monitoring function, except that if the Z_G is found outside of the defined monitoring zone (Z_{mon}) an alarm will be issued. It worth mentioning that this process will be run separately for each phase.

4.4   Case Study

To analyze the capabilities of proposed impedance based power factor monitoring technique, the IEEE 8500 Node Test Feeder (Figure 4.4) is chosen. It is a large 12 kV benchmark feeder introduced by the IEEE distribution system modeling working group. The 8500 node test feeder, according to (Arritt et Dugan, 2010), is a large network that has more than 2500 medium voltage nodes, all type of feeder configurations such as single, two and three-phase, overhead lines and cables, MV and LV lines. Four voltage regulators, one installed at substation and three distributed along the feeder, are used in this network. It has three controlled and one uncontrolled capacitors banks. This large and heavy loaded model, is a good case for testing the abilities of impedance based PF monitoring technique.

The OpenDSS (Dugan, 2012) and Matlab are used for simulation. The GridPV toolbox(Reno et Coogan, 2014) is used as a COM server interfaced between OpenDSS and the Matlab (Guide, 1998) for system simulation.

For RES penetration simulation, the solar PV model provided in OpenDSS is used as the RES model. Based on the simulation requirement, either the integrated and distributed model of PV system are installed at different locations. For analyzing the impact of RES generation on the measured impedance, the PV generation was increased from zero to 1.15 pu of the

nominal size of PV unit. The PV generation is increased one percent at each time step, and then a power flow was run by OpenDSS software. User written codes in Matlab are used to import the output data of all simulated cases produced by power flow in OpenDSS through the COM server interface. One-phase voltages of all buses, currents, active and reactive powers of all feeders, at each step saved in separate data file, were sent to MATLAB to use for impedance calculation. Then those data were analyzed by GridPV toolbox and user written scripts.
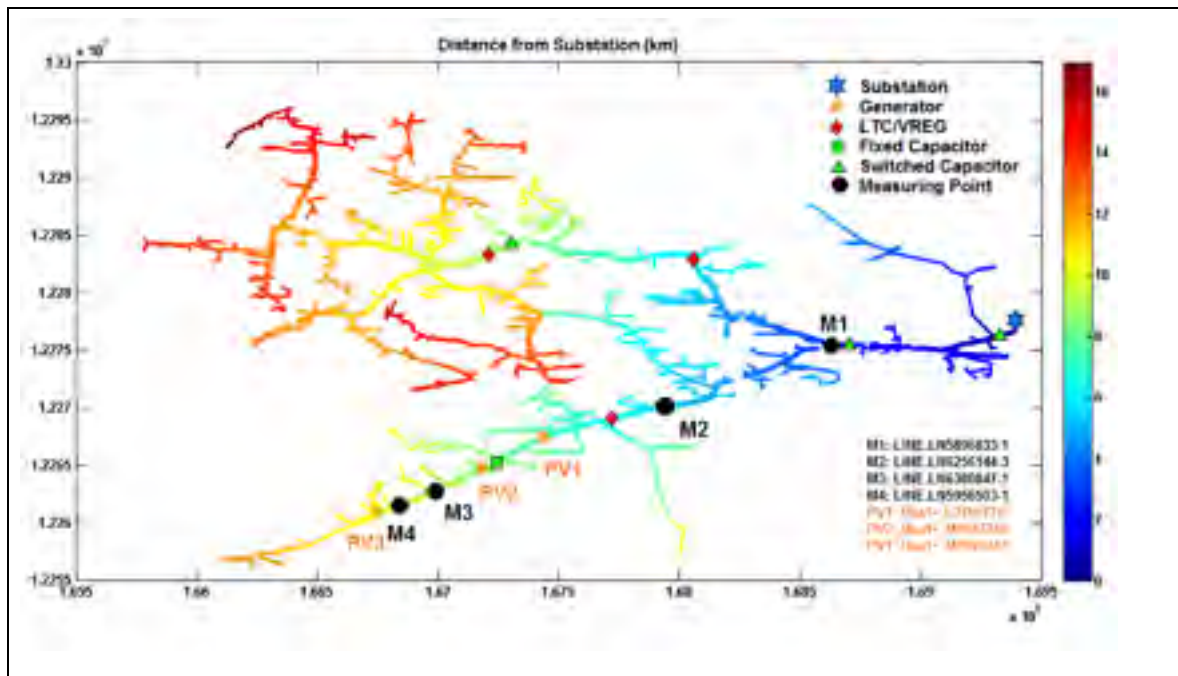
Figure 4.4 Schematic of the IEEE 8500 Node Test Feeder.
The lines coloring basis is the distance from the substation

Four measuring units were chosen at different locations on one of the main feeders to analyze the feeder behavior under changing conditions. The apparent impedance measuring units' locations are shown in Figure 4. 4. The basis of line color in Figure 4.4 is the distance (km) of each bus from the main substation.

Since in (Mortazavi et al.), the authors investigated the fault contribution of PV units and analyzed the capability of distance relay for distribution system protection and monitoring, the focus of this chapter will merely be on the monitoring applications of the distance relay.

4.5   Simulation Results and Discussion

4.5.1   Impedance and power factor trend due to normal load deviation

Distribution system has continuous load variation. In (Mortazavi et al., 2015a), it was shown that the apparent impedance seen by measuring devices has a distinctive changes due to different PV penetration levels. Figure 4.5 illustrate a typical normalized load patterns for which are applied to the IEEE 8500 test feeder.
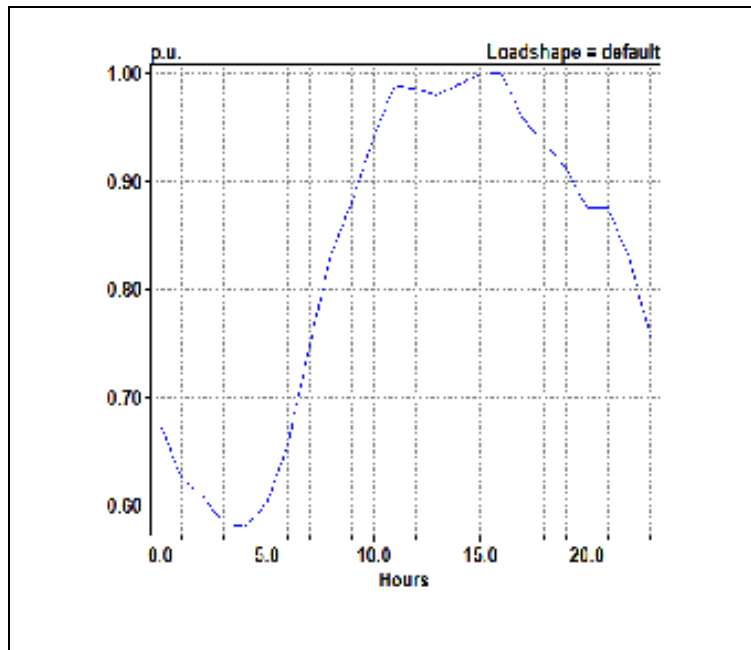
Figure 4.5 The normalized load patterns of residential loads

Figure 4.6 shows the exact value of active and reactive power for each feeder according to the distance from the substation for a snapshot of time series analysis (snapshot of t=24 h). The locations of four monitoring units are shown on the figure. As it can be seen, the reverse

reactive power happens at some locations (mostly caused by 900 Kvar fixed capacitor bank located downstream the monitor M2 and upstream of monitor M3).
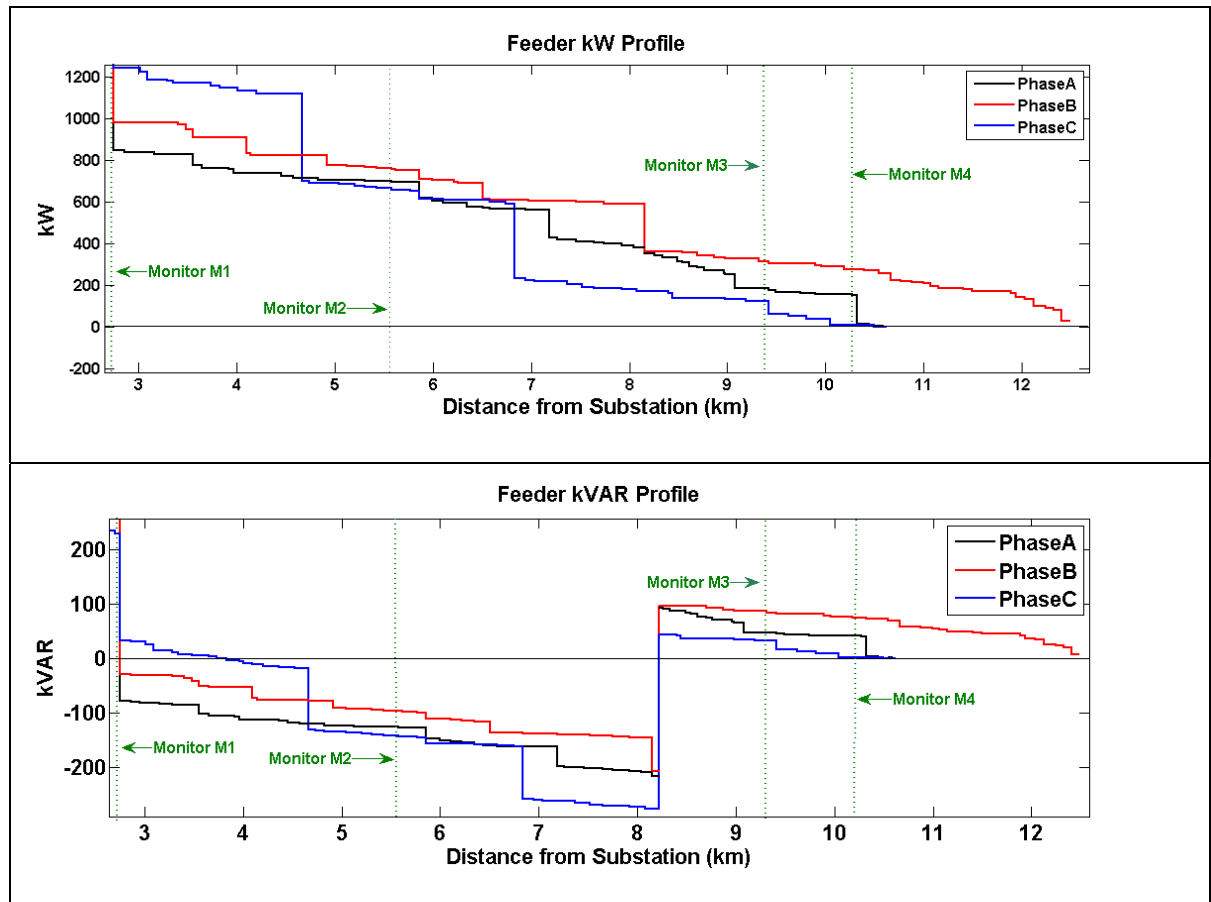
Figure 4.6 All feeder active and reactive power based on the
distance from substation (snapshot of t=24 h)

Figure 4.7 shows the measured impedance trajectories for *phase-A* at all the measuring point for typical load variation patterns. The second graph in Figure 4.7 is the zoom on the impedance variation for the sending-end of feeder measuring points (inside of circle). Due to big difference between the line loading at the sending-end and receiving end of the feeder the impedances variation are considerable.

 In this simulation, all the PV system generation set to zero. In (Mortazavi et al., 2015a), it was found that the small load variation shows its impact on the measured impedance. For this condition, while the measured impedance for *phase-A* at measuring point M1 changes from

13.023+j2.3074 (ohm) at the lightest load condition (58% of nominal load) to 13.645+j1.9465 (ohm) for the maximum daily load, the measured impedance at measuring point M4 changes from 8392+j2209 (ohm) to 8932+j2352 (ohm). The great difference between those measured impedances is due to the different load currents at measuring points (for the lightest load condition the current at M1 is bigger than 600 times of current at point M4).

Figure 4.8 shows the power factor variation due to the load variation based on the applied load pattern. While the PF has a small variation on the end of the selected feeder (M4 and M3) it has a detectable variation on the sending-end of feeder. This phenomenon happens due to impact of fixed and switched capacitor bank on the feeder PF.
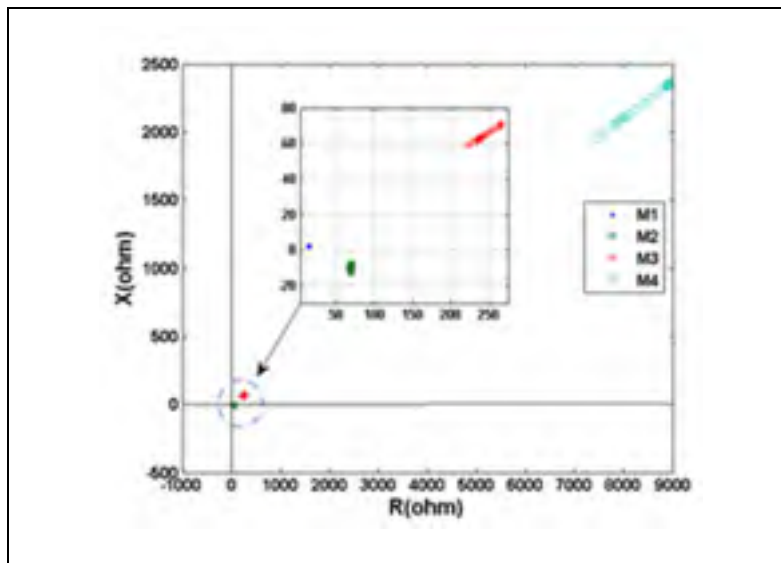
Figure 4.7 Phase-A measured impedance at four
measuring point for normal load variation condition
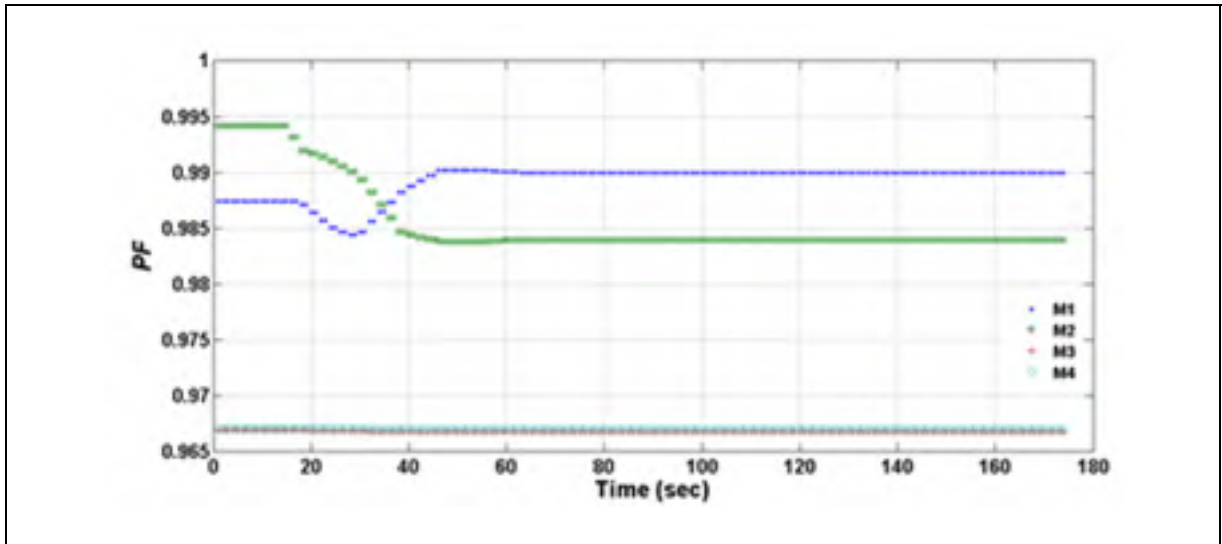
Figure 4.8 Phase-A measured PF at four measuring point
for normal load variation condition

4.5.2   The feeder PF monitoring with RES integration

Keeping the feeder PF close to unity could result in inadequate operation of feeder voltage regulator. Consequently, a range of power factor variation is defined by distribution system operation regulation. For example, in the Hydro-Quebec distributed generation interconnection guideline, a power factor range of 95% or higher is defined for large-power customers at the customer load point of connection. For medium- and small-power customers those ranges widen to 90% or higher at the connection point.

108
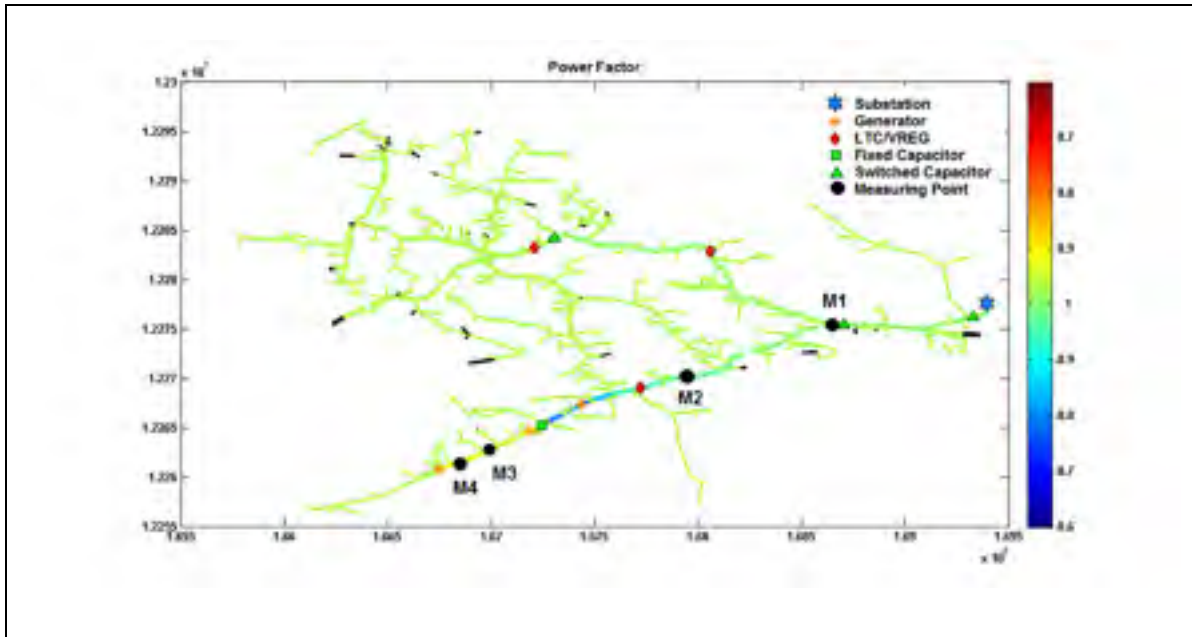
Figure 4.9 IEEE 8500 node test feeder power factor snapshot. The blue spectrum feeder
shows the lagging (capacitive) pf>1 and the red spectrum shows the leading
(inductive) pf<1. The PV units' location are shown by Orange stars

To simulate the feeder PF variations due to RES integration, three distributed PV units with
the same size of 300 kW are installed at three different locations, as they illustrated in Figure
4.9, on the selected feeder. Figure 4.9 shows a snapshot of the IEEE 8500, which the line
color is its PF. It can be clearly seen that most of feeders PF is in the range of +0.95 to 1. It
means that in this snapshot, the network PF is in the range except near the capacitor banks
and PVs location.

To simulate the impact of PV generation variation on the feeder PF profile a normalized
pattern of sun irradiance was chosen as the PV input. The data used to in this section for PV
unit generation are 1-second sun irradiation time series for 174 consecutive seconds is shown
in Figure 4.10.
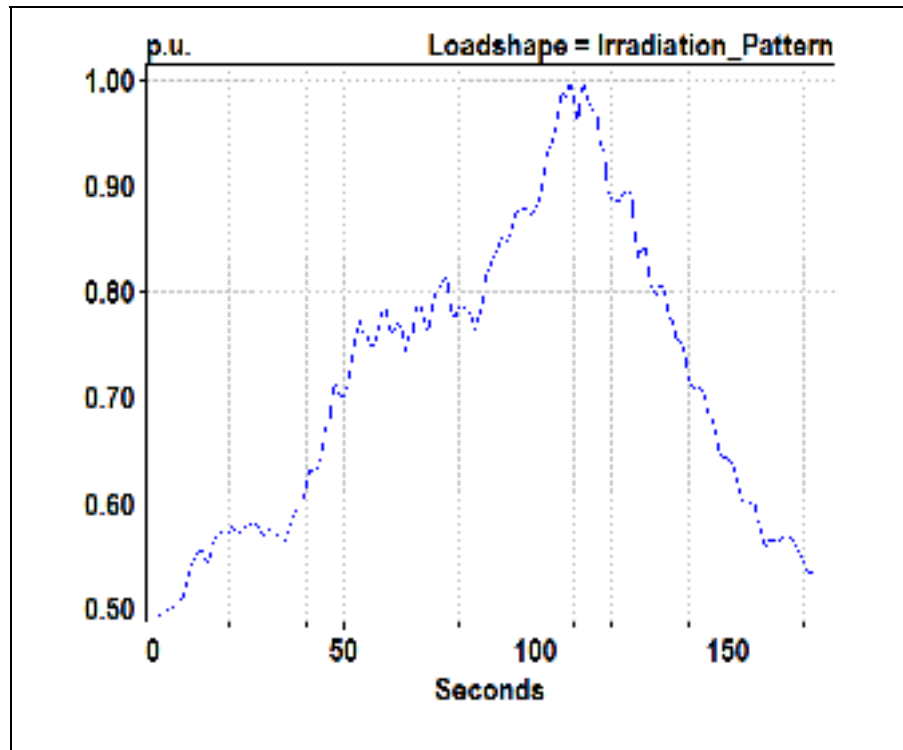
Figure 4.10 The normalized sun irradiation patterns on the PV units
Adapted from Dugan (2012)

Based on the Hydro-Quebec regulation the desired PF operation range is considered 90% and higher for monitoring purpose. The Figure 11 show the measured impedance variation due to the effect of sun irradiation fluctuations. The mapped PF limits for PF=± 0.9 are shown on the Figure 11. The pre-defined set points are defined for each monitor.

The impedance trend measured by each monitor shows unique patterns. While the impedance trend of measuring point M1 shows small reaction of measured impedance to sun irradiation on the PV units, the impedance trend of M2 shows the reverse of reactive power with the forward active power flow. Simultaneously, due to proximity to the PV units' location, the impedance trends in M3 and M4 shows a great reaction to sun radiation fluctuation. Furthermore, while the three phase impedance trends in M1 and M2 move inside the pre-defined PF limit, the impedance trend for each phase of monitors M3 and M4 has different patterns. For instance, while the PF in *phase-B* of M2 is inside the limit, for *phase-A* the impedance trend goes beyond the limit for some part of simulation, on the other hand,

phase-C impedance trend is outside of the limits for most of the time of simulation. While the *phase-A* and *B* of M4 shows the forward active and reactive power flow the *phase C* shows the reverse active and forward reactive power flow. Although in section III.A it was said that the PF will vary along the feeder length, here it was shown that not only the PF is not constant along the feeder, but also each phase PF is not the same as others.
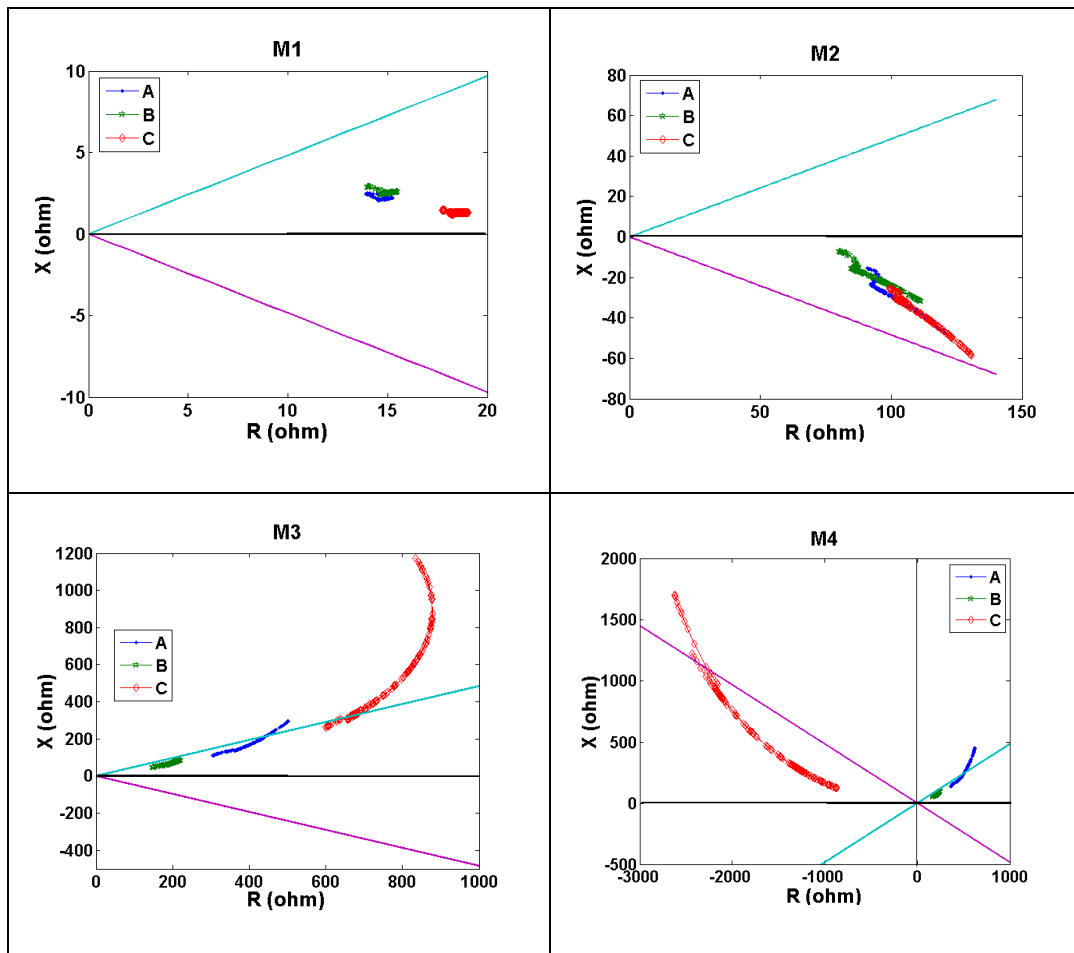
Figure 4.11 The measured impedance variations due to the effect of
sun irradiation patterns on the PV units

Figure 4.12 shows the PF trends for *phase-A* of four monitoring units due to sun radiation fluctuation effects on PV units. Comparing the Figures 4.8 and 4.12, shows that the RES integration has a substantial impact on the feeder PF profile and it must be considered as a side effect of RES integration to distribution system.
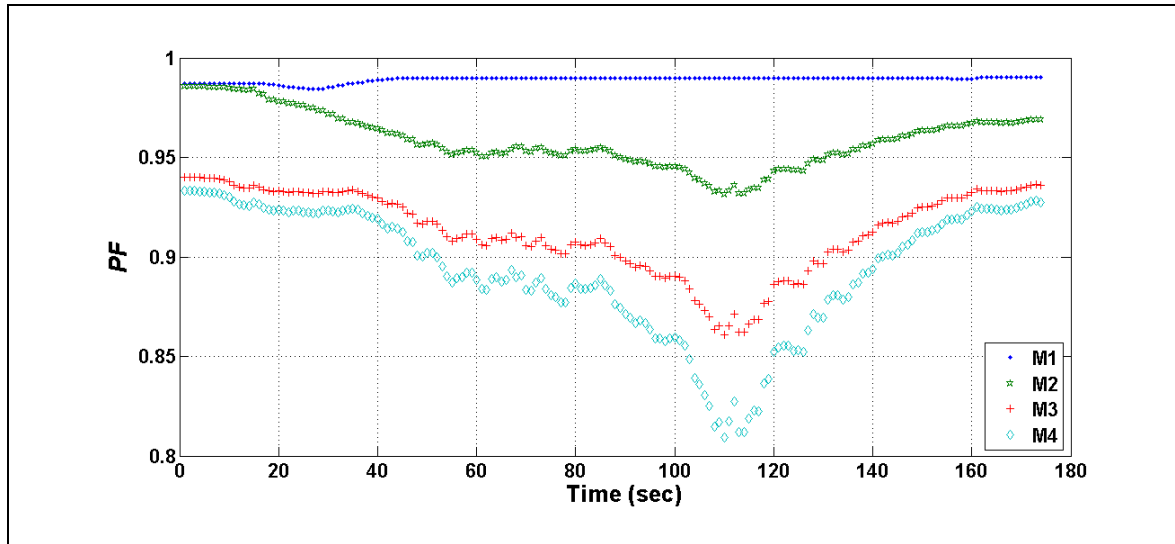
Figure 4.12 The PF variation due to the effect of sun irradiation patterns on the PV units

For awareness of the distribution network operator, a set of feeder PF alarms were defined. The set points are defined for pf = ±0.90 based on the Hydro-Quebec distributed generation interconnection guideline, for each monitor. The alarm will be issued, if the measured PF value goes beyond those limits. Figure 4.13 shows the output of alarm system for PV penetration level variation due to the effect of sun irradiation patterns on the PV units for measuring points M3 and M4.

It can be clearly seen by comparing the Figures 4.11 and 4.13, that monitor M3 detects inductive PF conditions for *phase-A* and *C* but at different times. The inductive PF alarms pick up and drop out are not the same for *phase-A* and *C*. Meanwhile, the defined alarm system only detects the inductive PF beyond the set point for the *phase-A* only. When power flows out, the load impedance is in the right of the X-axis. When power flows in, the load impedance is in the left-hand load impedance area. Since the distance relay is directional and it was set to look downward the feeder, the pre-defined alarm system did not react to *phase-C* reverse active power variation. Figure 4.14 shows the alarm output of the proposed method for reversed power flow PF detection. In this situation the distance relay can monitor reversed power flow PF variation.

112
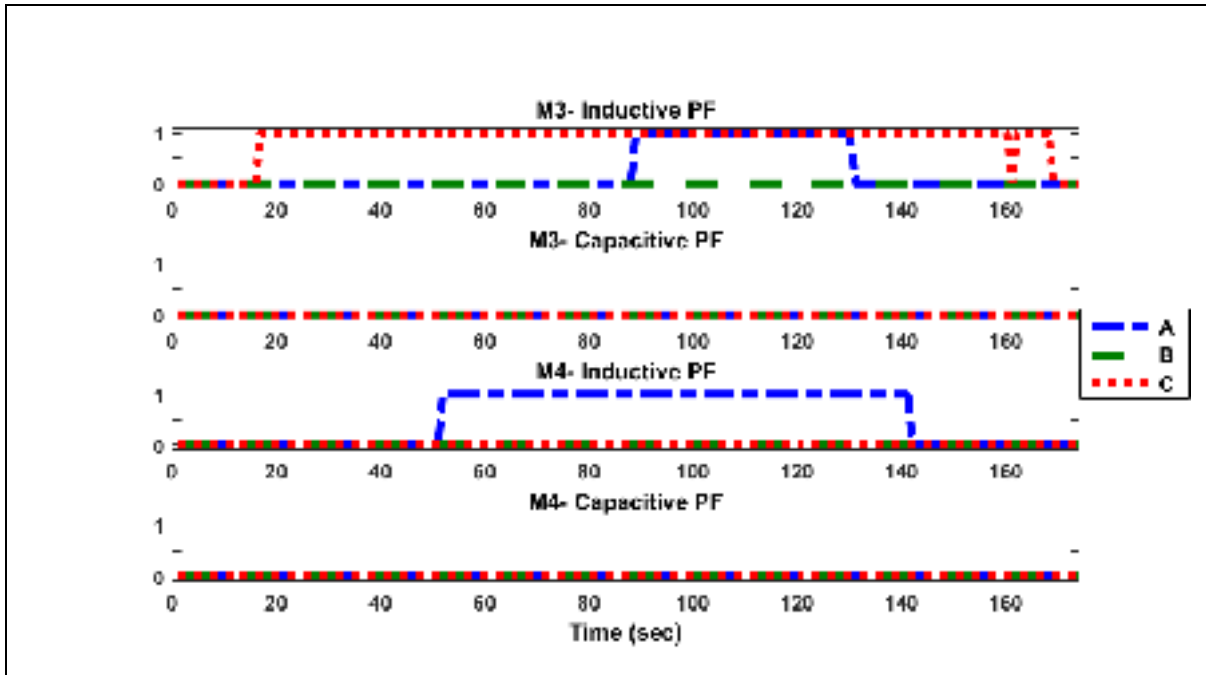
Figure 4.13 Alarm issued for PF beyond of the pre-defined limit,
for the same condition of the figure 4.12
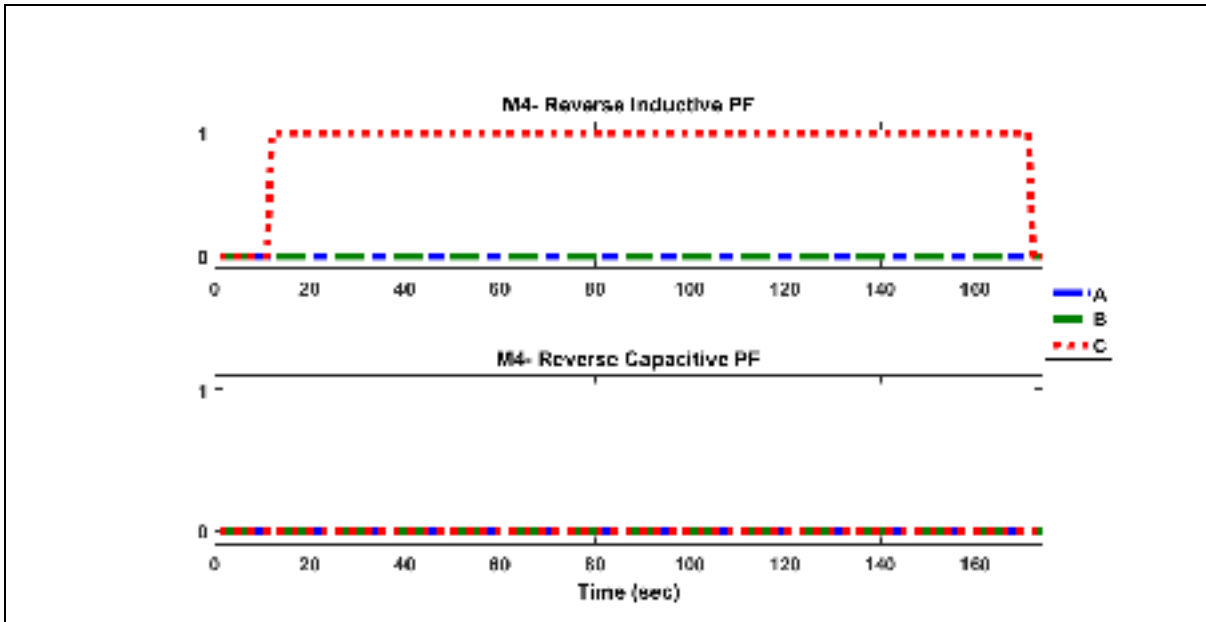
Figure 4.14 Alarm issued for reversed PF

The comparison of Figure 4.8 and Figure 4.11 shows that although the measuring point M2 shows the continuous under-excited condition (reversed reactive power only) for all the phases of that feeder, at any conditions the feeder power factor goes beyond the pre-defined settings (maintain its power factor between 0.90 and unity). Comparison of Figures 4.8, 4.9, 4.11 and Figure 4.12 emphasizes the necessity of the power factor monitoring units for critical feeder when there is high RES integration to that feeder. Because the feeder power factor may go beyond the distribution system designer limits, which its side effects were mentioned in section 4.3.

4.6 Conclusion

Based on the distributed generation interconnection standard, by RES integration to distribution system, utilities need to install distance relay as the main feeder protection device. In addition, the impedance of heavy loads can actually be less than the impedance of some faults. Yet, the distance protection must be made selective enough to discriminate between load and fault conditions. To perform this, modern digital distance relay utilizes the load encroachment scheme to ensure safe operation during the heavy load conditions.

This chapter shows the necessity of the power factor monitoring of the distribution system feeders. It was shown that the feeder power factor is not constant along the feeder and by RES integration the feeder power factor can be easily violated from the standard limits. In addition it was shown that the apparent impedance measured on the feeder has great capabilities for on line power factor monitoring of distribution feeder.

In this chapter, a load encroachment monitoring technique was proposed that is capable to monitor feeder power factor variations. The application of the proposed technique does not affect the normal operation of distance relay, because it is a modified load encroachment scheme. The only drawback of the proposed method is that it will use the cpu resource of digital distance relay, and it need more detailed investigation. Authors are working on using this method for power factor management in distribution system with high RES integration.

CONCLUSION

This thesis has investigated methods and techniques for distribution system monitoring with high RES integration. Through the measuring the sending-end voltage and current of the feeder and calculation of the apparent impedance, a novel impedance based monitoring technique has been successfully demonstrated for distribution system.

Integration of variable and intermittent source of electricity to the power system such as wind, solar and biomass to traditional power system not only improves the feeder voltage profile, decreases power loss and peak load shaving, but also raises a lot of challenges for the systems protection, control and operation. By integration of variable and intermittent renewable energy source, the power flow may reverse in the feeder. Therefore, considering the feeder load distribution and RES intermittent generation, unidirectional feeder will change to a bidirectional feeder for an unspecified of time, which impacts not only on the feeder voltage regulation, but also on the feeder protection philosophy. The introduction of a new methodology to monitor the feeder power flow have been the subject of this thesis.

The main impacts of integration RES intermittent generation on the feeder power flow and consequently on the feeder voltage profiles are presented in Chapter 1. Different approaches for mitigating the reverse power flow caused by RES integration were presented. In chapter one, it was argued that the modern distributions system vulnerability increases not only because of infrastructure aging, but also, because of RES generation. It increases the necessity of deployment of monitoring devices for different purposes. Therefore, the necessity of distribution system monitoring was presented in details in this chapter.

Due to necessity of monitoring technique for distribution system, first, a new impedance based methodology was presented in Chapter 2. It was shown that the calculated apparent impedance has high capability for detecting different states of distribution system in presence of RES integration. The results indicate that apparent impedance has the capability of monitoring for balanced and unbalanced system, is sensitive to load magnitude deviation,

116

feeder power factor variation and can detect fast transient phenomena such as cloud movement on centralized PV units.

Chapter 3 establishes the steady-state mathematical model for defining the monitoring zone in R-X plane as the main contribution. It was shown that the apparent impedance has a good potential for monitoring of feeder power factor, reverse and forward active and reactive power flow. In addition, it was shown that complex power curve can be transferred to R-X plane to monitor the reactive power requirement regulation issued by utilities for RES integration. The defining of the monitoring zone for different purpose and proposing this idea for online monitoring of wind farm reactive power capability cure are the most novel contributions of this chapter. The application of the proposed impedance based monitoring methodology has been validated through simulation with different case studies such as the IEEE 13 Node Test Feeder, the IEEE 34 Node Test Feeder and the IEEE 8500 Node Test Feeder.

As it was stated earlier, RES integration to distribution system, raises a lot of challenges for the systems protection, control and operation. From the feeder protection philosophy view, by RES integration the over current protection has not the capability to secure the safe operation of the feeder. One of the most popular solutions proposed in the literature to solve the over current protection problem is using the impedance based protection of distribution feeder in presence of RESs and DGs. In Chapter 4, it was shown that the so called distance relay as a protection device has the capability to monitor the RES integration to the feeder.The results indicate that a one-phase distance relay not only reacts to fault in its defined zone, but also can monitor the feeder for different RES penetration level and load variation. Since modern digital distance relay utilizes the load encroachment scheme to ensure safe feeder operation during the heavy load conditions, therefore a novel load encroachment monitoring technique was proposed in chapter 4 that is capable to monitor feeder power factor variations.

Future works

Some perspectives concerning the continuity of the present work and potential topics for future research are listed below:

Impedance based monitoring technique for electric vehicle integration

Develop techniques and model for analyzing the impact of electric vehicle integration on the feeder operation based on the apparent impedance monitoring technique. The time-series simulation is needed to be done to check the electric vehicle integration impacts on the feeder operation and the calculated impedance trends consecutively.

Power flow control method based on the calculated impedance

The focus of this thesis was on the monitoring application of the feeder apparent impedance. Based on the mathematics where proposed in the Chapter 3, some control action can be defined for proper feeder operation and control. An effort should be devoted in the development of a methodology for feeder power flow control based on the calculated impedance.
There are several techniques to use the calculated impedance for power flow control. Using the energy storage system for feeder power flow balancing is one of the recommendations. Based on the monitoring zone defined on the R-X plane and the calculated impedance, the charge or discharge command will be sent to the storage system control.

Application of PMU for distribution system monitoring

Phasor measurement unit (PMU) has different applications in power system protection, operation and control during normal and abnormal operation. Recently the application of PMU for distribution network is proposed in references. Normally the phasor value of voltage and currents are the output of PMU. Those phasor values can be used to calculate the

apparent impedance. Some techniques must be proposed to use the PMU data for implementing the impedance based monitoring technique.

Practical application of the proposed method by distance relay

Modern digital distance relay has a lot of calculation capabilities. Those capabilities can be used to test the practical application of the monitoring technique based on the distance relay. Implementing the proposed method as an extra function of relay or using the load encroachment function of relay will be the main focus of the idea. Different feeder grounding has substantial impact on the impedance calculation. Therefore a practical application guideline must be prepared to show different solutions for different grounding configuration.

Finding the optimal number of measuring points

Distribution network consists of numerous numbers of feeders. Due to financial constraints, monitoring of all feeders is impossible. Therefore optimization technique must be used to find the optimal location of measuring unit to reduce the number of measuring units for large distribution network.

Online monitoring the wind farm and micro-grid contract

In order of reliable operation of power system, the generating units must comply with certain active and reactive power requirement depending on the network they are connected. Although many of existing interconnection regulations have been based on traditional generating units' capabilities, the increasing rate of RES integration forces the power system regulators to consider variable type of generation in their standards and practical procedures. For example, some transmission service providers define certain reactive power requirements for wind power integration to their system. The proposed impedance based monitoring

technique has the capability of online monitoring of the utility active and reactive power requirement.

Analyzing the accuracy of the proposed method for harmonic distorted distribution network

Modern distribution system has higher total harmonic distortion (THD) in comparison with the traditional distribution system. Harmonics are the by-products of modern electronics appliances. Using solid state power switching technique in uninterruptible power supplies (UPSs), non-linear loads and power electronic drives are the main sources for high THD in modern distribution network. A harmonic sensitivity analysis is needed to be done to check the accuracy of the proposed monitoring technique in modern distribution network.

Impedance measurement details

In this section more details will be presented about the impedance measurement. The apparent impedance seen from any point on a feeder is calculated by three single phase measuring units. Each unit uses only a single phase current and a single phase voltage. Considering that V_{AN} is the phase A to ground voltage and I_A is the current flows through the phase A conductor, the apparent impedance seen for phase A is given by (Hase, 2007):

$$Z_A = \frac{V_{AN}}{I_A} \tag{AI.1}$$

The impedance calculated using (AI.1) is the positive sequence impedance for all system operation condition except fault conditions (Hase, 2007). For each feeder, 3 separate one-phase impedance measuring unit is installed for accurate measurement of apparent impedance.
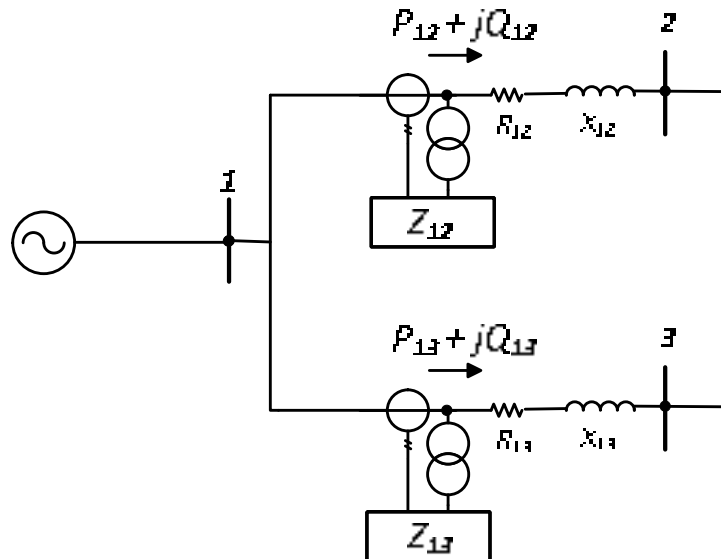
Figure AI.15 The impedance measuring unit is connected
to sending-end of each line connected to the bus i

Figure AI.1 shows a simple 3 buses system. For each feeder, for example feeder 1-2 three voltage transformer (VT) and current transformer (CT) are needed to be installed. The same

configuration will be replicated for any other feeder in the network that a measuring unit will be installed.

APPENDIX II

PV system and impedance measuring point data for IEEE Test Feeders

❖ **IEEE 13 Node Test Feeder**

Table AII.1 IEEE 13 Node Test Feeder

measuring point locations

Bus number	Line number
650632	650632
632670	632670
670671	670671
671680	671680

Table AII.2 IEEE 13 Node Test Feeder PV system locations

PV name	Bus number (Bus number)	Power (KW)
PV1	680	3800

❖ **IEEE 34 Node Test Feeder**

Table AII.3 IEEE 34 Node Test Feeder

measuring point locations

Bus number	Line number
800802	L1
850816	L24
854852	L27
858834	L29

Table AII.4 IEEE 34 Node Test Feeder PV system locations

PV name	Bus number (Bus number)	Power (KW)
PV1	816	200
PV2	832	200
PV3	828	200
PV4	852	200
PV5	888	200
PV6	848	200
PV7	860	200
PV8	840	200
PV9	862	200
PV10	842	200
PV11	864	300

❖ **IEEE 8500 Node Test Feeder**

Table AII.5 IEEE 8500 Node Test Feeder

measuring point locations

Monitor name	Line number
A	LN5815900-1
B	LN6381853-1
C	LN6109158-1
D	LN6380847-1

Table AII.6 IEEE 8500 Node Test Feeder PV system locations

PV name	Bus number (Bus number)	Power (KW)
PV1	m1026347	300
PV2	L2766718	300
PV3	m1026851	700
PV4	m1026808	300
PV5	m1027023	300
PV6	m1009805	300
PV7	m1026708	300
PV8	m1026854	300
PV9	m1047737	300
PV10	L3104136	200
PV11	m1069483	200
PV12	m1069424	300
PV13	m1026960	300

LIST OF REFERENCES

Appen, JV, Martin Braun, Thomas Stetz, Konrad Diwold et Dominik Geibel. 2013. « Time in the Sun: The Challenge of High PV Penetration in the German Electric Grid ». *Power and Energy Magazine, IEEE,* vol. 11, n° 2, p. 55-64.

Arritt, R. F., et R. C. Dugan. 2010. « The IEEE 8500-node test feeder ». In *Transmission and Distribution Conference and Exposition, 2010 IEEE PES*. (19-22 April 2010), p. 1-6.

Asari, Masahiro, et Hiromu Kobayashi. 2012. « Method of controlling reverse power flow of PV system with heat pump water heater ». In *Innovative Smart Grid Technologies (ISGT Europe), 2012 3rd IEEE PES International Conference and Exhibition on*. p. 1-6. IEEE.

Aziz, T, MJ Hossain, TK Saha et N Mithulananthan. 2013. « VAR Planning With Tuning of STATCOM in a DG Integrated Industrial System ». *Power Delivery, IEEE Transactions on,* vol. 28, n° 2, p. 875-885.

Baran, M. E., et I. El-Markaby. 2005. « Fault analysis on distribution feeders with distributed generators ». *Power Systems, IEEE Transactions on,* vol. 20, n° 4, p. 1757-1764.

Baran, M. E., H. Hooshyar, Shen Zhan et A. Huang. 2012. « Accommodating High PV Penetration on Distribution Feeders ». *Smart Grid, IEEE Transactions on,* vol. 3, n° 2, p. 1039-1046.

Baran, Mesut. 2012. « Branch current based state estimation for distribution system monitoring ». In *Power and Energy Society General Meeting, 2012 IEEE*. p. 1-4. IEEE.

Baran, Mesut E, et Arthur W Kelley. 1995. « A branch-current-based state estimation method for distribution systems ». *IEEE transactions on power systems,* vol. 10, n^o CONF-940702.

Basso, Thomas S, et Richard DeBlasio. 2004. « IEEE 1547 series of standards: interconnection issues ». *Power Electronics, IEEE Transactions on,* vol. 19, n° 5, p. 1159-1162.

128

Bernieri, Andrea, C Liguori et Arturo Losi. 1995. « Neural networks and pseudo-measurements for real-time monitoring of distribution systems ». In *Instrumentation and Measurement Technology Conference, 1995. IMTC/95. Proceedings. Integrating Intelligent Instrumentation and Control., IEEE*. p. 112. IEEE.

Billinton, Roy, Ronald Norman Allan et Ronald N Allan. 1984. *Reliability evaluation of power systems*, 2. Plenum press New York.

Bollen, Math H, et Fainan Hassan. 2011. *Integration of distributed generation in the power system*, 80. John Wiley & Sons.

Byung-Kwan, Kang, Kim Seung-Tak, Bae Sun-Ho et Park Jung-Wook. 2013. « Effect of a SMES in Power Distribution Network With PV System and PBEVs ». *Applied Superconductivity, IEEE Transactions on,* vol. 23, n° 3, p. 5700104-5700104.

Casali, F. 2013. « Field experience of phasors measurement in a distribution network with increased level of LV-connected PV ». In *Electricity Distribution (CIRED 2013), 22nd International Conference and Exhibition on*. (10-13 June 213), p. 1-3.

Cespedes, M., et Sun Jian. 2014. « Adaptive Control of Grid-Connected Inverters Based on Online Grid Impedance Measurements ». *Sustainable Energy, IEEE Transactions on,* vol. 5, n° 2, p. 516-523.

Chen, C. S., C. H. Lin, W. L. Hsieh, C. T. Hsu et T. T. Ku. 2013. « Enhancement of PV Penetration With DSTATCOM in Taipower Distribution System ». *Power Systems, IEEE Transactions on,* vol. 28, n° 2, p. 1560-1567.

Chilvers, I., N. Jenkins et P. Crossley. 2005. « Distance relaying of 11 kV circuits to increase the installed capacity of distributed generation ». *Generation, Transmission and Distribution, IEE Proceedings-,* vol. 152, n° 1, p. 40-46.

Christakou, K., J. LeBoudec, M. Paolone et D. C. Tomozei. 2013. « Efficient Computation of Sensitivity Coefficients of Node Voltages and Line Currents in Unbalanced Radial Electrical Distribution Networks ». *Smart Grid, IEEE Transactions on,* vol. 4, n° 2, p. 741-750.

Coffele, F., C. Booth et A. Dysko. 2015. « An Adaptive Overcurrent Protection Scheme for Distribution Networks ». *Power Delivery, IEEE Transactions on,* vol. 30, n° 2, p. 561-568.

Daratha, N., B. Das et J. Sharma. 2013. « Coordination Between OLTC and SVC for Voltage Regulation in Unbalanced Distribution System Distributed Generation ». *Power Systems, IEEE Transactions on,* vol. PP, n° 99, p. 1-11.

Das, S., S. Santoso et A. Maitra. 2014. « Effects of distributed generators on impedance-based fault location algorithms ». In *PES General Meeting | Conference & Exposition, 2014 IEEE*. (27-31 July 2014), p. 1-5.

David Smyth. *Using Distributed Pv For Volt/Var Control And Maximum Demand Reduction.* Energy Innovations Pty Ltd.

De Brabandere, Karel, Achim Woyte, Ronnie Belmans et Johan Nijs. 2004. « Prevention of inverter voltage tripping in high density PV grids ». *19th EU-PVSEC, Paris*.

Demirok, E., Gonza Casado, x, P. lez, K. H. B. Frederiksen, D. Sera, P. Rodriguez et R. Teodorescu. 2011. « Local Reactive Power Control Methods for Overvoltage Prevention of Distributed Solar Inverters in Low-Voltage Grids ». *Photovoltaics, IEEE Journal of,* vol. 1, n° 2, p. 174-182.

Distributed Generation Technical Interconnection Requirements - Interconnections at Voltages 50kv And Below, Hydro One Networks Inc Std, no: DT-10-015, Rev. 3, 2013

Dugan, R. C., et T. E. McDermott. 2011. « An open source platform for collaborating on smart grid research ». In *Power and Energy Society General Meeting, 2011 IEEE*. (24-29 July 2011), p. 1-7.

Dugan, Roger C. 2012. « Reference Guide: The Open Distribution System Simulator (OpenDSS) ». *Electric Power Research Institute, Inc*.

Ehara, T. 2009. « Overcoming PV grid issues in urban areas ». *International Energy Agency, Photovoltaic Power Systems Program, Rep. IEA-PVPS T10-06-2009*.

El-Khattam, W., et T. S. Sidhu. 2008. « Restoration of Directional Overcurrent Relay Coordination in Distributed Generation Systems Utilizing Fault Current Limiter ». *Power Delivery, IEEE Transactions on,* vol. 23, n° 2, p. 576-585.

El Itani, Samer, et Géza Joós. 2012. *Advanced wind generator controls: meeting the evolving grid interconnection requirements*. INTECH Open Access Publisher.

130

Ellis, Abraham, R Nelson, E Von Engeln, R Walling, J MacDowell, L Casey, E Seymour, W Peter, C Barker et B Kirby. 2012. « Reactive power performance requirements for wind and solar plants ». In *Power and Energy Society General Meeting, 2012 IEEE*. p. 1-8. IEEE.

Farivar, Masoud, Russell Neal, Christopher Clarke et Steven Low. 2012. « Optimal inverter var control in distribution systems with high pv penetration ». In *Power and Energy Society General Meeting, 2012 IEEE*. p. 1-7. IEEE.

Fenghai, Sui, M. Kostic et Zhang Zhiying. 2015. « Zone 2 distance protection coordination with distribution feeder protection ». In *Protective Relay Engineers, 2015 68th Annual Conference for*. (March 30 2015-April 2 2015), p. 248-261.

« FERC Order No. 661-A, December 12, 2005. ».

Ferdowsi, M., B. Zargar, F. Ponci et A. Monti. 2014. « Design considerations for artificial neural network-based estimators in monitoring of distribution systems ». In *Applied Measurements for Power Systems Proceedings (AMPS), 2014 IEEE International Workshop on*. (24-26 Sept. 2014), p. 1-6.

Godfrey, T., S. Mullen, R. C. Dugan, C. Rodine, D. W. Griffith et N. Golmie. 2010. « Modeling Smart Grid Applications with Co-Simulation ». In *Smart Grid Communications (SmartGridComm), 2010 First IEEE International Conference on*. (4-6 Oct. 2010), p. 291-296.

Goli, P., et W. Shireen. 2014. « PV Integrated Smart Charging of PHEVs Based on DC Link Voltage Sensing ». *Smart Grid, IEEE Transactions on,* vol. 5, n° 3, p. 1421-1428.

Guide, MATLAB User's. 1998. « The mathworks ». *Inc., Natick, MA,* vol. 5.

Hase, Yoshihide. 2007. *Handbook of Power System Engineering*.

Hatta, Hiroyuki, Satoshi Uemura et Hiromu Kobayashi. 2010. « Cooperative control of distribution system with customer equipments to reduce reverse power flow from distributed generation ». In *Power and Energy Society General Meeting, 2010 IEEE*. p. 1-6. IEEE.

Hepbasli, Arif, et Yildiz Kalinci. 2009. « A review of heat pump water heating systems ». *Renewable and Sustainable Energy Reviews,* vol. 13, n° 6, p. 1211-1229.

Hoke, Anderson, Rebecca Butler, Joshua Hambrick et Benjamin Kroposki. 2013. « Steady-state analysis of maximum photovoltaic penetration levels on typical distribution feeders ». *Sustainable Energy, IEEE Transactions on,* vol. 4, n° 2, p. 350-357.

IEEE Guide for the Application of Neutral Grounding in Electrical Utility Systems--Part IV: Distribution. 2015. « ». *IEEE Std C62.92.4-2014 (Revision of IEEE Std C62.92.4-1991)*, p. 1-44.

IEEE Standard Definitions for the Measurement of Electric Power Quantities Under Sinusoidal, Nonsinusoidal, Balanced, or Unbalanced Conditions. 2010. « ». *IEEE Std 1459-2010 (Revision of IEEE Std 1459-2000)*, p. 1-50.

Inoue, Kei, et Yumiko Iwafune. 2010. « Operation of heat pump water heaters for restriction of photovoltaic reverse power flow ». In *Power System Technology (POWERCON), 2010 International Conference on*. p. 1-7. IEEE.

Jahangiri, P., et D. C. Aliprantis. 2013. « Distributed Volt/VAr Control by PV Inverters ». *Power Systems, IEEE Transactions on,* vol. 28, n° 3, p. 3429-3439.

Khatami, Mehrdad, Hashem Mortazavi, Mostafa Rajabi Mashhadi et Mahdi Oloomi. 2013. « Designing an off-grid PV system: For a residential consumer in Mashhad-Iran ». In *AFRICON, 2013*. p. 1-5. IEEE.

Kersting, William H. 2012. *Distribution system modeling and analysis*. CRC press.

Kim, Chul-Hwan, Jeong-Yong Heo et Raj K Aggarwal. 2005. « An enhanced zone 3 algorithm of a distance relay using transient components and state diagram ». *Power Delivery, IEEE Transactions on,* vol. 20, n° 1, p. 39-46.

Kim, Young-Jin, James L. Kirtley et Leslie K. Norford. 2013. « Analysis of a building power system with a rooftop PV array and phevs as an aggregator ». In *Innovative Smart Grid Technologies (ISGT), 2013 IEEE PES*. (24-27 Feb. 2013), p. 1-6.

Kun, Yang, Cheng Xiaoxiao, Wang Yue, Chen Lei et Chen Guozhu. 2012. « PCC voltage stabilization by D-STATCOM with direct grid voltage control strategy ». In

Industrial Electronics (ISIE), 2012 IEEE International Symposium on. (28-31 May 2012), p. 442-446.

Lin, C. H., C. S. Chen, W. L. Hsieh, C. T. Hsu, H. J. Chuang et C. Y. Ho. 2012. « Optimization of photovoltaic penetration with DSTATCOM in distribution systems ». In *Power System Technology (POWERCON), 2012 IEEE International Conference on*. (Oct. 30 2012-Nov. 2 2012), p. 1-6.

Liu, Ellen, et Jovan Bebic. 2008. *Distribution system voltage performance analysis for high-penetration photovoltaics*. National Renewable Energy Laboratory.

Marra, F., Yang Guangya, C. Traeholt, J. Ostergaard et E. Larsen. 2014. « A Decentralized Storage Strategy for Residential Feeders With Photovoltaics ». *Smart Grid, IEEE Transactions on,* vol. 5, n° 2, p. 974-981.

Mason, C Russell. 1956. *The art and science of protective relaying*. Wiley.

Mortazavi, H., H. Mehrjerdi, M. Saad, S. Lefebvre, D. Asber et L. Lenoir. « Application of Distance Relay for Distribution System Monitoring ». In *PES General Meeting | Conference & Exposition, 2015 IEEE*

Mortazavi, H., H. Mehrjerdi, M. Saad, S. Lefebvre, D. Asber et L. Lenoir. 2015b. « A Monitoring Technique for Reversed Power Flow Detection With High PV Penetration Level ». *Smart Grid, IEEE Transactions on,* vol. 6, n° 5, p. 2221-2232.

Mortazavi, H., H. Mehrjerdi, M. Saad, S. Lefebvre, D. Asber et L. Lenoir. 2016. « An Impedance Based Method For Distribution System Monitoring ». *Smart Grid, IEEE Transactions on,* vol. PP, n° 99, p. 1-1.

Nikolaidis, V. C., E. Papanikolaou et A. S. Safigianni. 2015. « A Communication-Assisted Overcurrent Protection Scheme for Radial Distribution Systems With Distributed Generation ». *Smart Grid, IEEE Transactions on,* vol. PP, n° 99, p. 1-1.

Niazy, Ismail, J Ebadi, S Sabzevari, A Niazy, H Mortazavi et HR Poursoltani. 2010. « Participation in reactive power market considering generator aging ». In *IPEC, 2010 Conference Proceedings*. p. 1067-1072. IEEE.

Nykamp, S., A. Molderink, J. L. Hurink et G. J. M. Smit. 2013. « Storage operation for peak shaving of distributed PV and wind generation ». In *Innovative Smart Grid Technologies (ISGT), 2013 IEEE PES*. (24-27 Feb. 2013), p. 1-6.

Ogimoto, Kazuhiko, Izumi Kaizuka, Yuzuru Ueda et Takashi Oozeki. 2013. « A Good Fit: Japan?? s Solar Power Program and Prospects for the New Power System ». *Power and Energy Magazine, IEEE,* vol. 11, n° 2, p. 65-74.

Portillo, Ramon, Mohammad Sharifzadeh, Hani Vahedi, Leopoldo G. Franquelo et Kamal Al-Haddad. 2015. « Improved hybrid SHM-SHE modulation technique for four-leg three-level NPC inverters ». In *IECON 2015-41st Annual Conference of the IEEE Industrial Electronics Society*. (Japan, 9-12 Nov. 2015), p. 5415-5420.

Powalko, Michal, Krzysztof Rudion, Przemyslaw Komarnicki et Joerg Blumschein. 2009. « Observability of the distribution system ». In *Electricity Distribution - Part 1, 2009. CIRED 2009. 20th International Conference and Exhibition on*. (8-11 June 2009), p. 1-4.

Qiang, Fu, L. F. Montoya, A. Solanki, A. Nasiri, V. Bhavaraju, T. Abdallah et D. C. Yu. 2012. « Microgrid Generation Capacity Design With Renewables and Energy Storage Addressing Power Quality and Surety ». *Smart Grid, IEEE Transactions on,* vol. 3, n° 4, p. 2019-2027.

Qashqai, P., A. Sheikholeslami, H. Vahedi et K. Al-Haddad. 2015. « A Review on Multilevel Converter Topologies for Electric Transportation Applications ». In *VPPC 2015-Vehicular Power and Propulsion Conference*. (Canada), p. 1-6. IEEE.

Rajaei, N., M. H. Ahmed, M. M. A. Salama et R. K. Varma. 2014. « Fault Current Management Using Inverter-Based Distributed Generators in Smart Grids ». *Smart Grid, IEEE Transactions on,* vol. 5, n° 5, p. 2183-2193.

Reno, Matthew J, et Kyle Coogan. 2014. « Grid Integrated Distributed PV (GridPV) Version 2 ». *Sandia National Labs SAND2014-20141*.

Requirements for the Interconnection of Distributed Generation to the Hydro-Québec Medium-Voltage Distribution System (between 750 V to 44000 V), Hydro-Québec Std, no:E.12-01,2004.

134

Roberts, Jeff, Armando Guzman et Edmund O Schweitzer III. 1993. « Z= V/I does not make a distance relay ». *Proceedings of WPRC*.

Saleh, K. A., H. H. Zeineldin, A. Al-Hinai et E. F. El-Saadany. 2015. « Optimal Coordination of Directional Overcurrent Relays Using a New Time Current Voltage Characteristic ». *Power Delivery, IEEE Transactions on,* vol. 30, n° 2, p. 537-544.

Schoenung, Susan M, et William V Hassenzahl. 2003. « Long-vs. Short-Term Energy Storage Technologies Analysis. A Life-Cycle Cost Study. A Study for the DOE Energy Storage Systems Program ». *Sandia National Laboratories*.

Sharifzadeh, Mohammad, Hani Vahedi, Abdolreza Sheikholeslami, Philippe-Alexandre Labbé et Kamal Al-Haddad. 2015. « Hybrid SHM-SHE Modulation Technique for Four-Leg NPC Inverter with DC Capacitors Self-Voltage-Balancing ». *IEEE Trans. Ind. Electron.,* vol. 62, n° 8, p. 4890-4899.

Sharifzadeh, Mohammad, Abdolreza Sheikholeslami, Hani Vahedi, Philippe-Alexandre Labbé et Kamal Al-Haddad. 2015. « Optimized Harmonic Elimination Modulation Extended to Four-Leg NPC Inverter ». *IET Power Electron.*

Shateri, H., et S. Jamali. 2009. « Measured impedance by distance relay elements applied on a distribution feeder in a single phase to ground fault ». In *Power Systems Conference and Exposition, 2009. PSCE '09. IEEE/PES*. (15-18 March 2009), p. 1-7.

Shateri, H., et S. Jamali. 2010. « Measured impedance at source node of a distribution feeder for inter phase faults ». In *Transmission and Distribution Conference and Exposition, 2010 IEEE PES*. (19-22 April 2010), p. 1-6.

Short, Thomas Allen. 2014. *Electric power distribution handbook*. CRC press.

Sinclair, A., D. Finney, D. Martin et P. Sharma. 2014. « Distance Protection in Distribution Systems: How It Assists With Integrating Distributed Resources ». *Industry Applications, IEEE Transactions on,* vol. 50, n° 3, p. 2186-2196.

Singh, M., et V. Telukunta. 2014. « Adaptive distance relaying scheme to tackle the under reach problem due renewable energy ». In *Power Systems Conference (NPSC), 2014 Eighteenth National*. (18-20 Dec. 2014), p. 1-6.

Soleimani, Reza Nejad, Mostafa Rajabi Mashhadi et Hashem Mortazavi. 2014. « Voltage control and optimal capacitor placement in the presence of photovoltaic systems in distribution networks ». In *Electrical Power Distribution Networks (EPDC), 2014 19th Conference on*. p. 29-34. IEEE.

Taheri, H., O. Akhrif et A. F. Okou. 2013. « Contribution of PV generators with energy storage to grid frequency and voltage regulation via nonlinear control techniques ». In *Industrial Electronics Society, IECON 2013 - 39th Annual Conference of the IEEE*. (10-13 Nov. 2013), p. 42-47.

Tcheou, M. P., L. Lovisolo, M. V. Ribeiro, E. A. B. da Silva, M. A. M. Rodrigues, J. M. T. Romano et P. S. R. Diniz. 2014. « The Compression of Electric Signal Waveforms for Smart Grids: State of the Art and Future Trends ». *Smart Grid, IEEE Transactions on,* vol. 5, n° 1, p. 291-302.

Tholomier, Damien, T Yip et G Lloyd. 2009. « Protection of distributed generation (DG) interconnection ». In *Power Systems Conference, 2009. PSC'09.*, p. 1-15. IEEE.

Tonkoski, R., L. A. C. Lopes et T. H. M. El-Fouly. 2011a. « Coordinated Active Power Curtailment of Grid Connected PV Inverters for Overvoltage Prevention ». *Sustainable Energy, IEEE Transactions on,* vol. 2, n° 2, p. 139-147.

Tonkoski, Reinaldo, Luiz AC Lopes et Tarek HM El-Fouly. 2011b. « Coordinated active power curtailment of grid connected PV inverters for overvoltage prevention ». *Sustainable Energy, IEEE Transactions on,* vol. 2, n° 2, p. 139-147.

Tuffner, FK, MCW Kintner-Meyer, FS Chassin et K Gowri. 2012. « Utilizing Electric Vehicles to Assist Integration of Large Penetrations of Distributed Photovoltaic Generation ».

Turitsyn, Konstantin, Petr Sulc, Scott Backhaus et Michael Chertkov. 2010. « Distributed control of reactive power flow in a radial distribution circuit with high photovoltaic penetration ». In *Power and Energy Society General Meeting, 2010 IEEE*. p. 1-6. IEEE.

Ueda, Yuzuru, Kosuke Kurokawa, Takayuki Tanabe, Kiyoyuki Kitamura et Hiroyuki Sugihara. 2008. « Analysis results of output power loss due to the grid voltage rise in grid-connected photovoltaic power generation systems ». *Industrial Electronics, IEEE Transactions on,* vol. 55, n° 7, p. 2744-2751.

136

Uthitsunthorn, D., et T. Kulworawanichpong. 2010. « Distance protection of a renewable energy plant in electric power distribution systems ». In *Power System Technology (POWERCON), 2010 International Conference on*. (24-28 Oct. 2010), p. 1-6.

Vahedi, Hani, Kamal Al-Haddad, Youssef Ounejjar et Khaled Addoweesh. 2013. « Crossover switches cell (CSC): a new multilevel inverter topology with maximum voltage levels and minimum DC sources ». In *Industrial Electronics Society, IECON 2013-39th Annual Conference of the IEEE*. p. 54-59. IEEE.

Vahedi, H., et K. Al-Haddad. 2015a. « Real-Time Implementation of a Packed U-Cell Seven-Level Inverter with Low Switching Frequency Voltage Regulator ». *IEEE Trans. Power Electron.,* vol. PP, n° 99, p. 1-1.

Vahedi, H., P. Labbe et K. Al-Haddad. 2016. « Sensor-Less Five-Level Packed U-Cell (PUC5) Inverter Operating in Stand-Alone and Grid-Connected Modes ». *IEEE Trans. Ind. Informat.,* vol. 12, n° 1, p. 361-370.

Vahedi, H., K. Al-Haddad, P.-A. Labbe et S. Rahmani. 2014. « Cascaded Multilevel Inverter with Multicarrier PWM Technique and Voltage Balancing Feature ». In *ISIE 2014-23rd IEEE International Symposium on Industrial Electronics*. (Turkey), p. 2151-2156. IEEE.

Valverde, G., A. T. Saric et V. Terzija. 2013. « Stochastic Monitoring of Distribution Networks Including Correlated Input Variables ». *Power Systems, IEEE Transactions on,* vol. 28, n° 1, p. 246-255.

Verhoeven, Bas. 1998. *Utility aspects of grid connected photovoltaic power systems*. International Energy Agency.

Viawan, Ferry August. 2008. *Voltage control and voltage stability of power distribution systems in the presence of distributed generation*. Chalmers University of Technology.

Visconti, I. F., D. A. Lima, J. M. C. de Sousa Costa et N. Rabello de B.C.Sobrinho. 2014. « Measurement-Based Load Modeling Using Transfer Functions for Dynamic Simulations ». *Power Systems, IEEE Transactions on,* vol. 29, n° 1, p. 111-120.

Voima, S., et K. Kauhaniemi. 2014. « Using distance protection in smart grid environment ». In *Innovative Smart Grid Technologies Conference Europe (ISGT-Europe), 2014 IEEE PES*. (12-15 Oct. 2014), p. 1-6.

von Appen, J., T. Stetz, M. Braun et A. Schmiegel. 2014. « Local Voltage Control Strategies for PV Storage Systems in Distribution Grids ». *Smart Grid, IEEE Transactions on,* vol. 5, n° 2, p. 1002-1009.

Vu, Khoi, Miroslav M Begovic, Damir Novosel et Murari Mohan Saha. 1999. « Use of local measurements to estimate voltage-stability margin ». *Power Systems, IEEE Transactions on,* vol. 14, n° 3, p. 1029-1035.

Wei-Fu, Su, Huang Shyh-Jier et E. Lin Chin. 2001. « Economic analysis for demand-side hybrid photovoltaic and battery energy storage system ». *Industry Applications, IEEE Transactions on,* vol. 37, n° 1, p. 171-177.

Willis, H Lee. 2010. *Power distribution planning reference book*. CRC press.

Yaghobi, Hamid, et Hashem Mortazavi. 2015. « A novel method to prevent incorrect operation of synchronous generator loss of excitation relay during and after different external faults ». *International Transactions on Electrical Energy Systems,* vol. 25, n° 9, p. 1717-1735.

Yaghobi, Hamid, Hashem Mortazavi, Kourosh Ansari, Habib Rajabi Mashhadi et Hossein Borzoe. 2013. « Study on application of flux linkage of synchronous generator for loss of excitation detection ». *International Transactions on Electrical Energy Systems,* vol. 23, n° 6, p. 802-817.

Yang, Wang, Zhang Peng, Li Wenyuan, Xiao Weidong et A. Abdollahi. 2012. « Online Overvoltage Prevention Control of Photovoltaic Generators in Microgrids ». *Smart Grid, IEEE Transactions on,* vol. 3, n° 4, p. 2071-2078.